International Ph.D. Program in Neuroscience

XXXIII Cycle

New purinergic-based pharmacological targets for the treatment of retinal disorders

PhD thesis

Claudia Giuseppina Fresta

Coordinator & tutor: Prof. Claudio Bucolo
Tutor SIFI s.p.a: Dott.ssa Manuela Santonocito

Department of Clinical and Molecular Biomedicine-Section of Pharmacology and Biochemistry

University of Catania - School of Medicine

November 2021

TABLE OF CONTENTS

ABSTRACT

Diabetic retinopathy (DR) is a progressive disease representing a major microvascular complication of diabetes and a leading cause of visual loss among adults in most industrialized countries. The prevalence of DR is expected to raise worldwide due to aging population, longer life expectancy, and a higher prevalence of people with diabetes, although risk factors management in diabetes care has been improved. The hyperglycemic environment, typical of DR onset, induces blood retinal barrier (BRB) breakdown along with an enhanced expression of pro-inflammatory cell markers and oxidative stress-related mediators. Additionally, the high glucose (HG) levels observed during diabetes induce the activation of the purinergic signaling pathway, which includes the P2X7 receptor (P2X7R). This ATP-gated ion channel has been linked to vascular inflammation due to an over-expression of cytokines, contributing to BRB alteration. The integrity of this physical barrier is essential for a proper vision; indeed, the BRB dysfunction mainly contributes to the development of DR by leading to vascular leakage to surrounding tissues and the consequent vision impairments.

Based on the above, I focused my research project on the development of an innovative strategy for the early treatment of DR through the negative modulation of P2X7R and the decrease of inflammatory cytokines, both of them playing a pivotal role in BRB damage. First of all, I set up a BRB triple co-culture model entirely based on human cells (retinal endothelial cells, retinal pericytes, and retinal astrocytes), in order to mimic the human *milieu*, characterized by the same cellular numerical ratio and layer order observed *in vivo*. The results obtained by using this innovate system showed that an exposure for 48 hours to HG provoked the BRB breakdown, increased the barrier permeability (measured by trans-endothelial electrical

resistance (TEER)), and reduced the levels of junctional proteins such as vascular endothelial (VE)-cadherin and zonula occludens-1 (ZO-1). In our human inner BRB (iBRB) model, the hyperglycemic environment also led to the over-expression of inflammatory mediators (IL-1β, IL-6) and oxidative stress-related genes (iNOS, Nox2) along with a significant increase in reactive oxygen species (ROS) formation and the activation of nuclear factor (erythroid-derived 2)-like 2 (Nrf2)/heme-oxigenase-1 (HO-1) antioxidant axis. Once the model was established, I aimed to investigate the role played by P2X7R in the observed iBRB damage. I first indentified a novel P2X7R antagonist through a virtual screening analysis on a small in-house compound dataset. The results obtained by the computational analysis revealed that the diterpenoid dihydrotanshinone (DHTS) clustered with the well-known P2X7R antagonist JNJ47965567 (used as a positive P2X7R antagonist control in my experiments). In order to assess the potential protective effect of DHTS (as a possible P2X7R antagonist), I challenged the iBRB model with a combination of HG and 2′(3′)-O-(4-Benzoylbenzoyl)adenosine-5′-triphosphate (BzATP) (a selective P2X7R agonist) in absence or presence of this diterpenoid. I found that HG/BzATP stimulation led to an enhanced barrier permeability and reduced levels of junctional proteins at the membrane cell-cell interface along with reduced Cx-43 mRNA expression levels. Furthermore, this combination of stimuli determined an enhanced expression of the major markers of inflammation (TLR-4, IL-1β, IL-6, TNF-α, and IL-8) and others inflammatory mediators (P2X7R, VEGF-A, and ICAM-1) as well as the over-production of ROS. The pre-treatment with DHTS antagonized HG/BzATP stimulus and preserved the BRB integrity. In conclusion, the *in vitro* iBRB model demonstrated to be an useful tool for studying both the contribution of hyperglycemic conditions and P2X7R activation on iBRB dysfunction and

for testing the therapeutic potential of DHTS in preventing and/or counteracting such alterations typical of BRB-related disorders, such as DR.

ACKNOWLEDGEMENTS

It is strange to believe that this PhD chapter is coming to the end. Since I benefited from the input of several people for completing this degree and for supporting me during this period of my life, it is time to thank all of them.

First, I wish to express my gratitude to my supervisor, Professor Claudio Bucolo, for giving me the opportunity and the impetus to embark on this topic, for his expert academic support, for helping me design, conduct different subset studies within my project, and successfully complete this scientific research, but most importantly, for his human quality.

I would also like to thank Professor Salvatore Salomone for improving my knowledge during these years of working together, for his advice, feedbacks on this research work, and meticulous comments on different aspects of being a researcher.

I am deeply grateful to my husband for his insightful suggestions, availability, patience, and for supporting me during the writing of my thesis. He has been an enormous inspiration, both professionally and personally. Thanks a lot for trusting me with this project, for giving me constructive comments on the presentation and readability of the thesis, and for his perceptive guidance and encouragement. He is my role model!

I wish to express my sincere gratitude to my PhD colleagues for all the great moments shared during the last few years, for all the advice, friendship, help, and moral support along my research way, and for the funny moments and laughs we had in the lab. It has been an enormous pleasure to be a part of this great scientific group.

My heartfelt thanks and love are due to all the members of my family, for their love, understanding, and patience without which this project/thesis would have never been finished. Finally, my deepest thank goes to my daughter for her immeasurable ability to give me love and happiness. For this reason I dedicate this thesis to her!

LIST OF ABBREVIATIONS

DR: diabetic retinopathy

ADA: american diabetes association

NPDR: non-proliferative diabetic retinopathy

PDR: proliferative diabetic retinopathy

IRMA: intraretinal microvascular abnormalities

NVD: neovascularization of the disc

NVE: neovascularization elsewhere

VEGF: vascular endothelial growth factor

BRB: blood retina barrier

NFL: nerve fiber layer

GCL: ganglion cell layer

IPL: inner nuclear layer

OPL: outer plexiform layer

ONL: outer nuclear layer

PR: photoreceptor layer

RPE: retinal pigmented epithelium

RGCS: retinal ganglion cells

oBRB: outer blood-retinal barrier

ATP: adenosine triphosphate

BBB: blood-brain barrier

TEER: transendothelial electrical resistance

BAB: blood–aqueous barrier

iBRB: inner blood-retinal barrier

BL: basal lamina

TJs: tight junctions

AJs: adherents junctions

GJs: gap junctions

ZOs: zonula occludens

JAMs: junctional adhesion molecules

ZO-1: zonula occludens-1

VE-CADHERIN: vascular endothelial (VE)-cadherin

CX-43: connexin-43

ANG-1: angiopoietin-1

ANG-2: angiopoietin-2

TGF-β: transforming growth factor-beta

TNF-α: tumor necrosis factor-alpha

ROS: reactive oxygen species

DME: diabetic macular edema

AGEs: glycation end‑products

PKC: protein kinase C

AR: aldose reductase

HG: high glucose

COX-2: cyclooxygenase-2

iNOS: inducible nitric oxide synthase

ICAM-1: intercellular adhesion molecule-1

CCL2: chemokine ligand 2

PDGFB: platelet-derived growth factor beta

NOX: nadph oxidase

RNS: reactive nitrogen species

SOD: superoxide dismutase

NF-κB: nuclear factor kappa-light-chain-enhancer of activated B cells

NLRP3: NOD-like receptor family pyrin domain-containing 3

TXNIP: thioredoxin-interacting protein

TRX: thioredoxin

MAPK: mitogen-activated protein kinase

PKC: protein kinase C

RAS: renin-angiotensin system

G3P: glyceraldehyde-3-phosphate

eATP: extracellular ATP

P2X7R: P2X7 receptor

PANX1: pannexin-1

BzATP: 2′(3′)-o-(4-benzoylbenzoyl)-ATP

NA-F: sodium fluorescein

ETDRS: early treatment diabetes retinopathy study

PRP: panretinal photocoagulation

TA: triamcinolone acetonide

FA: fluocinolone acetonide

FDA: food and drug administration

DEX: dexamethasone

NRF2: nuclear factor erythroid-derived 2-like 2

HO-1: heme-oxigenase-1

DHTS: dihydrotanshinone

TLR-4: toll-like receptor 4

CX-43: connexin 43

INTRODUCTION

Diabetic retinopathy (DR) represents a severe eye condition mainly provoked by hyperglycemia and remains the leading cause of vision impairment and blindness in the working age populations worldwide [1]. DR has always been considered the most frequent and specific microvascular complication of type 2 diabetes mellitus for which diagnosis has been made by clinical manifestation of vascular irregularity; this notwithstanding, it has been shown that retinal microvascular abnormalities have been observed in patients without any evidences of microvascular alterations [2,3]. The American Diabetes Association (ADA) gave a new definition of this pathology as "neurovascular complication". According to the World Health Organization, DR due to the increased life expectancy of patients with diabetes as well as of older populations estimated to arise from 415 to 642 million by 2040 (International Diabetes Federation - IDF Diabetes Atlas 2017; www.diabetesatlas.org, accessed on 23 May 2021). Consequently, the progression and the prevalence of this disorder is linked to a new increase in health costs and represents a major public health concern [4]. Furthermore, according to some epidemiological data, it has been estimated that about 38 million of adults will develop the DR vision threatening by 2040 [5]. From a clinical point of view, DR has been divided into two stages by the ophthalmologists, mainly based on the manifestation of retinal neovascularization and the existence of visible ophthalmologic differences. These two stages are classified as early non-proliferative diabetic retinopathy (NPDR) and late proliferative diabetic retinopathy (PDR)[6]. The first stage in NPDR is known as preclinical retinopathy, where no visible eye alterations can be observed. The pathology then progresses to mild and moderate NPDR, defined by the presence of multiple microaneurysms and intraretinal hemorrhages (identified as red dots) and

hard exudates, respectively, detected by ophthalmoscopic examination and fundus photography. The arrangements of microaneurysms are related to capillary basement membrane alterations, loss of intramural pericytes, and endothelial cells proliferation. The fourth and last stage is represented by severe NPDR, in which is possible to observe increased signs of retinal ischemia characterized by the presence of intraretinal microvascular abnormalities (IRMA), considerable regions with lack of capillary perfusion, retinal cotton wool spots, and significant venous beading. At this stage, with a high probability, the patients progress to the PDR, that represents a more advanced stage of DR characterized by the proliferation of new abnormal blood vessels (neovascularization), the growth of which is variable, on the surface of the inner retina or vitreous (**Figure 1**).

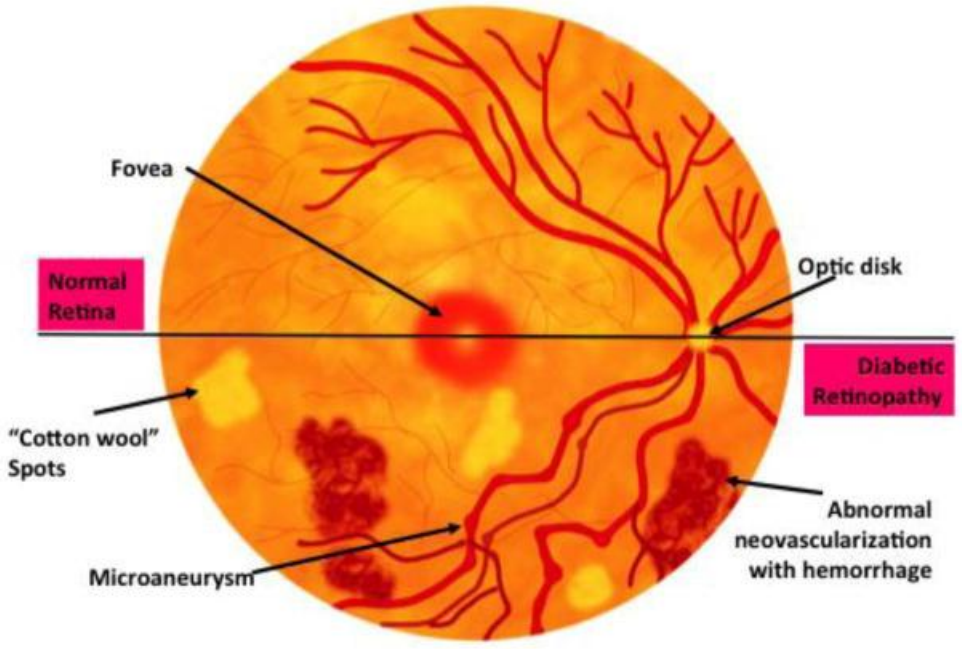

Figure 1. DR is marked by microvascular dysfunction, including abnormal neovascularization, hemorrhages, microaneurysms, and cotton wool spots, that will eventually, if not treated, lead to vision loss [7].

These new fenestrated and fragile vessels are usually accompanied by progressively increasing fibrous proliferation that can lead to vitreous hemorrhage, gliosis, and fibrovascular scar formation, resulting in retinal detachment and the consequent loss of vision [8,9]; indeed, patients at this disease' stage could present severe vision impairments. According to the location of the retinal vessels in PDR, the neovascularization can occur near to the optic disc (neovascularization of the disc, NVD) or elsewhere on the retina (neovascularization elsewhere, NVE). The formation of abnormal new vasculatures leads to complications such as pre-retinal hemorrhages, and may threaten the vision due to bleeding and retinal detachment [10]. Generally, the patients are considered at high-risk of vision loss following the retinal detachment if the NVD occupies more than one-third of the disc area [11]. Moreover, research evidence has been shown the involvement of vascular endothelial growth factor (VEGF) in the formation and progression of ischemia-driven angiogenic pathology in PDR [12]; in fact, it has been demonstrated an increased concentration of this protein in the vitreous of patients with PDR [13]. Several inflammatory, vascular, and neuronal mechanisms are implicated in the pathogenesis of DR. Additional factors contributing to the progression of DR are represented by the dysfunction of the blood retina barrier (BRB), hypoxia, oxidative stress, progressive microvascular damage, and excessive retinal neuronal and glial anomalies[14].

VASCULAR SUPPLY OF THE RETINA

The retina, located in the posterior part of the eye, is a innermost light-sensitive layer that transmits electrochemical signals to the visual center of the brain [15]. As a complex network, the retina is organized in a stratified manner consisting of the inner limiting membrane followed by the nerve fiber layer (NFL), the ganglion cell layer (GCL), the inner plexiform layer

(IPL), the inner nuclear layer (IPL), the outer plexiform layer (OPL), the outer nuclear layer (ONL), the photoreceptor layer (PR), while the last layer is represented by the retinal pigmented epithelium (RPE) (**Figure 2**).

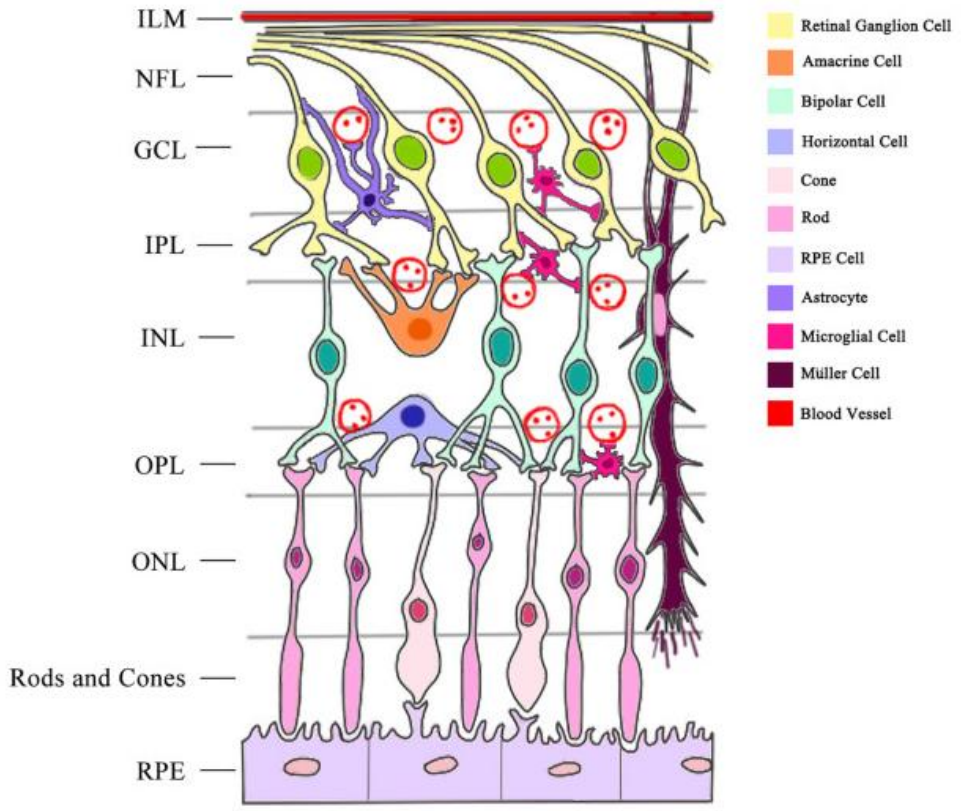

Figure 2. The schematic illustration of a retinal cross-section [16].

Furthermore, the retina is composed of different cell types such as neurons (ganglion cells, horizontal cells, amacrine cells and bipolar cells), glial cells (Müller cells and astrocytes), immune cells (microglia), and vascular cells (endothelial cells and pericytes). Since the neural retina is highly stratified, the light needs to crisscross the retinal neuronal circuit in order to reach the retinal ganglion cells (RGCs), which transmit the electrical impulses, previously converted into a light signal by the photoreceptors, to the visual cortex via the optic nerve (formed by RGCs axons). The RGCs, representing

the retinal output neurons, are located inside the IPL along with bipolar, horizontal, and amacrine cell bodies [17], while the ONL contains photoreceptor cells (mainly rods and cones). The neuronal cells rely on the vasculatures to supply oxygen and nutrients and, along with glial cells and pericytes, regulate the local blood flow [18,19]. The RPE, forming the outer blood-retinal barrier (oBRB), contains cells able to interact with photoreceptors and are crucial for maintaining the homeostasis of the retina through the transport of nutrients and deportation of waste compounds [20]. In the retina, the vessels are highly organized into two distinct complex vascular systems: the choriocapillaris system (outer retina) and the central retinal artery system (inner retina); this circulation is regulated by both blood vessels themselves and the surrounding tissue. Generally, retinal blood vessels are highly concentrated in the central retina and start to decline towards the periphery. Since the retina is a high metabolic-demanding tissue, it requires high levels of oxygen and nutrients that are provided by the retinal vessels; thus, the integrity of the vascular systems is crucial for maintaining the normal visual function [21,22]. The retina is considered an immune privileged tissue since the retinal vasculatures provide a BRB that restricts the access to toxins and pathogens. Collectively, the functional coupling between retinal blood vessels, ganglion cells, and glial cells is known as “neurovascular unit” (**Figure 3**), in which each component regulates, in close coordination, the vasodilatation and vasoconstriction in order to better combine the metabolic activity with the retinal blood flow [23].

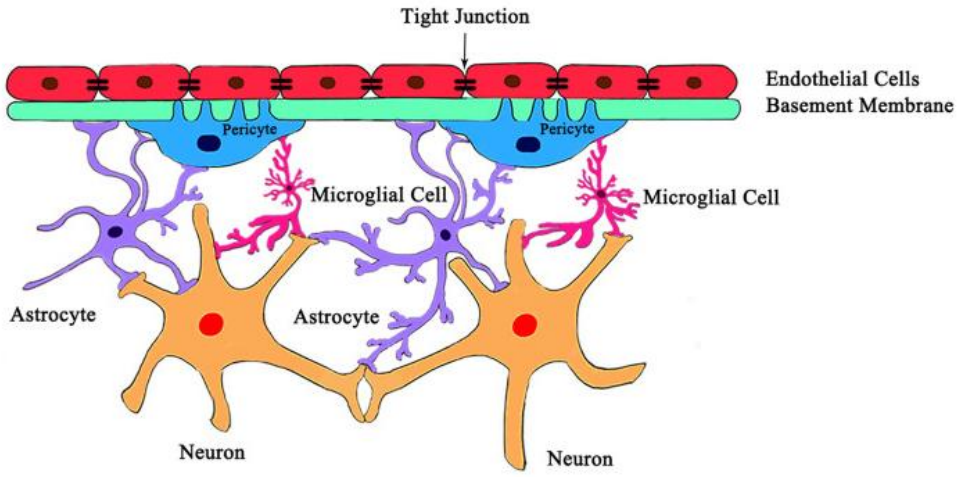

Figure 3. The schematic illustration of the neurovascular unit in the retina [16].

Several studies have shown that the above-mentioned physiologic responses are defective in patients with DR prior to the onset of the early clinical symptoms [24,25], underling the crucial role played by the interactions between the neurosensory retina and its blood vessels. Furthermore, alterations of several molecules such as adenosine triphosphate (ATP), nitric oxide as well as of several lipids interfere with these interactions, triggering DR progression [26]. Lastly, since the neurovascular unit represents the retinal fundamental regulatory mechanism, it becomes more susceptible to oxidative stress-induced damage [27].

OCULAR BARRIERS: THE BRB

The presence of neuronal activity makes both the brain and the retinal tissue the highest energy-demanding systems in the body. The cerebral and retinal circulations are structurally and functionally comparable and share essential properties as “endothelial barrier”. Indeed, both the BRB and the blood-brain barrier (BBB) are constituted of endothelial cells which play a fundamental role for the protection of neuronal *milieu* by providing the transport of nutrients (glucose and amino acids) and oxygen, and reducing

the flow of blood cells. Furthermore, these endothelial barriers are involved in the enzymatic degradation of several compounds [28]. Retinal e cerebral endothelial cells are assembled in a single layer, all around the capillary lumen, and integrated to the adjacent cells through junctional complexes consisting of several proteins such as zonulae occludentes or occluding junctions, and adhesion molecules; these protein complexes represent the basis of the mechanical component of both BBB and BRB [29]. With specific regard to BRB, this physiological barrier is highly restrictive towards the retinal metabolic flux [30]; indeed, the integrity of the BRB determines a high transendothelial electrical resistance (TEER) and reduced paracellular permeability.

In the eye it is possible to distinguish two major barrier systems: the BRB and the blood–aqueous barrier (BAB) that, by acting in equilibrium, regulate both the content of the inner fluids and the discharge of waste products, preserving the ocular tissue environment [31]. The retinal vascular leakage due to BRB alteration is the central cause of visual loss in several ocular diseases, as observed in the case of DR. Unfortunately, despite the recent advances, the cellular mechanisms underlying the BRB dysfunction in pathological conditions have not been fully elucidated.

Structurally, the BRB consist of two distinct compartments: the oBRB and the inner BRB (iBRB) (**Figure 4**).

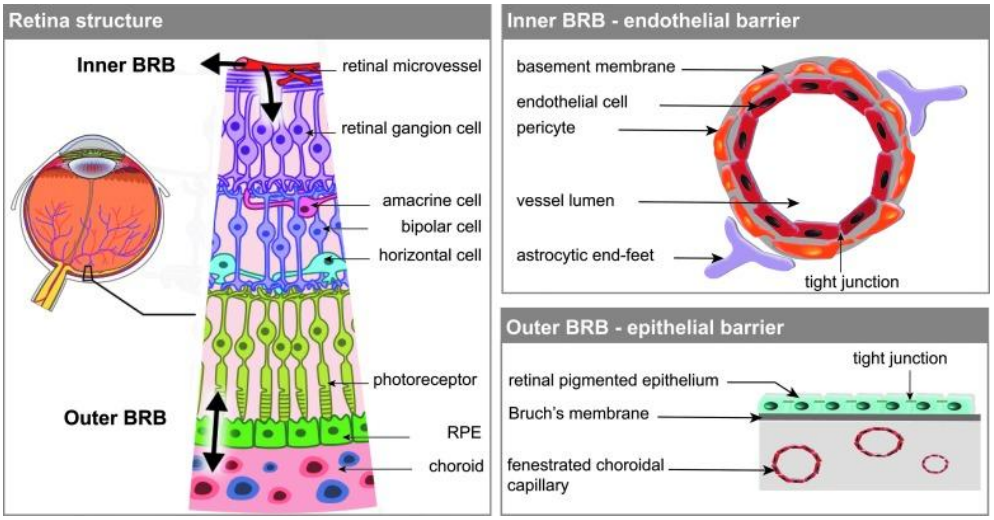

Figure 4. BRB compartments: iBRB and oBRB [32].

The oBRB is established by junctional complexes between neighboring RPE cells and it is involved in the regulation of the transport between the choriocapillaris and the retina [33]. The RPE regulates the exchange of nutrients between the blood and the photoreceptors; this metabolic communication is critical for maintaining the proper visual function.

The iBRB is composed by retinal endothelial cells, connected by junctional proteins ,that are surrounded by pericytes that, in turn, are supported by the processes of glial cells, such as astrocytes and Müller cells. Müller cells promote the integrity of tight junction complexes, induce endothelial cells and pericytes differentiation, being responsible for the BRB maintenance [34]. Differently from endothelial cells, pericytes do not form a continuous layer and, even though they are firmly associated with endothelial cells, they do not contribute to the diffusion barrier. Pericytes provide structural support to the microvasculature and, along with astrocytes and Muller cells, supervise endothelial cells activity by releasing regulatory molecules that act as signals indicating changes of the retinal microenvironment. The BRB plays a pivotal role in the retinal microenvironment through the regulation

of transport across retinal capillaries and the management of fluids and molecules, avoiding the retinal leakage and the passage of harmful agents into the retina [33]; indeed, the loss of BRB integrity can be detrimental and greatly contributes to the pathophysiology of DR [35]. Therefore, a better understanding of the mechanisms underlying BRB dysfunction will help the development of DR therapies

Retinal endothelial cells and junctional proteins

As stated above, retinal endothelial cells are non-fenestrated cells that form a continuous and single layer, known as basal lamina (BL), around the vasculatures. Along with pericytes, astrocytes, and microglia, endothelial cells represent the "supporting columns" of the neurovascular unit and are responsible of the BRB polarization [36]. In several ocular pathologies, such as DR, the structural damage of endothelial cell has been linked to BRB dysfunction, since they are the fundamental iBRB structures [37]. Indeed, it has been shown in diabetic rats that the endothelial cells death leads to the formation of acellular capillaries [38]. Furthermore, hyperglycemic and hypoxic conditions along with oxidative stress trigger endothelial cells apoptotic process [39].

The endothelial barrier selectively regulates the transport of molecules that can occur through two dynamic pathways: the transcellular transport, mainly mediated by the presence of specialized transport vesicles, and the paracellular pathway, which involves the inter-endothelial cells junctions.

The junctional complexes consist of tight junctions (TJs), adherents junctions (AJs), and gap junctions (GJs) (**Figure 5**).

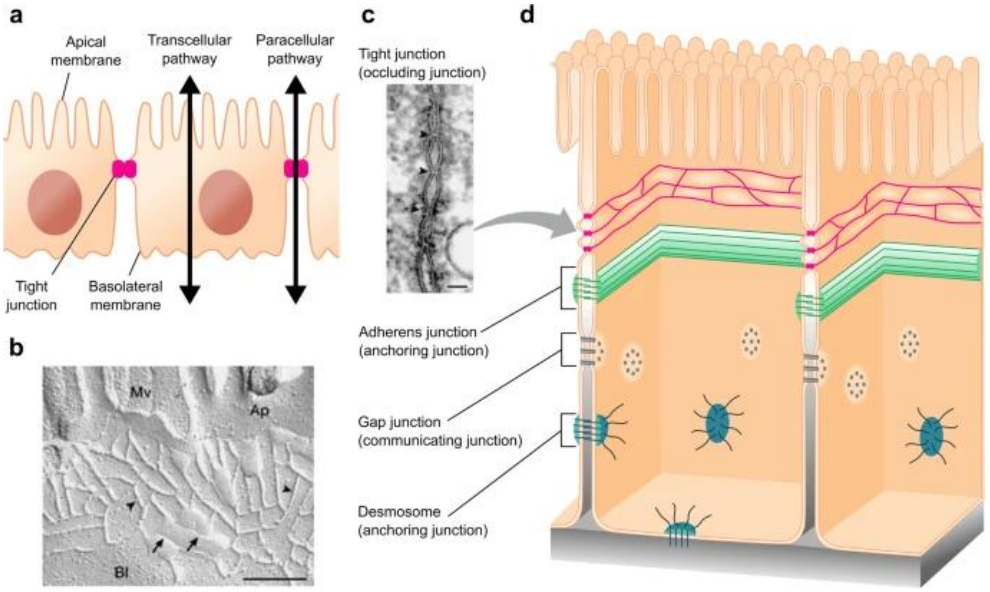

Figure 5. Transepithelial transport routes and intercellular junctions [40].

These protein complexes are dynamic structures involved in the regulation of cell-to-cell adhesion, cell survival, and endothelial cells contact inhibition; likewise, the junctional complexes are crucial for the regulation of the paracellular permeability and the maintenance of cell polarity. With regard to AJs and TJs, the lateral adhesion is mediated by the interaction, along the cell border, of adhesive membrane proteins organized in zipper-like structures.

In the BRB, TJs represent multifunctional complexes involved in two main functions:

1. the control of fluid and solute fluxes through the paracellular space;
2. the conferment of cell polarity by marking a boundary line between basolateral and apical plasma membranes.

Differently from epithelial cells, in which TJs are more concentrated at the apical side of the cell, in endothelial cells the TJs are entangled with AJs and GJs, and mediate the adhesion and communication between adjacent cells. The TJs family consist of more than 40 transmembrane proteins

including intracellular scaffold proteins such as the zonula occludens family (ZOs), junctional adhesion molecules (JAMs), occludin, claudins, and other membrane associated proteins. ZOs is a family of large proteins (>200 kDa) which includes zonula occludens-1 (ZO-1), the first intracellular component of TJs discovered, and two closely related proteins represented by zonula occludens-2 and zonula occludens-3. They exert an important role regarding the TJs organization, since these proteins mediate the connection between transmembrane proteins and the cytoskeletal components.

AJs represent another class of junctional proteins connecting endothelial cells at BRB level. They develop in early stages of intercellular contact, prior to TJs formation, and are formed by adhesion proteins of the cadherin superfamily; the latter provides the formation of multimeric complexes at the cell-to-cell borders [41]. BRB endothelial cells express a distinct cadherin called vascular endothelial (VE)-cadherin, a transmembrane Ca^{2+}-dependent protein that is present in all endothelial cells part of the vessels, while it cannot be found in any other cell types; indeed, it represents a kind of signature of endothelial lineage [42]. VE-cadherin has a conserved cytoplasmic tail that binds multiple intracellular partners, including β-catenin. Since VE-cadherin promotes claudin-5 expression [43], the presence of this adhesion molecule is crucial for TJs organization. Additionally, VE-cadherin is essential for the maintenance of newly formed vessel and for the appropriate formation of their lumen [44].

Lastly, another intracellular junction involved in the formation of the BRB structure is represented by GJs family, composed by connexin proteins. GJs play an important role in cellular communication, allowing the passage of small molecules between two neighboring cells. In the retina and in the brain, GJs are predominant in astrocytes where are involved in K^+ and glutamate redistribution as well as in TJs assembly [45,46].

Retinal pericytes

Pericytes are important constituents of the BRB, having a crucial role in the maintenance of BRB stability and the regulation of homeostatic processes through the communication with other cell types part of the neurovascular unit. They are branched mural cells that envelope capillary walls; indeed, these cells share the BL with endothelial cells with which establish the cell-cell contacts through N-cadherin and connexin-43 (Cx-43) [47,48]. Furthermore, pericytes, by interacting with the adjacent endothelial cells,astrocytes and microglia, regulate endothelial functions ,growth, and differentiation as well as the maintenance of the vascular system through the secretion of different factors [49], such as angiopoietin-1 (Ang-1). Ang-1, by binding its receptor Tie-2, induces endothelial remodeling processes and maturation [50]. On the other hand, the secretion of angiopoietin-2 (Ang-2) along with an overproduction of VEGF induce angiogenic processes by activating a cascade of events in endothelial cells [51]. The interaction between VEGF and Ang-2 has considerable implications in the progression of DR since it triggers the angiogenic switch from non-proliferative to proliferative stage [52]. Additionally, it has been shown that transforming growth factor-beta (TGF-β) signaling inside the pericytes, inhibits retinal endothelia cells proliferation and migration, preserving BRB integrity [53]; indeed, the loss of pericytes leads to an increased BRB permeability due to retinal vasculature damage [7].

Retinal glial cells

In addition to pericytes, retinal glial cells, including Müller cells, astrocytes and microglia, play an important role in regulating and maintaining the BRB integrity; they also actively participate in the uptake of nutrients and in the removal of waste products [54]. Müller cells and astrocytes have processes

that surround all the retinal blood vessels and are separated from endothelial cells by the BL only. Glial cells are involved in the regulation of several endothelial cell functions as well as in the survival of retinal cells through the release of neurotrophic and antioxidant factors. Both cell types are also implicated in the mechanism that regulates vasodilation and vasoconstriction, and provide metabolic support to neurons by setting the metabolism and transport of neurotransmitters (such as glutamate) [54]. This proves that Müller cells and astrocytes support the BRB by regulating the communication between vascular and neural cells.

The alteration of glial cells function has been linked with retinal pathologies, including BRB breakdown [55]. Indeed, under pathological conditions, glial cells start to overproduce angiogenic cytokines, such as VEGF and tumor necrosis factor-alpha (TNF-α), leading to the degradation of tight junctional proteins and, in turn, BRB alterations [56]. Retinal astrocytes are crucial for maintaining the integrity of retinal vasculatures, and the alteration of astrocytes function contributes to the pathogenesis of several retinal pathologies, including DR [57]. Of note, activated retinal microglia, following a retinal damage, are able to release pro-inflammatory cytokines that trigger retinal pericytes apoptosis [58]. In addition, Müller cells dysfunction due to high glutamate concentrations, leads to an overproduction of reactive oxygen species (ROS), giving toxic effects on retinal tissues [59].

MOLECULAR MECHANISMS OF BRB DYSFUNCTION IN DR

The pathogenesis of DR is very complex and involves several mechanisms, many of which are not fully understood yet. The main processes underlying the onset of DR are hyperglycemia, hypoxia, oxidative stress, and

inflammation. One of major cause of vision loss in DR is the BRB dysfunction; indeed, the vascular leakage and the consequent exposure of blood constituents to retinal microenvironment occurs simultaneously with the BRB degradation, often leading to diabetic macular edema (DME). Usually, the genetic predisposition along with the hyperglycemia boost several pathophysiological events that are linked to the progression of DR [60]; in fact, hyperglycemic episodes promote metabolic dysfunctions that determine the generation of ROS and thus oxidative stress [27]. To date, several major biomechanical mechanisms along with sustained hyperglycemia have been involved in the development of microvascular damage and correlated to retinal stress in DR: accumulation of advanced glycation end‑products (AGEs), activation of protein kinase C (PKC), polyol pathway, inflammation, and oxidative stress [6] (**Figure 6**).

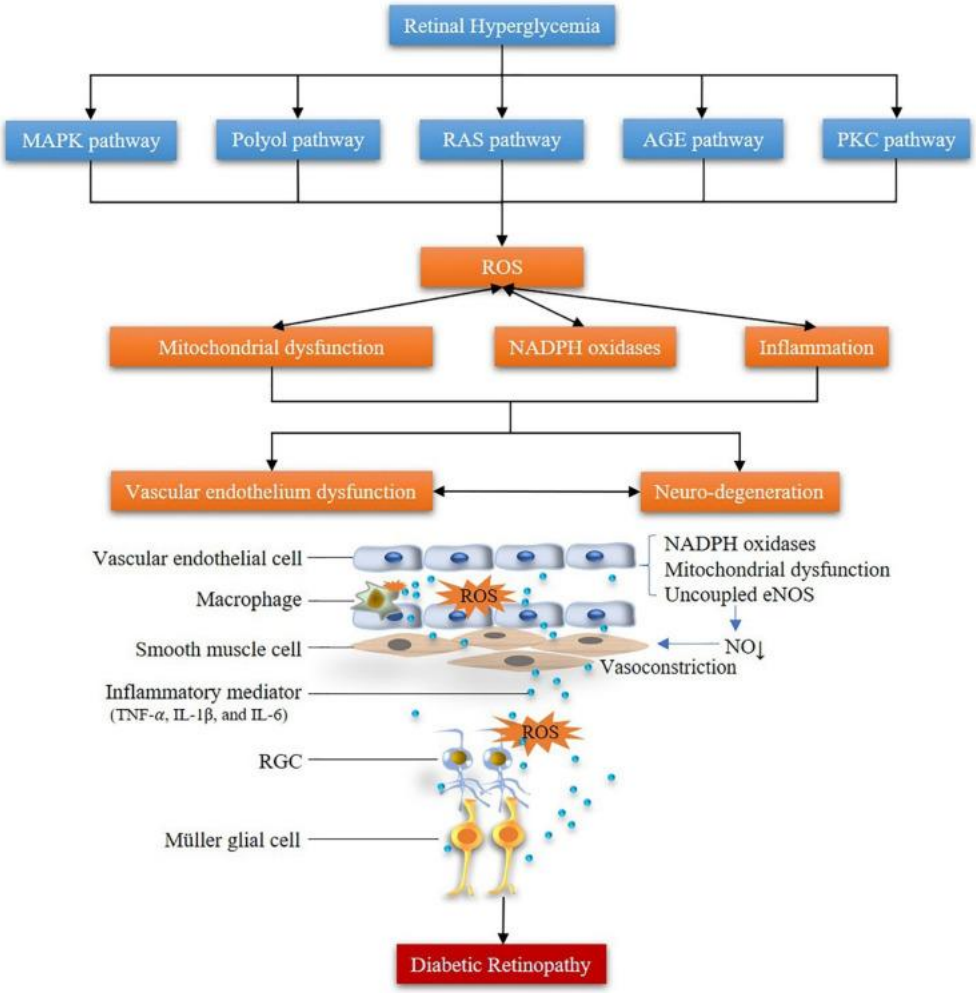

Figure 6. Pathophysiological mechanisms of ROS in diabetic retinopathy [27].

Hyperglycemia

Hyperglycemia is considered the main long-term determinant of the retinal microvascular damage and plays a pivotal role in the pathogenesis of DR. Hyperglycemic episodes lead to blood vessels dilation and cause variation of the blood flow; these changes represent a metabolic auto-regulation that enhance retinal metabolism in diabetic patients [61]. The molecular events associated to an excessive glucose concentration in the bloodstream remain poorly defined. Hyperglycemia leads to aberrant regulation of polyol

pathway in which the excess of glucose is metabolized in sorbitol through the action of aldose reductase (AR), an enzyme expressed in endothelial cells and pericytes. Since it is impermeable to cellular membranes, sorbitol accumulates inside the cell and induces osmotic damage to the retinal vascular endothelium, pericytes death, and other harmful effects [62]. High glucose (HG) levels determine mitochondrial dysfunction with a consequent increase of ROS that, along with deficient anti-oxidative defense systems, lead to metabolic disturbances in retinal endothelial cells [63].

Another side effect of hyperglycemia is represented by the formation of AGEs. These post-translationally modified lipids and proteins have the ability to cross-link intracellular and transmembrane proteins and/or initiating signaling cascades, altering their function [64]. AGEs have been implicated in the development of DR pathology since the modification of key molecules by these modified products leads to vascular damage [64].

Notably, several growth factor including VEGF-A are induced by the diabetic environment and hence are involved in BRB breakdown and the pathogenesis of DR. Indeed, an over-expression of VEGF-A has been linked to vascular permeability and angiogenesis phenomena [65]. Antibodies directed to this grow factor (anti-VEGF) are widely used for the treatment for PDR since they are able to reduce bleeding during vitrectomy [66].

Inflammation

Molecular and physiological changes due to hyperglycemia are correlated with the onset of the inflammatory processes that represent the key drivers of hypoxia, capillary occlusion, and vascular alteration, all characteristic factors of DR, considered by many as an inflammatory disease [67]. An enhanced production of pro-inflammatory cytokines such as interleukin (IL)-6, IL-8, IL-1β, TNF-α, cyclooxygenase-2 (COX-2) and inducible nitric

oxide synthase (iNOS) pro-oxidant enzymes, as well as chemokines (e.g. CCL2, CCL5, CCL12) have been found in the retina of DR subjects [68] (**Figure 7**).

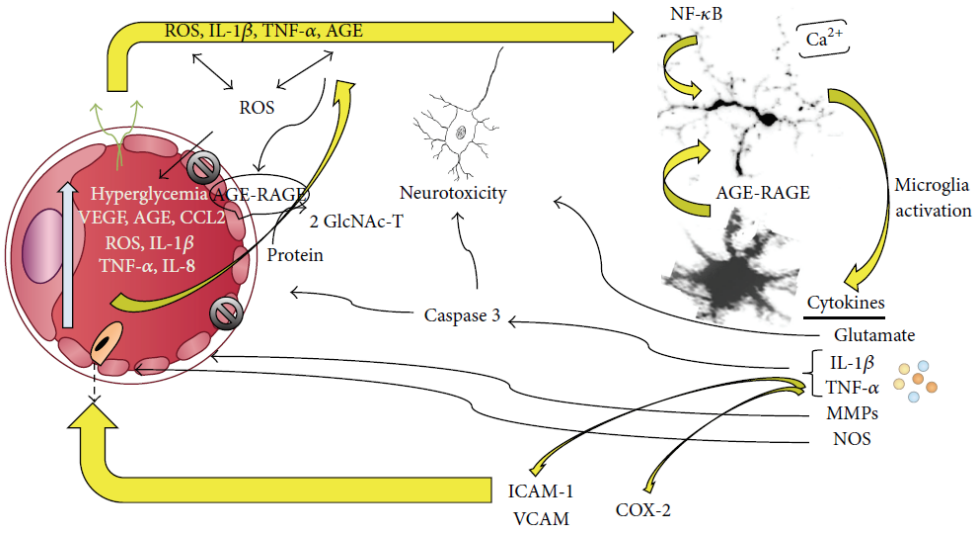

Figure 7. Inflammation during DR [69].

These inflammatory mediators promote junctional protein complexes modification and redistribution in the retinal vessels, contributing to increase the BRB permeability. Worthy of interest is the role played by IL-1β in the barrier dysfunction. This multifunctional pro-inflammatory cytokine has been found to be up-regulated in the retinal endothelial cells, astrocytes, and Müller cells due to HG concentrations [70]. The over-expression of IL-1β induces leukocyte adhesion and migration and the up-regulation of other pro-inflammatory cytokines, leading to BRB breakdown [71]. TNF-α is an important inflammatory mediator of leukostasis that is involved in the apoptotic processes taking place in vascular endothelial cells and retinal neurons [72]; indeed, its gene silencing prevents some pathological events that are linked to the progression of DR, including the BRB breakdown [72]. Leukostasis is a crucial mechanism of the

inflammatory process and has been found to be significantly raised in the retina of diabetic animals [73]. It occurs through the binding between the adhesion molecules (e.g., intercellular adhesion molecule-1 (ICAM-1)) part of the endothelial cell surface and leukocyte counter-receptor CD18. It has been shown that patients with diabetes have high levels of ICAM-1, especially in retinal blood vessels and fibrovascular membranes [74]. Furthermore, it has been shown that ICAM-1 knockout diabetic mice are characterized by lower retinal capillary degeneration and retinal leukostasis [75], demonstrating the involvement of this adhesion molecule in the progression of DR.

Chemokines are also involved in the inflammatory processes that characterize the diabetic retina. In particular, the C-C motif chemokine ligand 2 (CCL2), responsible of the monocytes recruitment and activation, is involved in the regulation of retinal vascular permeability and it is highly concentrated in the vitreous of patients with DR [76,77]. Furthermore, CCL2 plays a fundamental role in BRB breakdown due to the release of pro-inflammatory cytokines and growth factors by activated monocytes [76]. A study conducted by Bartels *et al*. revealed that the treatment with salicylate-based drugs of patients with rheumatoid arthritis reduced the incidence of these subjects to develop DR [78]; these data pointed out the interest on anti-inflammatory compounds as possible drugs for the modulation of DR progression.

Pericytes dropout

Pericytes death has been considered one of the main hallmarks of retinal vascular integrity alteration in subjects with DR [79]. Indeed, hyperglycemia along with basement membrane thickening and AGEs boost

apoptosis and dropout in both retinal endothelial cells and retinal pericytes [80] (**Figure 8**).

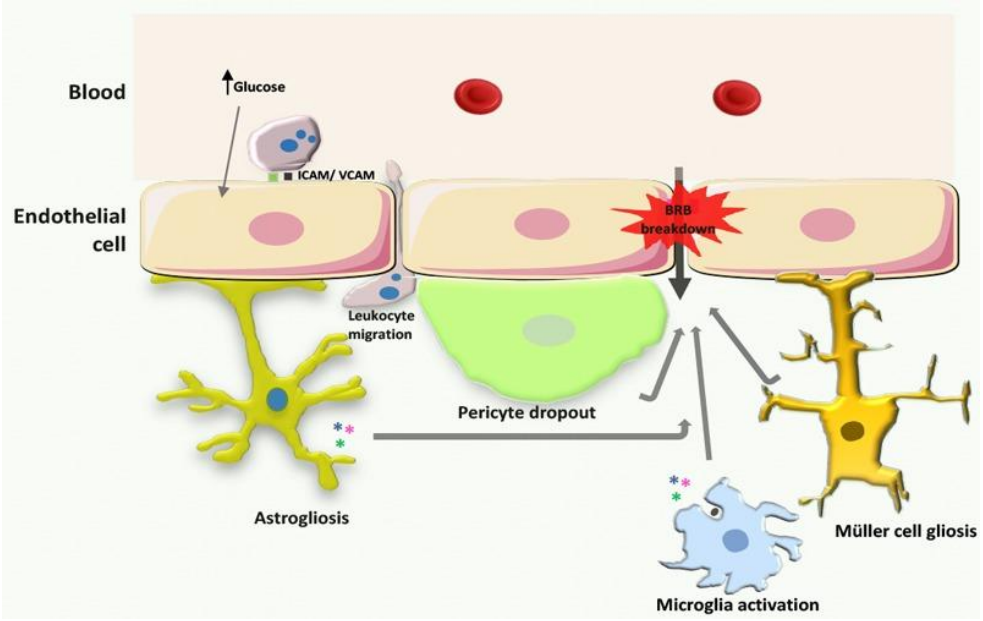

Figure 8. Processes leading to BRB breakdown in diabetic retinopathy [14].

Differently from endothelial cells, pericytes cannot be replaced and their absence in the capillary wall is indicated as "ghost cells". Additionally, pericytes death is associated to pathologic angiogenesis since they are involved in the regulation of endothelial cells proliferation [49]. Recent evidence revealed that under hyperglycemic conditions pericytes start to form bridges across two or more capillaries and the presence of these bridges represents an indicator of retinal vascular damage; indeed. enhanced pericyte bridges can be observed some months before the loss of pericytes and/or endothelial cells in diabetic animal models [81].With the loss of pericytes, endothelial cells start to become feeble and an increased iBRB permeability along with vascular leakage and microaneurysms formation can be observed, all signs indicating the progression of NPDR [82]. A study conducted by Cai and co-workers showed that the interaction between Ang-

2 and its receptors enhanced the apoptotic process in bovine retinal pericytes underhyperglycemic conditions [83]. These results were consistent with other data showing that Ang-2 deficient mice are characterized by reduced pericytes loss [84]. Furthermore, the selective inactivation of platelet-derived growth factor beta (PDGFB) gene in endothelial cells led to a decreased number of pericytes and, as a consequence of this decrease, the animals developed DR [85]. There are other signaling pathways involved in diabetes-induced pericytes loss, even though the underlying mechanisms that reveal their association with pericytes dropout have not been fully elucidated yet [86] .

Oxidative stress

Hyperglycemia-induced oxidative stress, which represents the imbalance between ROS generation and the ability of antioxidant defense systems to eliminate them, is one of the key factors that contribute to DR pathogenesis [87] (**Figure 9**).

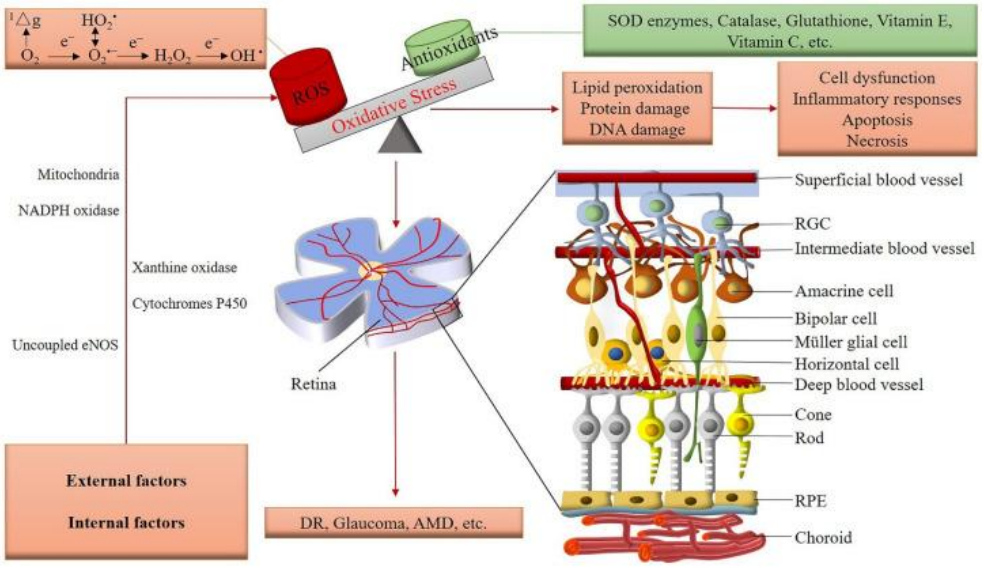

Figure 9. Oxidative stress in the retina [27].

The production of ROS occurs primarily in the electron transport chain of mitochondria, where the unintended leakage of electrons and their reaction with molecular oxygen lead to the production of free radicals [88]. The enzymatic complex of NADPH oxidase (NOX) greatly contributes to ROS production [89].

The free radicals species are mainly classified into ROS and reactive nitrogen species (RNS) [90]. Under normal physiological conditions, ROS are involved in eliminating pathogens, but if their level becomes excessively high, it can induce oxidative damage to proteins (protein misfolding and destruction), lipids (via lipid peroxidation), and nucleic acids, resulting in tissue and mitochondrial injury, cell dysfunction, and inflammatory responses [91]. The antioxidant defense systems consist of several enzymes with detoxification ability such as superoxide dismutase (SOD), catalase, heme oxygenase, and direct antioxidants such vitamin C, vitamin E, and glutathione [92]. As stated above, the ROS generation processes are enhanced under several pathological conditions, as in the case of DR. Indeed, persistent hyperglycemia stimulates the generation of ROS, that in turn determines the dysfunction of the neurovascular unit, leading to retinal vascular diseases[18]. Since oxidative stress originates in mitochondria of endothelial cells, ROS accumulation within these cell type causes endothelial cell dysfunction (characterized by reduced endothelium-dependent vasodilation) along with a pro-thrombotic tand pro-inflammatory state [39]. An over-production of ROS stimulates the generation of several pro-inflammatory cytokines that contribute to cell damage and promotes vascular dysfunction and inflammatory processes by activating several transcription factors such as nuclear factor kappa-light-chain-enhancer of activated B cells (NF-κB) [93]. It has also been demonstrated that ROS activate the NOD-like receptor family pyrin domain-containing 3 (NLRP3)

inflammasome, a multiprotein cytoplasmic complex involved in mediating cellular inflammation through the activation of caspase-1 and the consequent formation of IL-1β and IL-18 mature cytokines [94].

Data reported in literature shown that NLRP3 inflammasome activation (via the ROS-sensitive thioredoxin-interacting protein, TXNIP) andVEGF-A over-expression promote retinal capillary cell apoptosis and enhance retinal vascular permeability in the retina of DR subjects [95,96]. Indeed, it has been shown that the pro-oxidant TXNIP is up-regulated in DR since the link between this protein and thioredoxin (Trx) inhibits Trx ability to reduce thiols and scavenge pro-oxidant molecules [97]. The over-generation of ROS promotes the modification of several signaling pathways such as mitogen-activated protein kinase (MAPK), AGEs, the protein kinase C (PKC),and the renin-angiotensin system (RAS) pathways, all of them contributing to the pathophysiology of DR [98]. In addition to the above, hyperglycemic conditions induce ROS production by altering glycolysis as well as the citric acid cycle pathways with the consequent overproduction of superoxide radical. This radical species induces an increment in the levels of glyceraldehyde-3-phosphate (G3P), that in turn up-regulates the formation and deposition of AGEs [64]. Furthermore, the superoxide radical has been found to be enhanced in retinal endothelial cells exposed to HG concentrations and in a streptozotocin rat model of type I diabetes [99]. Oxidative stress plays a crucial role in the mitochondrial function changes; in line with this, the alteration of bioenergetic pathways in the diabetic neural retina is supported by studies showing the link between inherited mitochondrial disorders and visual impairment, highlighting the contribution of neural retinal cell mitochondria to oxidative stress [100-102].

P2X7 receptor

HG concentrations trigger alterations of retinal blood vessels that induce ATP-mediated apoptosis through the activation of the purinergic signaling. ATP is an excitatory transmitter present at high concentrations (1-10 mM) in the intracellular compartment, whereas its concentration is considerably lower at the extracellular site [103]. During an acute inflammation, injured cells start to release ATP in the extracellular environment and consequently the amount of extracellular ATP (eATP) increases rapidly. High levels of eATP at the site of inflammation represent a danger signal that promotes the infiltration of inflammatory cells, triggering the inflammatory response with the release of pro-inflammatory mediators. The purinergic signaling is mediated by purinergic receptors consisting of two different families: P1 and P2. These purinergic receptors bind adenosine and ATP (or other nucleotide analogs), respectively. The P2 receptor family includes two sub-types: P2X and P2Y [104]. To date, seven P2X receptor sub-types and eight P2Y receptor sub-types have been identified. P2X receptors are a family of ligand-gated ion channels that are activated by eATP and widely distributed in most cell types, including brain glial cells, macrophages,f ibroblasts, erythrocytes, granulocytes, bone cells, epithelial, and endothelial cells [105]. Furthermore, this class of receptors mediates the synaptic transmission in the central and peripheral nervous systems, macrophage activation, platelet aggregation, and are also involved in cell death and immunomodulation phenomena [106,107]. P2X receptors have two transmembrane (2TM) motifs and, since three molecules of ATP seem to bind to the extracellular portions, it has been proposed that these ion channels are composed by three subunits. Differently from the other P2X purinoreceptors, the P2X7 receptor (P2X7R) possess unique features with both physiological and pathological significance. This receptor is highly polymorphic and requires higher

concentrations of ATP to be activated compared to the other ionotropic receptors of the P2X family. P2X7R has been found to be expressed in several retinal cell types including vascular cells and neurons [108,109]. Furthermore, this receptor has also been detected in processes presynaptic to photoreceptors, suggesting a potential role in the retinal neurotransmission [110].The tri-dimensional analysis of P2X7R structure reveals the presence of an extracellular region and two transmembrane helices (TM1 and TM2). Its structure resembles the shape of a dolphin. As in the case of the other P2X sub-types, P2X7R possesses three ATP-binding pockets with three ATP sites of each pair of two adjacent monomers [111]. Interestingly, this receptor has other three drug-binding pockets, juxtaposed to the ATP-binding one, that are able to bind different molecules with both allosteric and/or inhibitory modulatory properties [112]. Under physiological conditions P2X7R is silent, whereas, if the eATP concentration raises following cellular injury or metabolic distress, this purinoreceptor becomes activated. Depending on eATP exposure duration, P2X7R activation leads to two specific responses:

1. permeabilization to a non-selective cationic current ($Ca^{2+}$and Na^{+} influx, and K^{+} efflux) in the case of a relatively short exposure to the agonist (0.1-1sec);
2. formation of a non-selective transmembrane pore, permeable to molecules up to 900Da, when the levels of divalent cations are low and eATP exposure is prolonged.

The “pore formation” response can be easily detected, since it has been associated with cell swelling and apoptotic or necrotic cell death [113]. Additionally, when eATP binds P2X7R it is also possible to observe the activation of pannexin-1 (Panx1), that in turn activates the inflammasome with the consequent release of IL-1β [114] (**Figure 10**).

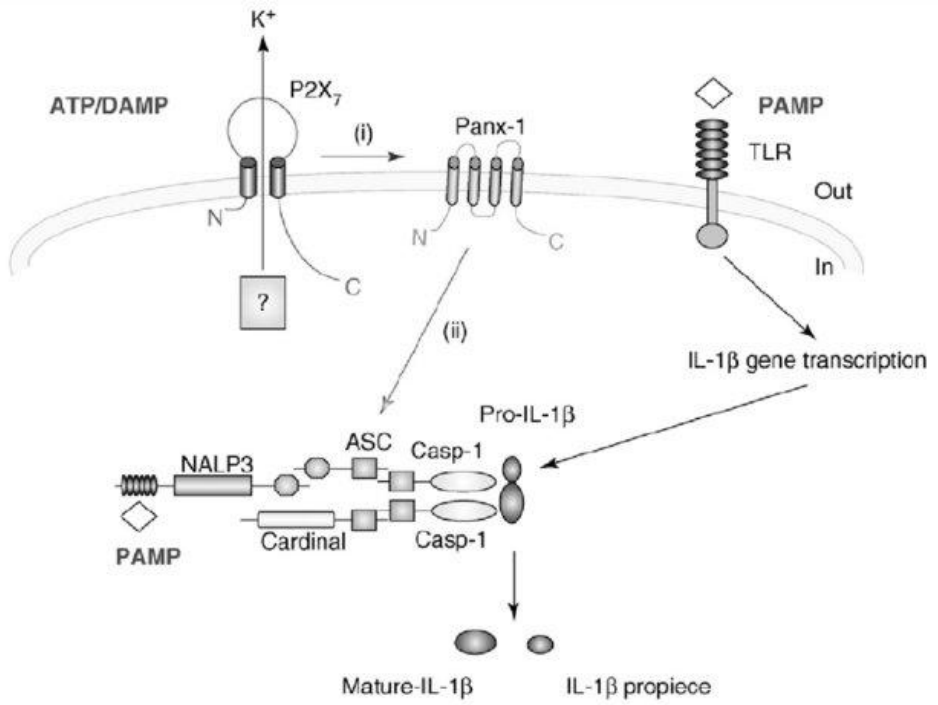

Figure 10. Sequence of events leading to P2X7 receptor and Panx1-mediated inflammasome activation [115].

P2X7R is sensitive to its agonist 2′(3′)-O-(4-Benzoylbenzoyl)-ATP (BzATP) which is 10 to 30-times more potent than ATP [116]. It has been shown that this P2X7R agonist is involved in the mechanisms that lead to the microvascular cell death associated with early changes in DR [117]. Evidence in literature has shown how the activation of P2X7R induces alterations of retinal microvasculature in an *in vitro* model consisting of pericyte-containing retinal microvessels [118]. Additionally, the activation of P2X7R along with the formation of transmembrane pores lead to increased extracellular NAD^+ causing retinal microvessels death [119]. The activation of this purinoreceptor has also been linked to retinal ganglion cell damage following an elevated intraocular pressure paralleled by an excessive release of eATP [120]. Further studies have revealed that P2X7R triggers the vascular inflammatory reactions as a consequence of an over-

expression of inflammatory mediators, contributing to retinal vascular occlusion and BRB dysfunction [121]. To date, the role played by P2X7R in activating inflammatory processes has been established and, since DR is considered an inflammatory diseases, several compounds modulating P2X7R function have been using as possible DR treatments [115].

IN VITRO MODELS OF BRB

The development and maintenance of multicellular organisms occur through the formation of physical barriers such as endothelial and epithelial biological barriers, whose aim is the separation of numerous and often very different compartments. These vital barriers possess several physiological functions that include the protection against pathogens and their toxins, the transport of ions and small molecules and, the elimination of waste products. They also provide nutrients and are involved in the fluids filtration as well as in the regulation of internal homeostasis [40]. The alteration of these biological barriers contributes to the onset and progression of several ocular diseases, such as DR. Indeed, it has been shown that the dysfunction of BRB junctional complexes contributes to the neuronal signaling damage and consequent neural apoptosis [122]. BRB plays a central role in maintaining the proper retinal environment and function and its breakdown is characterized by enhanced permeability. The latter leads to the leakage of neurotoxic compounds, infiltration of inflammatory cells, and accumulation of extracellular fluids, all these factors directly or indirectly contributing to the development of major retinal diseases characterized by an impaired visual function [123]. Furthermore, several mediators such as oxidative stress, inflammation, and hyperglycemia are involved in the increased BRB permeability and are then connected to retinal disorder, where the BRB dysfunction represents one of the main cause of vision impairment [124].

Taking the above into account, the develop of proper and representative *in vitro* models that allow to study and target BRB permeability and to test potential drugs is of utmost importance. Indeed, one of the aim of the *in vitro* models is to closely mimic the BRB environment and consequently allow to better predict the behavior of its cell components at *in vivo* level. Additionally, the investigation of the most important physiological aspects of this biological barrier could allow a better understanding of the pathophysiology as well as of the mechanisms underlying BRB dysfunction-related diseases. Notably, the BRB *in vitro* models are considered useful approaches to prevent and/or limiting vascular leakage or eventually restore the barrier function in several ocular disorders [16]. Ideally, an appropriate *in vitro* BRB model should recapitulate the BRB crucial features and integrate human cells in order to provide a more solid understanding of ocular disease biology. By the use of BRB *in vitro* models it is possible to recreate a controlled environment and investigate both the key molecular pathways and the detailed mechanisms underlying BRB alteration with reproducible conditions; the use of these systems could also make it possible the acceleration of pharmaceutical procedures through the improvement of early-stage compound screening. Furthermore, by employing the *in vitro* models, it is possible to mitigate the costs and the time-intensive ethical approval procedures typical of animal models, even though one of the drawbacks is to strictly mimic the complexity of BRB *in vivo* along with the difficulty to efficiently observe cell–cell interaction due to the thickness of the BL [125]. Since the main function of the cell barrier is the separation of two physiological compartments, the current *in vitro* models are 2-dimensional (2D) cell culture devices that rely on the compartmentalization of distinct environments by using physical interfaces supported by cells (e.g.,transwell) [126]. BRB *in vitro* systems usually use co-cultures of

endothelial cells and pericytes, cultured on permeable support membranes, with or without other cell types such as astrocytes [127]. Transwell are semipermeable filters that favor the cell growth and, at the same time, allow the passage of secrete molecules (**Figure 11**).

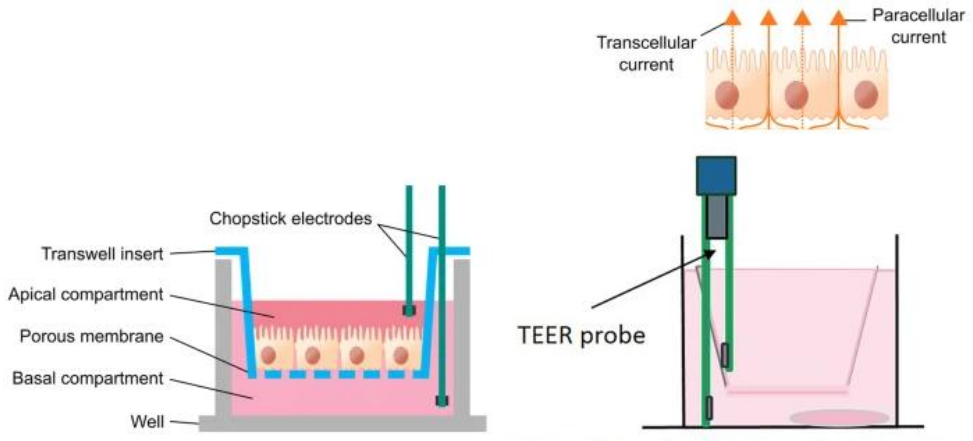

Figure 11. Use of transwell inserts and TEER to study BRB integrity. Adapted from [40,128].

These permeable supports define two compartments: the apical (upper) and the basolateral (lower) chambers. These devices also permit the cell polarization by mimicking the *in vivo* cellular scenario as well as the collection of samples from both tissue sides; the latter function gives the possibility to better elucidate the mechanisms of transport. *In vitro* models based on retinal cells co-cultures grown on transwell supports have been extensively used to deeply investigate the BRB-related diseases, such as DR [129-131]. In these *in vitro* systems, the cells are challenged with HG levels (whose concentration ranges from 25 to 50 mM) with the aim to mimic the hyperglycemic environment and then increase the expression of inflammatory mediators; two typical features of the early phase of NPDR. The measurement of BRB permeability is essential to assess the integrity and/or alteration of the barrier as well as to identify the mediators that may

contribute to its dysfunction and consequently the progression of DR. The BRB tightness can be monitored by using TEER (**Figure 11**), which involves the use of two electrodes, one placed in the upper chamber while the other is placed in the lower chamber; the results obtained by TEER measurement are expressed as Ohm×cm^2. With this non-invasive technique is also possible to determine ion selectively and trans-endothelial transports [132]. The barrier function can also be evaluated by measuring the permeability of the cells to several fluorescence dyes, such as sodium fluorescein (Na-F) and fluorescein isothiocyanate–dextran, with known molecular weight. The tracers are added in the donor chamber and quantified in the received compartment during the time. The permeability of these soluble inert tracers can be analyzed by fluorescence and/or using the following formula: P_{app} = dQ/(dT×A×C0), where dQ is the transported amount, dT the incubation time, A the surface area of membrane, and C_0 the initial concentration in the donor chamber [133].

The progresses in biomaterials and in microfabrication technologies made during the last decades allow the use of new compartmentalization approaches to develop barrier models as the“organs-on-a-chip” systems. These small microfluidic devices provide a tissue-like architecture (at the micro- and nano-levels) and the physio-chemical microenvironment of human barriers by integrating 3-dimensional (3D) cell organization, co-cultures, and perfusion [134]. These technological small systems are physiologically relevant for investigating the cellular response to treatments; furthermore, their use facilitate the predictive personalized medicine applications [135-137], even though the exactly knowledge on3D co-culture stability of multiple cell types is required.

TREATMENT STRATEGIES IN BRB-BREAKDOWN-RELATED DISEASES

For the treatment of early DR, the drug delivery through the systemic administration is limited into the intraocular tissue, since the drugs must pass the BRB in order to reach therapeutic levels in the retina [138]. The penetration of drugs and the concentration that reaches the retina is really low (less than 5% of the administered dosage) even because the drug entrance depends on several factors including the volume of drug distribution and profile, the plasma protein binding, and the relative BRB permeability. By using animal models of DR, it has been recently demonstrated that a number of drugs could reach the posterior segment of the eye at effective concentrations when administered topically, even though there are no supporting data from clinical trials [139-141].Thus, new strategies have been considered in order to obtain pharmacological therapeutic concentrations within the retina including:

1. the delivery of polymeric nanoparticles that are able to bypass all ocular barriers [142,143];
2. the coupling of drugs to vectors, as for example in the case of the addition of cell-penetrating peptides [144] and/or a hydrogel ring made of hydroxyethyl methacrylate in the eye drops, to improve the delivery of topically administered drugs into the retina/choroid, obtaining the therapeutic efficacy observed for intravitreal injection [145,146];
3. chemical modification of drugs that mimic the substrates to be taken up by receptors or particular transporters present in the BRB.

The development of new drug delivery systems led to the use of topical administration as preferred choice for the delivery of drugs into the retina in

the early phase of DR, even if eye drops are generally considered to be of limited benefit; therefore, the use of intravitreal injections, a form of administration that circumvents the BRB, seems to be the most appropriate choice. To date, only PDR stage can be pharmacologically or surgically treated including the treatment options described below.

Laser and panretinal photocoagulation

Before the advent of anti-VEGF drugs, this focal laser treatment has been considered the gold standard for the treatment of PDR. This therapeutic option is based on the use of a laser on leaking microaneurysms that reduces the leakage of blood and fluid in the eye also improving the oxygenation. It has been shown that the focal therapy reduced the risk of moderate visual loss in the three-year Early Treatment Diabetes Retinopathy Study (ETDRS) by 50%, with no deleterious effects on visual fields [147]. Another treatment used for the treatment of PDR is the panretinal photocoagulation (PRP), a scatter laser treatment that reduces the risk of severe visual loss, as observed in the case of vitreous hemorrhage [148], and represents the standard treatment for PDR patients. Although the laser therapy could lead to mild central visual loss and reduce night vision due to its destructive nature [149], it still plays an important role as a rescue therapy or adjuvant treatment [150].

Anti-inflammatory therapy

Intravitreal corticosteroids are potent anti-inflammatory agents that represent an important therapy for the treatment of vitreoretinal and inflammatory disease, including DR. Since the corticosteroids have a broad spectrum of action, they are involved in several biological processes by reducing, on a large scale, the expression of several inflammatory mediators

such as chemokines, leukostasis, and inflammatory cytokines involved in the pathogenesis of DR and DME. Corticosteroids can also inhibit intracellular pathways of inflammatory lipid mediators. Furthermore, it has been shown that corticosteroids play an important role in reassembling BRB by the increase of junctional complexes between capillary endothelial cells through the inhibition of VEGF-A activity [151]. These anti-inflammatory agents are efficient in several delivery systems and can be used in combination with macular laser therapies. Currently, the intravitreal corticosteroids used in the clinical trials for the treatment of vitreoretinal diseases include triamcinolone acetonide (TA), fluocinolone acetonide (FA), and the Food and Drug Administration (FDA)-approved dexamethasone (DEX). TA intravitreal injection has shown to reduce the thickness of the central retina in patients with DME and improve their visual acuity although, after 24 weeks of therapy, its effectiveness started to drop due to adverse ocular episodes [152]. Moreover, scientific evidence reveals that TA is also involved in the reduction of the PDR progression [153]. In pseudophakic patients, the combination of intravitreal TA with laser photocoagulation therapy has shown a comparable effectiveness to ranibizumab monotherapy [150]. Corticosteroids can be used as drug delivery implants such as the DEX intravitreal one which provides prolonged drug exposure and reduces the frequency of injections. However, despite that, these treatments have several adverse effects consisting in, just to name a few, the enhanced prevalence of glaucoma and high rate of cataract formation. Given the elevate incidence of corticosteroids side effects and the uncertainty on the efficacy of their use in the treatment of PDR, corticosteroid therapy is considered as a second-line option for patients that showed a weak response to other therapeutic options.

The inflammatory therapy also includes the use of non-steroid anti-inflammatory drugs. Since the IL-6 represents the most important pro-inflammatory cytokine present in the vitreous of DR subjects [154], it has been considered a promising target for the treatment of patients with DR. This anti-inflammatory therapy is based on the use of antibodies against both IL-6 (EBI-031) and its receptor (tocilizumab). Furthermore, an antagonist of the adhesion molecule integrin (Luminate) provided promising responses in improving visual acuity in patients with DME, even though its efficacy still needs to be further tested.

Anti-VEGF drugs

With the anti-VEGF therapy advent more opportunities have become available to prevent and/or reduce the visual impairments typical of DR and DME. VEGF plays a crucial role in the development and progression of ocular disorders since this growth factor leads to enhanced vascular permeability and angiogenesis mediators [155]. Based on the above, the use of VEGF inhibitors as pharmacologic therapy for the treatment of these diseases has captured enormous interest among the scientific community [156]. The anti-VEGF medications that have been tested in clinical trials for the treatment of DR include the FDA-approved pegaptanib, ranibizumab, aflibercept, and the off-label intravitreal bevacizumab. Among these agents, ranibizumab is the most evaluated drug in several clinical trials and was the first anti-VEGF approved by FDA. Indeed, intravitreal injections of the Fab fragment ranibizumab improved visual acuity of DME subjects by reducing macular edema [157]. Moreover, it has been shown by different studies that ranibizumab monotherapy is more effective than macular laser photocoagulation in reducing DME; these studies have also evinced no additional benefits of the combined ranibizumab/macular laser therapy [158-

160]. Differently from bevacizumab, ranibizumab has a higher affinity for VEGF-A by binding with all the VEGF-A isoforms, with the consequent reduction of VEGFR1 and VEGFR2 receptors activation [161].

Aflibercept is another anti-VEGF agent that received FDA approval for the treatment of DME in 2014 [162]. This fusion protein bears two binding domains of VEGF receptors and in its C-terminal region is located the fragment crystallizable region of human immunoglobulin [163]. Results obtained from a study aimed to evaluate the relative effectiveness and safety of aflibercept revealed that this drug achieved greater average values in improving visual acuity compared to bevacizumab and ranibizumab [164]. Unfortunately, anti-VEGF agents have a short half-life, then monthly injections are needed in order to ensure its efficacy. The most important drawback is represented by the elevate incidence of adverse effects. Additionally, even though VEGF plays a neuroprotective role, the use of high-dose of anti-VEGF drugs can be deleterious for the retina and then requires careful consideration [165].

CHAPTER 1

Int J Mol Sci. 2020 Feb 27;21(5):1636. doi: 10.3390/ijms21051636.
PMID: 32121029.

A New Human Blood-Retinal Barrier Model Based on Endothelial Cells, Pericytes and Astrocytes

Claudia G. Fresta[1], Annamaria Fidilio[2], Giuseppe Caruso[3], Filippo Caraci[2,3], Frank J. Giblin[4], Gian M. Leggio[1,5], Salvatore Salomone[1,5], Filippo Drago[1,5] and Claudio Bucolo[1,4,5]

[1] Department of Biomedical and Biotechnological Sciences, School of Medicine, University of Catania, Italy
[2] Department of Drug Sciences, University of Catania, Catania, Italy
[3] Oasi Research Institute - IRCCS, Troina, Italy
[4] Eye Research Institute, Oakland University, Rochester, Michigan, USA
[5] Center for Research in Ocular Pharmacology-CERFO, University of Catania, Catania, Italy

Abstract

Blood-retinal barrier (BRB) dysfunction represents one of the most significant changes occurring during diabetic retinopathy. We set up a high-reproducible human-based *in vitro* BRB model using retinal pericytes, retinal astrocytes, and retinal endothelial cells in order to replicate the human *in vivo* environment with the same numerical ratio and layer order. Our findings showed that high glucose exposure elicited BRB breakdown, enhanced permeability and reduced the levels of junction proteins such as ZO-1 and VE-cadherin. Furthermore, an increased expression of pro-inflammatory mediators (IL-1β, IL-6) and oxidative stress-related enzymes (iNOS, Nox2) along with an increased production of reactive oxygen species were observed in our triple co-culture paradigm. Finally, we found an activation of immune response-regulating signaling pathways (Nrf2 and HO-1). In conclusion, the present model mimics the closest human *in vivomilieu* providing a valuable tool to study the impact of high glucose in the retina and to develop novel molecules with potential effect on diabetic retinopathy.

Keywords: diabetic retinopathy; blood-retinal barrier; astrocytes; oxidative stress; inflammation.

Introduction

Blood-retinal barrier (BRB) is crucial for proper vision and the loss of the integrity of this physical barrier greatly contributes to the vision loss in retinal diseases such as diabetic retinopathy. The BRB consists of two compartments: inner BRB, formed by adherents and tight junctions between adjacent retinal capillary endothelial cells, and outer BRB, composed of retinal pigment epithelial cells, representing a highly selective barrier for molecules and solutes moving from the choroid into the retina [1,2]. With regard to the inner BRB, the retinal endothelial cells are covered by pericytes, which, in turn, are supported by glial cells such as astrocytes. The latter are involved in the maintenance of both retinal neurons and blood vessels and are able to modulate the BRB function through the release of trophic factors and antioxidants in the retinal microenvironment [3]. Astrocytes play also an important role in the maintenance of the BRB since their processes enfold retinal endothelial cells, with a more defined maturation of the tight junction proteins [1,4].

The integrity of BRB is maintained by endothelial tight and adherence junctions, which create a very tight monolayer, so that macromolecules cannot easily penetrate between the cells forming the retinal unit [5]. The loss of tight junctions, connected to the actin cytoskeleton through zonula occludens-1 (ZO-1), leads to the disruption of the inner barrier[6]. The vascular endothelial (VE)-cadherin, a member of the super-family of cadherins, acts as a plasma membrane attachment site for the cytoskeleton and plays a pivotal role in the regulation of endothelial cell behavior [7,8]. The integrity of both classes of the above-mentioned junctional proteins is crucial for the normal settlement of the barrier functionality [9].

Hyperglycemia can contribute to the BRB breakdown that is the hallmark of diabetic retinopathy associated by pericytes death, and endothelial junctions loss [6,10,11]. It is worth of note that, in the last decade, diabetic retinopathy has been shifted from "microvascular disease" towards "neurovascular disease" [12].

High glucose conditions alter several cellular functions affecting, among others, intracellular calcium levels, NADPH oxidase (Nox2) activity, and nuclear factor kappa-light-chain-enhancer of activated B cells (NF-κB) signaling [13-15]. Hyperglycemia has also been linked to the over production of inflammatory mediators (e.g. IL-1β, TNF-α, IL-6) and reactive oxygen species (ROS), with a consequent increase in inflammation and oxidative stress [16-20].

Increased levels of reactive oxygen (ROS) and nitrogen (RNS) species, including nitric oxide ($NO^{\bullet}$) and superoxide anion ($O_2^{-\bullet}$), have been observed in the retina of diabetic rats [21-23]. Under pathological conditions inducible nitric oxide synthase (iNOS) and NADPH oxidase (Nox), responsible for NO and $O_2^{-\bullet}$production respectively [24,25], are over-activated in several cell types including endothelial and immune cells [24,26]. The iNOS-mediated NO production has been associated with the induction of early vascular changes [27], while Nox2-derived ROS are involved in retinal inflammation [28-30]. Furthermore, an overproduction of ROS and RNS has been correlated with the BRB breakdown occurring in the early stage of diabetic retinopathy [31].

An important mechanism in the cellular defense against oxidative stress is represented by the activation of nuclear factor (erythroid-derived 2)-like 2 (Nrf2) pathway, which in turn regulates ROS-sensitive genes including heme oxygenase-1 (HO-1) [32-34]. With specific regard to astrocytes, Nrf2 pathway has been shown to play a key role in counteracting oxidative stress-induced cell death [35].

In vitro models of BRB provide a valuable tool to better understand the retinal pathophysiology as well as the trafficking occurring in the barrier [36,37]. In particular, co-cultures of BRB are widely used in order to clarify the cross-talk between the cells of the retinal unit. According to Nakagawa *et al.*, *in vitro* models of rat blood brain barrier (BBB) in which endothelial cells and pericytes are co-cultured on opposite sides of a transwell insert and astrocytes are located at the bottom of the culture dish well represent the *in vivo* anatomical position of the cells at the BBB[38] that, as know, it shares histological and functional similarities with the BRB [39]. Recently, Wisniewska-Kruk *et al.*[40] set up a BRB based on a triple co-culture, even though they did not used human cells. These authors employed bovine endothelial cells, bovine pericytes and rat astrocytes, therefore a bit far from human BRB. In order to set up a better BRB *in vitro* model closer to human *in vivo* environment, we characterize an *in vitro* human primary culture based on triple co-culture BRB model using human retinal endothelial cells, human retinal pericytes, and human retinal astrocytes, keeping the same cellular layer order present in human, and the same numerical ratio.

In the present study, we first evaluated barrier tightness and paracellular permeability of our BRB system by measuring the trans-epithelial electrical resistance (TEER) and the flux of the water-soluble inert tracer, sodium fluorescein (Na-F). Next, we examined the functional integrity of the BRB by immunofluorescence staining. The effects of high glucose exposure were also assessed by ROS production, pro-inflammatory mediators, and oxidative stress

related genes by quantitative real time PCR (qRT-PCR). Lastly, we investigated the effect of high glucose exposure on NF-κB, Nrf2 as well as on its downstream gene heme oxygenase 1 (HO-1) by western blot analysis.

Results

BRB integrity

The effect of high glucose conditions on BRB integrity were first assessed by performing TEER measurements. As shown in Figure 1 the permeability was significantly altered by high glucose conditions compared to normal glucose (control) conditions at both time points. A reduction of 41% was observed after 24 h ($p < 0.0001$ vs. normal glucose), that further increased (-52%) after 48 h of treatment.

Paracellular permeability was assessed in cells subjected to normal or high glucose conditions for 48 hours using the fluorescent marker Na-F (Figure 2). As expected, an inverse correlation was observed between the TEER values and the Na-F permeability (Figure 2).

Unlike the difference in fluorescence due to Na-F passage (permeability) measured in the two different media collected by cells cultured under normal and high glucose conditions after 5 min (+4.9%, not significant), significant differences were observed after 15 min and 30 min ($p < 0.01$ and $p < 0.05$ vs. normal glucose, respectively).

ZO-1 and VE-cadherin levels

Figure 3 depicts the results of the immunocytochemistry analysis performed in the endothelial cells monolayer, part of the in vitro BRB model, grown under normal and high glucose conditions.

The presence of ZO-1 was significantly reduced in cells exposed to high glucose (Figure 3A,ii) compared to normal glucose conditions ($p < 0.001$; Figure 3A,i), where a distinct ZO-1 staining at the cell-cell borders was observed. The quantification of ZO-1 intensity, measured as fluorescence arbitrary units (AUs), under both normal and high glucose conditions is shown in Figure 3B. It is worthy to note that high glucose exposure affected the presence of VE-cadherin in a similar way to ZO-1. In fact, the staining of VE-cadherin appeared to be markedly reduced and discontinuous in endothelial cell monolayers under high glucose conditions (Figure 3C,ii), while endothelial cells under normal glucose conditions show a continuous Ve-cadherin brush border (Figure 3C,i). The quantification of VE-cadherin intensity (AU) under both normal and high glucose conditions, clearly

showing the significant difference ($p < 0.001$) between both conditions, is reported in Figure 3D.

Biomarkers of inflammation and oxidative stress

Astrocytes are able to modulate the BRB function through the release of trophic factors and antioxidants in the retinal microenvironment [3]. The over-activation as well as the dysfunction of astrocytes represent key contributors to the BRB injury and other retinal vascular diseases [41]. Since high glucose conditions have been shown to compromise retinal astrocytes function [17,42] and to be connected to the inflammatory cytokine secretion and to the induction of neuronal death [43], we measured the expression of two well-known pro-inflammatory cytokines (IL-6 and IL-1β) in astrocytes, part of the in vitro BRB model, grown under normal as well as high glucose conditions. As clearly shown in Figure 4A,B, the expression levels of both pro-inflammatory cytokines were significantly increased by high glucose conditions compared to normal glucose conditions ($p < 0.01$ for IL-6; $p < 0.05$ for IL-1β).

In order to assess whether the ability of high glucose conditions to enhance IL-6 and IL-1β expression level is also linked to oxidative stress, we measured the gene expression of enzymes related to the oxidative stress as well as the total ROS production in astrocytes. High glucose conditions significantly raised both iNOS ($p < 0.001$; Figure 5A) and Nox2 ($p < 0.01$; Figure 5B) expression levels compared to normal glucose conditions.

As shown in Figure 5C, high glucose conditions were also responsible for a higher accumulation of intracellular ROS in astrocytes compared to normal glucose conditions ($p < 0.01$).

NF-κB, Nrf2, and HO-1 levels

To address whether the propensity to increase inflammation and oxidative stress was also connected to other molecular events, the effect of high glucose conditions on pNF-κB and Nrf2 nuclear translocation as well as HO-1 expression was studied in astrocytes. Compared to normal glucose levels, high glucose conditions promoted an increase in the nuclear protein fraction of pNF-κB ($p < 0.05$; Figure 6A) and Nrf2 ($p < 0.05$; Figure 6B) nuclear translocation, while, as expected, an opposite situation was observed for the cytoplasmic protein fractions ($p < 0.05$ for both of them; Figure 6A-B).

It is also worth underlining that the total levels of both proteins (NF-κB and Nrf2),were not affected by high glucose (data not shown). Figure 6C shows the significant increment in

HO-1 protein levels observed in astrocyte extracts obtained by cells challenged with high glucose conditions compared to normal glucose conditions ($p < 0.05$).

Discussion

Cell culture models can be simply set up and represent valuable tools to investigate several biological phenomena occurring on complex systems such as BRB and BBB, under physiological and pathological conditions. Unfortunately, so far there are no BRB triple co-culture model that used human retinal cells. Therefore, the first aim of this study was to characterize a new and reproducible in vitro human primary culture based triple co-culture BRB model based on retinal perycites, retinal astrocytes, and retinal endothelial cells, mimicking the human milieu [44]. Keeping in mind this goal, we tried to maintain the same position and order of the cellular layers in human. We also investigated the alterations of the inner BRB responsible for the biological retinal modifications occurring in ocular pathological conditions such as diabetic retinopathy. Our BRB co-culture system was build-up by placing endothelial cells and pericytes on the opposite sites of a porous membrane of a trans-well insert, and astrocytes on the luminal compartment of the well (Figure 7).

Once our BRB system has been assembled, we evaluated: i) the overall barrier tightness and paracellular permeability; ii) the distribution of junctional adhesion molecules in endothelial cells; iii) the expression of genes related to inflammation and oxidative stress as well as total ROS production in astrocytes; iiii) the protein expression levels of elements of immune response-regulating signaling pathways in astrocytes. In order to better understand the BRB alterations occurring in diabetic retinopathy, we evaluated the above-mentioned paramenters in our system under normal (5 mM) and high (40 mM) glucose conditions.

The structural integrity variations of the in vitro BRB model following high glucose insult were assessed after 24 and 48 h, since a well-defined BRB damage can be detected at these time points [45]. A significant decrease of TEER values was observed after both 24 (-41%) and 48 (-48%) h challenge with high glucose exposure as compared with control cells (normal glucose) (Figure 1). The loss of BRB integrity was further confirmed by a significant increase in Na-F permeability from the apical to the basolateral compartment of the insert (Figure 2). The results of the experiments showed in Figure 1 and Figure 2 indicates a leaky retinal barrier under high glucose conditions, in accordance to what has been observed in patients with diabetic retinopathy [46].

Among the tight junction-associated proteins, ZO-1 plays a key role in BRB integrity and its deficiency has been connected to a setback in the formation of the tight junction protein

complex [47,48] and an increased permeability of the BRB in patients affected by diabetic retinopathy [49]. In accordance with the aforementioned, the challenge of the endothelial cells, part of our BRB model, with high glucose exposure caused a robust decrease in terms of ZO-1 protein levels (Figure 3B) as depicted by a discontinuous brush border at the cell-cell contact (Figure 3A,ii), very different from the distinct ZO-1 staining observed at the cell-cell borders under normal glucose conditions (Figure 3A,i). We also investigated the VE-cadherin modifications, another protein implicated in the BRB breakdown during diabetic retinopathy [50,51]. As observed for ZO-1, the immunocytochemistry analysis carried out on endothelial cell monolayers challenged with high glucose showed an evident alteration of organization pattern of VE-cadherin staining (Figure 3C,ii) that is significantly different compared to normal glucose conditions (Figure 3D). Overall, these results showed that high levels of glucose lead to mechanical disruption of both adherents and tight junction proteins in BRB and then to the loss of cell-to-cell contactin endothelial cell monolayers.

During both early and late stages of diabetic retinopathy, inflammation and oxidative stress take place [52]. It is well known that astrocytes, the major glial cell within the central nervous system, participate in different pathophysiological mechanisms by releasing pro- and anti-inflammatory mediators [53,54]. These cells also play a central role in the development of the retinal vessells and in the maintenance of BRB [35]. As previously mentioned, high glucose conditions negatively influence the integrity of the BRB and this phenomenon is due, at least in part, to the ability of high glucose to compromise retinal astrocytes function as well as their morphology and viability [17,42]. Nevertheless, the precise molecular mechanisms leading to astrocytes dysfunction is currently poorly understood and under debate. With the aim to better clarify the role of astrocytes in the context of BRB, we analyzed the expression level of IL-1β, IL-6, iNOS, and Nox2 mRNAs as well as the total ROS production in astrocytes exposed to high glucose levels. Our results showed a significant increase in the expression levels of the above-mentioned pro-inflammatory molecules (IL-1β, IL-6) (Figure 4) and pro-oxidant (iNOS, Nox2) (Figure 5A,B) mediators coupled to the increased production of ROS (Figure 5C). The present data clearly demonstrate that high glucose levels boost the pro-oxidant and pro-inflammatory behavior of astrocytes, part of our BRB system. These results are in agreement with previous findings showed the link between the inflammatory mediators and the up-regulation of iNOS and Nox2 in in vivo models of diabetic retinopathy [55,56].

Additionally, several papers have shown that hyperglycemia-induced ROS production plays an important role in different pathological conditions such as diabetic retinopathy [57-59]. Inflammation and oxidative stress may be related to pro-inflammatory and pro-oxidant mediators increase or to a deficiency and/or impairment of endogenous defense signaling pathways. For this reason the effects of high glucose on NF-κB, Nrf2, and HO-1 protein expression levels in astrocytes were also investigated. By protein extracts of astrocytes, we found that high glucose exposure significantly promoted the nuclear translocation and the following activation of pNF-κB and Nrf2, also enhancing HO-1 expression (Figure 6), compared to normal glucose conditions. This finding is in line with previous data pointing out that: 1) NF-κB represents one of the most common intracellular targets of hyperglycemia [60] and its translocation to the nucleus regulates the expression of several factors including pro-inflammatory cytokines [61]; 2) Nrf2, a transcription factor that is involved in the regulation of ROS-sensitive genes during oxidative stress events, translocates to the nucleus [62] allowing the transcription of genes directly involved in the protection against oxidative stress such as HO-1 [63]. The latter has been shown to exert a protective role in diabetic retinopathy [64].

Materials and Methods

Materials and reagents

Human retinal endothelial cells, human retinal pericytes, human retinal astrocytes, endothelial cell medium (ECM), fetal bovine serum (FBS), endothelial cell growth supplement (ECGS), pericyte cell medium (PM), pericyte supplement factor (PGS), astrocyte cell medium (AM), astrocytes supplement factor (AGS), polylysine (PLL), and penicillin-streptomycin (P/S) were purchased from INNOPROT (Derio, Bizkaia, Spain). Cell culture inserts, 75 cm^2 polystyrene culture flasks, 12-wells plate, 96-wells plate, and rat-tail collagen type I were obtained from Corning Inc. (Corning, NY, USA). Paraformaldehyde (PFA), normal goat serum (NGS), Triton-X 100, Tween 20, phosphatases and proteases inhibitors, RIPA buffer, D-Glucose, and tris buffered saline (TBS) were all supplied by Sigma–Aldrich (St. Louis, MO, USA). Cy3 goat anti-mouse secondary antibody (ab97035), FITC-conjugated goat anti-rabbit (ab97050), anti-von Willebrand factor (ab6994) and anti-HO-1 (ab13248) primary antibodies, and 2',7'-dichlorofluorescin diacetate (DCFDA) - Cellular ROS Assay Kit were purchased from Abcam (Cambridge, UK). Odissey®blocking buffer (PBS) and IRDye® 800CW

(92632211) or 680LT (92668020) secondary antibodies were obtained from LiCor (Lincoln, USA). Anti-VE-cadherin (2500), anti-Phospho-NF-κB p65 (anti-pNFκB) (3033), anti-NFκB (8242), and anti-Nrf2 (12721) primary antibodies were supplied by Cell Signaling (Leiden, Netherlands). Anti-ZO-1 primary antibody (61-7300), mounting medium, TRIzol reagent, SuperScript III first-strand synthesis system for RT-PCR, Pierce™ BCA protein assay kit, Ne-PER nuclear and cytoplasmic extraction reagents, NuPage™ 4-12% bis-tris gel, and 4',6-diamidine-2'-phenylindole dihydrochloride (DAPI) (D1306) were purchased from ThermoScientific (Waltham, MA USA). Sodium fluorescein (Na-F), anti-β-actin (sc-47778) and anti-lamin B (sc-365214) primary antibodies were obtained from Santa Cruz Biotechnology, Inc. (Dallas, Texas, USA). Anti-GFAP primary antibody (NB120-10062) was supplied by Novus Biologicals (Milan, Italy). Anti-α-SMA primary antibody (M0851) was purchased from Dako (Santa Clara, California, USA).

Nitrocellulose blotting membrane was purchased from GE Healthcare Life Sciences (Amersham, UK). LightCycler®fast start DNA master SYBR Green I was purchased from Roche Diagnostics (Indianapolis, IN, USA). QuantiTect primer assays were purchased from Qiagen (Hilden, Germany).

Cells

Endothelial cells were grown as previously described [65]. Briefly, the cells were maintained in ECM containing 5% FBS, 1% penicillin-streptomycin, and 1% ECGS under a humidified atmosphere (95% air/5% CO_2 at 37 °C). Endothelial cells were routinely seeded in a 75 cm^2 polystyrene culture flask, split at a confluence of 80–90%, and used for the BRB in vitro model assembly. Cell passage number was always between 2 and 4.

Pericytes were fed with PM supplemented with 100 U/ml penicillin, 100 μg/ml streptomycin, 2% FBS, and 1% PGS. The cells were cultured at 37 °C and in humidified atmosphere with 95% air/5% CO_2. As in the case of endothelial cells, pericytes were passaged after reaching 80–90% of confluence and used for the BRB in vitro model assembly. Cell passage number was always between 2 and 4.

Astrocytes were seeded in PLL-coated 75 cm^2 polystyrene culture flasks and cultured in AM enriched with 100 U/ml penicillin, 100 μg/ml streptomycin, 2% FBS, and 1% AGS. The cells were maintained in a humidified environment at 37 °C and 95% air/5% CO_2 and passaged every 3–5 days to avoid cell overgrowth. Astrocytes following the first passage were used for the BRB in vitro model assembly.

BRB model set up

In order to generate the in vitro BRB model, both inserts and 12-well plates were coated with PLL (2 μg/cm^2) for 1 h at 37 °C followed by 3 washing steps: two with water and one with PBS. Pericytes were then seeded (1.5 × 10^4 cells/cm^2) on the bottom side of polycarbonate inserts and placed upside down. After 4 h of incubation, the inserts were inverted and inserted into 12-well plates containing pericyte medium. During the same day, astrocytes were plated (7.5 × 10^4 cells/cm^2) on 12-well plates pre-coated with PLL. The cells were allowed to adhere firmly (overnight, 37 °C in 95% air/5% CO_2). The following day, the inserts containing pericytes were positioned into the 12-well plates holding astrocytes, while endothelial cells (7.5 × 10^4 cells/cm^2) were seeded on the luminal compartment of the inserts having pericytes on the other side. The three cell lines were co-cultured in a humidified environment at 37 °C and 95% air/5% CO_2 with a medium consisting of a mixture of the three cell lines' media (1:1:1). Primary cells were co-culture at a ratio of 1:5:5 for pericytes, endothelial cells, and astrocytes, respectively, according to Bonkowski et al. [66], in order to replicate the in vivo numerical ratio. Under the above-mentioned conditions, the in vitro BRB model was established within 3 days after setting of the cells. The day of the experiment, the medium was added of glucose (at the final concentration of 40 mM) for 48 h, while the co-culture medium containing a physiological glucose concentration (5 mM) was used as control, as recently described elsewhere [67].
Figure 7 depicts the experimental procedure followed for the in vitro human primary culture based triple co-culture BRB model assembly.

BRB integrity assessment

The barrier integrity of the established co-culture was evaluated by TEER measurements using a Millicel-Electrical Resistance System (ERS2) (Merck, Millipore, Burlington, MA, USA) as described elsewhere [68]. Final TEER values of coated filters containing cells, shown as ω × cm^2, were calculated by subtracting the TEER values of coated cell-free filters. The results, recorded at 0 (T0), 1 (T24), and 2 (T48) after challenging the cells with high glucose conditions, were multiplied for the surface area (1.12 cm^2). A 20 minutes equilibration period at room temperature (RT) was performed prior to the first measurement. TEER values were obtained from five independent experiments.
In order to evaluate the BRB paracellular permeability, we measured the apical-to-basolateral movements of Na-F across endothelial cells monolayer, subjected to normal or high glucose conditions for 48 hours, as previously described [38]. After 5, 15, and 30 min

the medium from the lower chamber was collected and the quantification of fluorescence (Na-F: excitation 480 nm, emission 535 nm) was carried out using a Varioskan Flash microplate reader (Thermo Scientific, MA, USA).

Immunofluorescence staining

All necessary information of the experimental conditions of the immunofluorescence staining (primary antibodies list, source, dilution, function/characteristics) are reported in Table 1.

Endothelial cells and pericytes were characterized by their positive immunostaining for von Willebrand factor and α-SMA, respectively, as previously described [69] (Supplementary Figure 1A,B).

In order to characterize the astrocytes, these cells were grown on PLL-coated coverslip, fixed by using 4% PFA for 20 min at 4 °C, washed three times (5 min each) with 10 mM PBS, and permeabilized with a 10 mM PBS solution containing 5% NGS and 0.1% Triton-X 100 for 30 min at RT. Next, cells were incubated overnight, at 4 °C, with anti-GFAP primary antibody (dilution 1:200). The day after, cells were washed three times with 10 mM PBS and incubated for 1 h, at RT, with Cy3 goat anti-mouse secondary antibody (1:300). As a final step, cell nuclei were stained by using DAPI (1:10000) (10 min). Cell imaging of GFAP-positive astrocytes (Supplementary Figure 1C) was performed by using a fluorescence microscope Zeiss Observer Z1 equipped with the Apotome.2 acquisition system connected to a digital camera (Carl Zeiss, Oberkochen, Germany).

Immunohistochemistry analysis of ZO-1 and VE-cadherin were carried on endothelial cells under normal and high glucose conditions. In the case of ZO-1, endothelial cell monolayers were washed three times with 10 mM PBS, fixed with ice-cold acetone (100%) at -20 °C for 15 min followed by incubation with ice-cold methanol (100%) at -20 °C for 20 min. Cells were then washed three times with 10 mM PBS and permeabilized with a 10 mM PBS solution containing 5% NGS and 0.1% Triton-X 100 for 10 min at RT. Fixed cells were incubated overnight at 4 °C with ZO-1 antibody (1:100). Washing steps were performed before and after 1 h of incubation with FITC-conjugated goat anti-rabbit antibody (1:300). As a final step, cell nuclei were stained by using DAPI (1:10000) (10 min).

To assess VE-cadherin, endothelial cells were fixed in 4% PFA and permeabilized with 0.3% Triton-X 100 at RT for 5 min followed by three washing steps. After a blocking step with 1% BSA/10 mM PBS for 1 h at RT, cells were incubated overnight at 4 °C with anti-

VE-cadherin antibody (1:100) previously diluted in 10 mM PBS containing 1% BSA. The following day, the coverslips were incubated with FITC-conjugated goat anti-rabbit (1:300) for 1 h followed by PBS washes.

Semi-quantitative evaluation of ZO-1 and VE-cadherin expression was carried out as previously described [67], with slight modifications. Coverslips were mounted on glass slides by using mounting medium and analyzed with a Leica TCS SP8 confocal laser scanning microscope (Leica Biosystems, Wetzlar, Germany) or Nikon A1RHD25confocal microscope (Nikon Instruments S.p.A, Florence, Italy). Images for ZO-1 and VE-cadherin immunostaining were acquired at 20× or 60× magnification. The images were analyzed by the use of ImageJ [70] or NIS-Elements software programs. Measurements of average gray scale intensity were carried out at the cell-cell interface in 7 random areas of 7 image rotations. More than 30 cells for each condition were analyzed.

Measurement of intracellular ROS in astrocytes, part of the in vitro BRB model, was performed by using DCFDA Cellular ROS Assay Kit according to the manufacturer's recommendations. Astrocytes, challenged with high glucose conditions for 48 h, were stained with DCFDA (25 µM, for 45 min at 37 °C), then fluorescence at 485 nm excitation/535 nm emission was measured by employing a Varioskan Flash microplate reader to determine total ROS formation. The final fluorescent intensity, after background subtraction, was then normalized to the fluorescent intensity of control cells (normal glucose conditions).

qRT-PCR

Total RNA was extracted from astrocytes, part of the in vitro BRB model, in TRIzol reagent according to the instructions provided by the manufacturer, and re-dissolved in RNAse-free water. Reverse transcription of RNA (2 µg) into cDNA was accomplished by using SuperScript III [68]. Quantitative real-time PCR was carried out to determine the expression levels of four selected genes by employing LightCycler® FastStart DNA Master SYBR Green Iin a final volume of 20 µL (0.5 µM primers, 1.6 mM Mg^{2+}, 1X SYBR Green I).

The QuantiTect Primer Assays (Qiagen) used for gene expression analysis are enlisted in Table 2, with the exception of IL-1β (forward: 5'-AGC TAC GAA TCT CCG ACC AC-3'; reverse: 5'-CGT TAT CCC ATG TGT CGA AGA A-3') and 18S rRNA (forward: 5'-AGT CCC TGC CCT TTG TAC ACA-3'; reverse: 5'-GAT CCG AGG GCC TCA CTA AAC-3') that were purchased by Eurofins MWG Synthesis GmbH (Ebersberg, Germany).

Negative controls (no template control, NTC) were included in each assay. Amplifications were carried out in a Light Cycler 1.5 instrument (Roche Diagnostics, Indianapolis, IN, USA). The relative RNA expression level for each gene of interest was calculated using the $2^{-\Delta\Delta CT}$ method [76] by the comparison of the threshold cycle (CT) value of the gene of interest to the CT value of the selected internal control (18S rRNA gene).

Western Blot Analysis

HO-1 protein expression was analyzed by the evaluation of protein concentration in astrocytes, part of the in vitro BRB model, challenged with high glucose conditions for 48 h. Cells were collected and subsequently lysed in RIPA buffer supplemented by phosphatases and proteases inhibitors (1:100). Protein quantification was performed using Pierce™ BCA Protein Assay Kit, according to the manufacturer's instructions.

The activation of both Nrf2 and NF-κB on astrocytes under the same experimental conditions described above was measured by employing Ne-PER Nuclear and Cytoplasmic Extraction Reagents as previously described in details [77].

Approximately 25 µg of total, cytoplasmic, and nuclear proteins were separated on 4-12% tris-glycine gels and transferred to nitrocellulose membranes. The membranes were blotted with anti-HO-1 (1:500), anti-pNFκB (1:1000), anti-NFκB (1:1000), anti-Nrf2 (1:1000), anti-β-actin (1:1000), and lamin B (1:1000) primary antibodies in blocking buffer at 4 °C overnight. The day after the membranes were washed three times in TBS/Tween 20 0.1%, followed by incubation for 1 h with IRDye® 800CW or 680LT secondary antibodies (1:15000). Bands were visualized using Odyssey® Infrared Imaging system (LI-COR Biosciences, Lincoln, NE, USA) and the densitometric analysis were performed by Image J software.

Statistical analysis

Statistical analysis was performed by using GraphPad Prism 7 (GraphPad Software, La Jolla, CA). Student's t-test was used to assess the statistical differences between two experimental groups.Two-way analysis of variance (ANOVA), followed by Bonferroni's post hoc test, was used for multiple comparisons. Only two-tailed p-values of less than 0.05 were considered statistically significant. All experiments were repeated at least three times and the data are reported as mean ± standard deviation (SD).

Conclusions

We developed, the first high-reproducible in vitro BRB model mimicking the inner retinal barrier, entirely based on human cells (retinal perycites, retinal astrocytes, and retinal endothelial cells). The effects of high glucose exposure were investigated in our BRB model. High glucose elicited remarkable changes in our triple co-culture system: first of all, the high glucose significantly reduced ZO-1 and VE-cadherin in endothelial cells decreasing BRB integrity; secondly, high glucose elicited genes expression related to inflammation and oxidative stress as well as antioxidant response. Taken together, the present findings show that our in vitro paradigm mimics the in vivo human inner BRB suggesting that this model represents a useful tool for drug discovery process in ocular pharmacology.

Author Contributions: Conceptualization, C.G.F., A.F. and C.B.; Validation, C.G.F., A.F. and G.C.; Formal Analysis, C.G.F., A.F. and G.C.; Investigation, C.G.F., A.F. and G.C.; Resources, F.C., G.M.L., S.S., F.D. and C.B.; Data Curation, C.G.F., A.F. and G.C.; Writing – Original Draft Preparation, C.G.F., A.F. and G.C.; Writing – Review & Editing, C.G.F., A.F., G.C., F.C., F.J.G., G.M.L., S.S., F.D. and C.B.; Visualization, C.G.F., A.F. and G.C.; Supervision, C.B.; Project Administration, F.C., G.M.L., S.S., F.D. and C.B.; Funding Acquisition, F.C. and C.B..

Funding: This research was funded by National Grant PRIN 2015JXE7E8 from Ministry of Education, University and Research (MIUR), "Piano Triennale per la Ricerca – Linea Intervento 2, University of Catania, Italy", and Italian Ministry of Economic Development (MISE) PON-Innovative PhD Program XXXIII code E37H18000340006.

Conflicts of Interest: The authors declare no conflict of interest.

References

1. Klaassen, I.; Van Noorden, C.J.; Schlingemann, R.O. Molecular basis of the inner blood-retinal barrier and its breakdown in diabetic macular edema and other pathological conditions. *Prog Retin Eye Res* **2013**, *34*, 19-48.
2. Bucolo, C.; Drago, F.; Lin, L.R.; Reddy, V.N. Sigma receptor ligands protect human retinal cells against oxidative stress. *Neuroreport* **2006**, *17*, 287-291.

3. Abbott, N.J.; Ronnback, L.; Hansson, E. Astrocyte-endothelial interactions at the blood-brain barrier. *Nat Rev Neurosci* **2006**, *7*, 41-53.
4. Roy, S.; Kim, D.; Lim, R. Cell-cell communication in diabetic retinopathy. *Vision Res* **2017**, *139*, 115-122.
5. Rangasamy, S.; McGuire, P.G.; Das, A. Diabetic retinopathy and inflammation: Novel therapeutic targets. *Middle East Afr J Ophthalmol* **2012**, *19*, 52-59.
6. Leal, E.C.; Martins, J.; Voabil, P.; Liberal, J.; Chiavaroli, C.; Bauer, J.; Cunha-Vaz, J.; Ambrosio, A.F. Calcium dobesilate inhibits the alterations in tight junction proteins and leukocyte adhesion to retinal endothelial cells induced by diabetes. *Diabetes* **2010**, *59*, 2637-2645.
7. Carmeliet, P.; Lampugnani, M.G.; Moons, L.; Breviario, F.; Compernolle, V.; Bono, F.; Balconi, G.; Spagnuolo, R.; Oosthuyse, B.; Dewerchin, M.; Zanetti, A.; Angellilo, A.; Mattot, V.; Nuyens, D.; Lutgens, E.; Clotman, F.; de Ruiter, M.C.; Gittenberger-de Groot, A.; Poelmann, R.; Lupu, F.; Herbert, J.M.; Collen, D.; Dejana, E. Targeted deficiency or cytosolic truncation of the ve-cadherin gene in mice impairs vegf-mediated endothelial survival and angiogenesis. *Cell* **1999**, *98*, 147-157.
8. Shay-Salit, A.; Shushy, M.; Wolfovitz, E.; Yahav, H.; Breviario, F.; Dejana, E.; Resnick, N. Vegf receptor 2 and the adherens junction as a mechanical transducer in vascular endothelial cells. *Proc Natl Acad Sci U S A* **2002**, *99*, 9462-9467.
9. Diaz-Coranguez, M.; Ramos, C.; Antonetti, D.A. The inner blood-retinal barrier: Cellular basis and development. *Vision Res* **2017**, *139*, 123-137.
10. Navaratna, D.; McGuire, P.G.; Menicucci, G.; Das, A. Proteolytic degradation of ve-cadherin alters the blood-retinal barrier in diabetes. *Diabetes* **2007**, *56*, 2380-2387.
11. Vinores, S.A.; Xiao, W.H.; Aslam, S.; Shen, J.; Oshima, Y.; Nambu, H.; Liu, H.; Carmeliet, P.; Campochiaro, P.A. Implication of the hypoxia response element of the vegf promoter in mouse models of retinal and choroidal neovascularization, but not retinal vascular development. *J Cell Physiol* **2006**, *206*, 749-758.
12. Heng, L.Z.; Comyn, O.; Peto, T.; Tadros, C.; Ng, E.; Sivaprasad, S.; Hykin, P.G. Diabetic retinopathy: Pathogenesis, clinical grading, management and future developments. *Diabet Med* **2013**, *30*, 640-650.

13. Song, J.H.; Jung, S.Y.; Hong, S.B.; Kim, M.J.; Suh, C.K. Effect of high glucose on basal intracellular calcium regulation in rat mesangial cell. *Am J Nephrol* **2003**, *23*, 343-352.
14. Gray, S.P.; Di Marco, E.; Okabe, J.; Szyndralewiez, C.; Heitz, F.; Montezano, A.C.; de Haan, J.B.; Koulis, C.; El-Osta, A.; Andrews, K.L.; Chin-Dusting, J.P.; Touyz, R.M.; Wingler, K.; Cooper, M.E.; Schmidt, H.H.; Jandeleit-Dahm, K.A. Nadph oxidase 1 plays a key role in diabetes mellitus-accelerated atherosclerosis. *Circulation* **2013**, *127*, 1888-1902.
15. Andreasen, A.S.; Kelly, M.; Berg, R.M.; Moller, K.; Pedersen, B.K. Type 2 diabetes is associated with altered nf-kappab DNA binding activity, jnk phosphorylation, and ampk phosphorylation in skeletal muscle after lps. *PLoS One* **2011**, *6*, e23999.
16. Geraldes, P.; Hiraoka-Yamamoto, J.; Matsumoto, M.; Clermont, A.; Leitges, M.; Marette, A.; Aiello, L.P.; Kern, T.S.; King, G.L. Activation of pkc-delta and shp-1 by hyperglycemia causes vascular cell apoptosis and diabetic retinopathy. *Nat Med* **2009**, *15*, 1298-1306.
17. Kumar, S.; Zhuo, L. Longitudinal in vivo imaging of retinal gliosis in a diabetic mouse model. *Exp Eye Res* **2010**, *91*, 530-536.
18. Zhang, W.; Liu, H.; Rojas, M.; Caldwell, R.W.; Caldwell, R.B. Anti-inflammatory therapy for diabetic retinopathy. *Immunotherapy* **2011**, *3*, 609-628.
19. Lamers, M.L.; Almeida, M.E.; Vicente-Manzanares, M.; Horwitz, A.F.; Santos, M.F. High glucose-mediated oxidative stress impairs cell migration. *PLoS One* **2011**, *6*, e22865.
20. Giacco, F.; Brownlee, M. Oxidative stress and diabetic complications. *Circ Res* **2010**, *107*, 1058-1070.
21. Carmo, A.; Cunha-Vaz, J.G.; Carvalho, A.P.; Lopes, M.C. Effect of cyclosporin-a on the blood--retinal barrier permeability in streptozotocin-induced diabetes. *Mediators Inflamm* **2000**, *9*, 243-248.
22. Du, Y.; Smith, M.A.; Miller, C.M.; Kern, T.S. Diabetes-induced nitrative stress in the retina, and correction by aminoguanidine. *J Neurochem* **2002**, *80*, 771-779.
23. Kowluru, R.A.; Engerman, R.L.; Kern, T.S. Abnormalities of retinal metabolism in diabetes or experimental galactosemia viii. Prevention by aminoguanidine. *Curr Eye Res* **2000**, *21*, 814-819.

24. de Campos, R.P.; Siegel, J.M.; Fresta, C.G.; Caruso, G.; da Silva, J.A.; Lunte, S.M. Indirect detection of superoxide in raw 264.7 macrophage cells using microchip electrophoresis coupled to laser-induced fluorescence. *Anal Bioanal Chem* **2015**, *407*, 7003-7012.

25. Caruso, G.; Fresta, C.G.; Siegel, J.M.; Wijesinghe, M.B.; Lunte, S.M. Microchip electrophoresis with laser-induced fluorescence detection for the determination of the ratio of nitric oxide to superoxide production in macrophages during inflammation. *Anal Bioanal Chem* **2017**, *409*, 4529-4538.

26. Cristina de Assis, M.; Cristina Plotkowski, M.; Fierro, I.M.; Barja-Fidalgo, C.; de Freitas, M.S. Expression of inducible nitric oxide synthase in human umbilical vein endothelial cells during primary culture. *Nitric Oxide* **2002**, *7*, 254-261.

27. Leal, E.C.; Manivannan, A.; Hosoya, K.; Terasaki, T.; Cunha-Vaz, J.; Ambrosio, A.F.; Forrester, J.V. Inducible nitric oxide synthase isoform is a key mediator of leukostasis and blood-retinal barrier breakdown in diabetic retinopathy. *Invest Ophthalmol Vis Sci* **2007**, *48*, 5257-5265.

28. Al-Shabrawey, M.; Bartoli, M.; El-Remessy, A.B.; Ma, G.; Matragoon, S.; Lemtalsi, T.; Caldwell, R.W.; Caldwell, R.B. Role of nadph oxidase and stat3 in statin-mediated protection against diabetic retinopathy. *Invest Ophthalmol Vis Sci* **2008**, *49*, 3231-3238.

29. Al-Shabrawey, M.; Rojas, M.; Sanders, T.; Behzadian, A.; El-Remessy, A.; Bartoli, M.; Parpia, A.K.; Liou, G.; Caldwell, R.B. Role of nadph oxidase in retinal vascular inflammation. *Invest Ophthalmol Vis Sci* **2008**, *49*, 3239-3244.

30. Rojas, M.; Zhang, W.; Xu, Z.; Lemtalsi, T.; Chandler, P.; Toque, H.A.; Caldwell, R.W.; Caldwell, R.B. Requirement of nox2 expression in both retina and bone marrow for diabetes-induced retinal vascular injury. *PLoS One* **2013**, *8*, e84357.

31. El-Remessy, A.B.; Behzadian, M.A.; Abou-Mohamed, G.; Franklin, T.; Caldwell, R.W.; Caldwell, R.B. Experimental diabetes causes breakdown of the blood-retina barrier by a mechanism involving tyrosine nitration and increases in expression of vascular endothelial growth factor and urokinase plasminogen activator receptor. *Am J Pathol* **2003**, *162*, 1995-2004.

32. Foresti, R.; Bucolo, C.; Platania, C.M.; Drago, F.; Dubois-Rande, J.L.; Motterlini, R. Nrf2 activators modulate oxidative stress responses and bioenergetic profiles of human retinal epithelial cells cultured in normal or high glucose conditions. *Pharmacol Res* **2015**, *99*, 296-307.

33. Foresti, R.; Bains, S.K.; Pitchumony, T.S.; de Castro Bras, L.E.; Drago, F.; Dubois-Rande, J.L.; Bucolo, C.; Motterlini, R. Small molecule activators of the nrf2-ho-1 antioxidant axis modulate heme metabolism and inflammation in bv2 microglia cells. *Pharmacol Res* **2013**, *76*, 132-148.
34. Pittala, V.; Fidilio, A.; Lazzara, F.; Platania, C.B.M.; Salerno, L.; Foresti, R.; Drago, F.; Bucolo, C. Effects of novel nitric oxide-releasing molecules against oxidative stress on retinal pigmented epithelial cells. *Oxid Med Cell Longev* **2017**, *2017*, 1420892.
35. Shin, E.S.; Huang, Q.; Gurel, Z.; Sorenson, C.M.; Sheibani, N. High glucose alters retinal astrocytes phenotype through increased production of inflammatory cytokines and oxidative stress. *PLoS One* **2014**, *9*, e103148.
36. Barar, J.; Asadi, M.; Mortazavi-Tabatabaei, S.A.; Omidi, Y. Ocular drug delivery; impact of in vitro cell culture models. *J Ophthalmic Vis Res* **2009**, *4*, 238-252.
37. Hornof, M.; Toropainen, E.; Urtti, A. Cell culture models of the ocular barriers. *Eur J Pharm Biopharm* **2005**, *60*, 207-225.
38. Nakagawa, S.; Deli, M.A.; Nakao, S.; Honda, M.; Hayashi, K.; Nakaoke, R.; Kataoka, Y.; Niwa, M. Pericytes from brain microvessels strengthen the barrier integrity in primary cultures of rat brain endothelial cells. *Cell Mol Neurobiol* **2007**, *27*, 687-694.
39. Abuhaiba, S.I.; Cordeiro, M.; Amorim, A.; Cruz, A.; Quendera, B.; Ferreira, C.; Ribeiro, L.; Bernardes, R.; Castelo-Branco, M. Occipital blood-brain barrier permeability is an independent predictor of visual outcome in type 2 diabetes, irrespective of the retinal barrier: A longitudinal study. *J Neuroendocrinol* **2018**, *30*.
40. Wisniewska-Kruk, J.; Hoeben, K.A.; Vogels, I.M.; Gaillard, P.J.; Van Noorden, C.J.; Schlingemann, R.O.; Klaassen, I. A novel co-culture model of the blood-retinal barrier based on primary retinal endothelial cells, pericytes and astrocytes. *Exp Eye Res* **2012**, *96*, 181-190.
41. Yao, H.; Wang, T.; Deng, J.; Liu, D.; Li, X.; Deng, J. The development of blood-retinal barrier during the interaction of astrocytes with vascular wall cells. *Neural Regen Res* **2014**, *9*, 1047-1054.
42. Ly, A.; Yee, P.; Vessey, K.A.; Phipps, J.A.; Jobling, A.I.; Fletcher, E.L. Early inner retinal astrocyte dysfunction during diabetes and development of hypoxia,

retinal stress, and neuronal functional loss. *Invest Ophthalmol Vis Sci* **2011**, *52*, 9316-9326.

43. Bahniwal, M.; Little, J.P.; Klegeris, A. High glucose enhances neurotoxicity and inflammatory cytokine secretion by stimulated human astrocytes. *Curr Alzheimer Res* **2017**, *14*, 731-741.
44. Hamilton, N.B.; Attwell, D.; Hall, C.N. Pericyte-mediated regulation of capillary diameter: A component of neurovascular coupling in health and disease. *Front Neuroenergetics* **2010**, *2*.
45. Maugeri, G.; D'Amico, A.G.; Gagliano, C.; Saccone, S.; Federico, C.; Cavallaro, S.; D'Agata, V. Vip family members prevent outer blood retinal barrier damage in a model of diabetic macular edema. *J Cell Physiol* **2017**, *232*, 1079-1085.
46. Lobo, C.L.; Bernardes, R.C.; Cunha-Vaz, J.G. Alterations of the blood-retinal barrier and retinal thickness in preclinical retinopathy in subjects with type 2 diabetes. *Arch Ophthalmol* **2000**, *118*, 1364-1369.
47. Umeda, K.; Matsui, T.; Nakayama, M.; Furuse, K.; Sasaki, H.; Furuse, M.; Tsukita, S. Establishment and characterization of cultured epithelial cells lacking expression of zo-1. *J Biol Chem* **2004**, *279*, 44785-44794.
48. McNeil, E.; Capaldo, C.T.; Macara, I.G. Zonula occludens-1 function in the assembly of tight junctions in madin-darby canine kidney epithelial cells. *Mol Biol Cell* **2006**, *17*, 1922-1932.
49. Deissler, H.L.; Deissler, H.; Lang, G.K.; Lang, G.E. Vegf but not plgf disturbs the barrier of retinal endothelial cells. *Exp Eye Res* **2013**, *115*, 162-171.
50. Lee, C.S.; Kim, Y.G.; Cho, H.J.; Park, J.; Jeong, H.; Lee, S.E.; Lee, S.P.; Kang, H.J.; Kim, H.S. Dipeptidyl peptidase-4 inhibitor increases vascular leakage in retina through ve-cadherin phosphorylation. *Sci Rep* **2016**, *6*, 29393.
51. He, J.; Wang, H.; Liu, Y.; Li, W.; Kim, D.; Huang, H. Blockade of vascular endothelial growth factor receptor 1 prevents inflammation and vascular leakage in diabetic retinopathy. *J Ophthalmol* **2015**, *2015*, 605946.
52. Al-Kharashi, A.S. Role of oxidative stress, inflammation, hypoxia and angiogenesis in the development of diabetic retinopathy. *Saudi J Ophthalmol* **2018**, *32*, 318-323.
53. Deng, Y.; Xie, D.; Fang, M.; Zhu, G.; Chen, C.; Zeng, H.; Lu, J.; Charanjit, K. Astrocyte-derived proinflammatory cytokines induce hypomyelination in the

periventricular white matter in the hypoxic neonatal brain. *PLoS One* **2014**, *9*, e87420.

54. Sofroniew, M.V. Multiple roles for astrocytes as effectors of cytokines and inflammatory mediators. *Neuroscientist* **2014**, *20*, 160-172.
55. Mishra, A.; Newman, E.A. Inhibition of inducible nitric oxide synthase reverses the loss of functional hyperemia in diabetic retinopathy. *Glia* **2010**, *58*, 1996-2004.
56. Peng, J.J.; Xiong, S.Q.; Ding, L.X.; Peng, J.; Xia, X.B. Diabetic retinopathy: Focus on nadph oxidase and its potential as therapeutic target. *Eur J Pharmacol* **2019**, *853*, 381-387.
57. Di Meo, S.; Reed, T.T.; Venditti, P.; Victor, V.M. Role of ros and rns sources in physiological and pathological conditions. *Oxid Med Cell Longev* **2016**, *2016*, 1245049.
58. Liguori, I.; Russo, G.; Curcio, F.; Bulli, G.; Aran, L.; Della-Morte, D.; Gargiulo, G.; Testa, G.; Cacciatore, F.; Bonaduce, D.; Abete, P. Oxidative stress, aging, and diseases. *Clin Interv Aging* **2018**, *13*, 757-772.
59. Volpe, C.M.O.; Villar-Delfino, P.H.; Dos Anjos, P.M.F.; Nogueira-Machado, J.A. Cellular death, reactive oxygen species (ros) and diabetic complications. *Cell Death Dis* **2018**, *9*, 119.
60. Brownlee, M. The pathobiology of diabetic complications: A unifying mechanism. *Diabetes* **2005**, *54*, 1615-1625.
61. Evans, J.L.; Maddux, B.A.; Goldfine, I.D. The molecular basis for oxidative stress-induced insulin resistance. *Antioxid Redox Signal* **2005**, *7*, 1040-1052.
62. Vomund, S.; Schafer, A.; Parnham, M.J.; Brune, B.; von Knethen, A. Nrf2, the master regulator of anti-oxidative responses. *Int J Mol Sci* **2017**, *18*.
63. Tonelli, C.; Chio, I.I.C.; Tuveson, D.A. Transcriptional regulation by nrf2. *Antioxid Redox Signal* **2018**, *29*, 1727-1745.
64. Fan, J.; Xu, G.; Jiang, T.; Qin, Y. Pharmacologic induction of heme oxygenase-1 plays a protective role in diabetic retinopathy in rats. *Invest Ophthalmol Vis Sci* **2012**, *53*, 6541-6556.
65. Platania, C.B.M.; Fidilio, A.; Lazzara, F.; Piazza, C.; Geraci, F.; Giurdanella, G.; Leggio, G.M.; Salomone, S.; Drago, F.; Bucolo, C. Retinal protection and distribution of curcumin in vitro and in vivo. *Front Pharmacol* **2018**, *9*, 670.

66. Bonkowski, D.; Katyshev, V.; Balabanov, R.D.; Borisov, A.; Dore-Duffy, P. The cns microvascular pericyte: Pericyte-astrocyte crosstalk in the regulation of tissue survival. *Fluids Barriers CNS* **2011**, *8*, 8.

67. Platania, C.B.M.; Lazzara, F.; Fidilio, A.; Fresta, C.G.; Conti, F.; Giurdanella, G.; Leggio, G.M.; Salomone, S.; Drago, F.; Bucolo, C. Blood-retinal barrier protection against high glucose damage: The role of p2x7 receptor. *Biochem Pharmacol* **2019**, *168*, 249-258.

68. Giurdanella, G.; Lazzara, F.; Caporarello, N.; Lupo, G.; Anfuso, C.D.; Eandi, C.M.; Leggio, G.M.; Drago, F.; Bucolo, C.; Salomone, S. Sulodexide prevents activation of the pla2/cox-2/vegf inflammatory pathway in human retinal endothelial cells by blocking the effect of age/rage. *Biochem Pharmacol* **2017**, *142*, 145-154.

69. Giurdanella, G.; Montalbano, G.; Gennuso, F.; Brancati, S.; Lo Furno, D.; Augello, A.; Bucolo, C.; Drago, F.; Salomone, S. Isolation, cultivation, and characterization of primary bovine cochlear pericytes: A new in vitro model of stria vascularis. *J Cell Physiol* **2019**, *234*, 1978-1986.

70. Rueden, C.T.; Schindelin, J.; Hiner, M.C.; DeZonia, B.E.; Walter, A.E.; Arena, E.T.; Eliceiri, K.W. Imagej2: Imagej for the next generation of scientific image data. *BMC Bioinformatics* **2017**, *18*, 529.

71. Hira, V.V.V.; Breznik, B.; Vittori, M.; Loncq de Jong, A.; Mlakar, J.; Oostra, R.J.; Khurshed, M.; Molenaar, R.J.; Lah, T.; Van Noorden, C.J.F. Similarities between stem cell niches in glioblastoma and bone marrow: Rays of hope for novel treatment strategies. *J Histochem Cytochem* **2020**, *68*, 33-57.

72. Peyvandi, F.; Garagiola, I.; Baronciani, L. Role of von willebrand factor in the haemostasis. *Blood Transfus* **2011**, *9 Suppl 2*, s3-8.

73. Hol, E.M.; Pekny, M. Glial fibrillary acidic protein (gfap) and the astrocyte intermediate filament system in diseases of the central nervous system. *Curr Opin Cell Biol* **2015**, *32*, 121-130.

74. Bauer, H.; Zweimueller-Mayer, J.; Steinbacher, P.; Lametschwandtner, A.; Bauer, H.C. The dual role of zonula occludens (zo) proteins. *J Biomed Biotechnol* **2010**, *2010*, 402593.

75. Vestweber, D. Ve-cadherin: The major endothelial adhesion molecule controlling cellular junctions and blood vessel formation. *Arterioscler Thromb Vasc Biol* **2008**, *28*, 223-232.

76. Caruso, G.; Fresta, C.G.; Musso, N.; Giambirtone, M.; Grasso, M.; Spampinato, S.F.; Merlo, S.; Drago, F.; Lazzarino, G.; Sortino, M.A.; Lunte, S.M.; Caraci, F. Carnosine prevents abeta-induced oxidative stress and inflammation in microglial cells: A key role of tgf-beta1. *Cells* **2019**, *8*.

77. Caruso, G.; Fresta, C.G.; Fidilio, A.; O'Donnell, F.; Musso, N.; Lazzarino, G.; Grasso, M.; Amorini, A.M.; Tascedda, F.; Bucolo, C.; Drago, F.; Tavazzi, B.; Lazzarino, G.; Lunte, S.M.; Caraci, F. Carnosine decreases pma-induced oxidative stress and inflammation in murine macrophages. *Antioxidants (Basel)* **2019**, *8*.

Figure 1. Assessment of barrier integrity in the in vitro human primary culture based triple co-culture BRB model by TEER. TEER values were measured at time 0 (TO), and after 24 (T24) and 48 (T48) h. NG = normal glucose condition (5 mM); HG = high glucose condition (40 mM). Values are means ± SD of five independent experiments. Two-way ANOVA with Bonferroni's post-hoc analysis. *p < 0.0001 vs. NG.

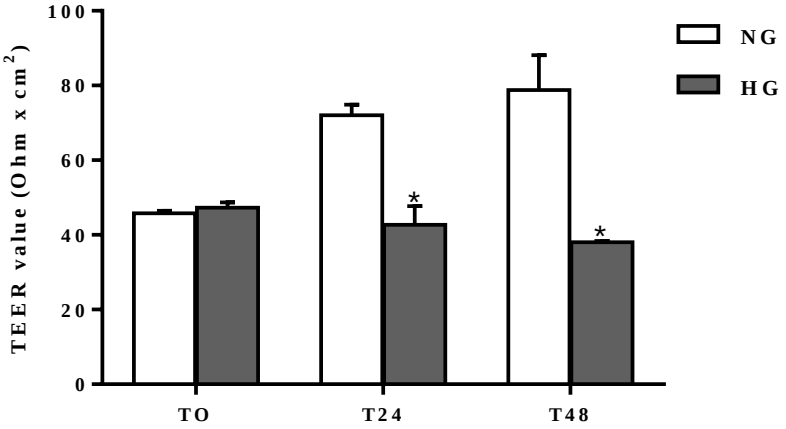

Figure 2. Measurement of the apical-to-basolateral movements of Na-F in the in vitro human primary culture based triple co-culture BRB model. Na-F permeability was measured after 5, 15, and 30 min. NG = normal glucose condition (5 mM); HG = high glucose condition (40 mM). Values, presented as a mean of relative fluorescence units (RFUs), are means ± SD of three independent experiments. Two-way ANOVA with Bonferroni's post-hoc analysis. *p < 0.01 vs. NG; **p < 0.05 vs. NG.

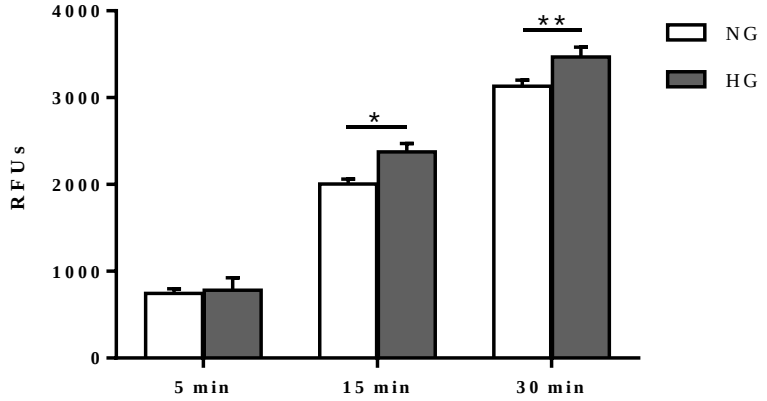

Figure 3. Confocal analysis of ZO-1 (A) and VE-cadherin (C) in endothelial cells subjected to normal or high glucose conditions for 48 hours. ZO-1 and VE-cadherin were labeled with FITC (green) while nucleus were labeled with DAPI (blue). The continuous brush border showed for normal glucose conditions (Ai and Ci) is interrupted under high glucose conditions (Aii and Cii). The average intensity (AU) of the data from more than 30 cells per coverslip for ZO-1 and VE-cadherin under normal and high glucose conditions are reported in (B) and (D), respectively. Images for ZO-1 and VE-cadherin immunostaining were acquired at 20 or 60× magnification. NG = normal glucose condition (5 mM); HG = high glucose condition (40 mM). Values are means ± SD of three independent experiments. Statistical analysis was performed using Student's t-test. *p < 0.001 vs. NG.

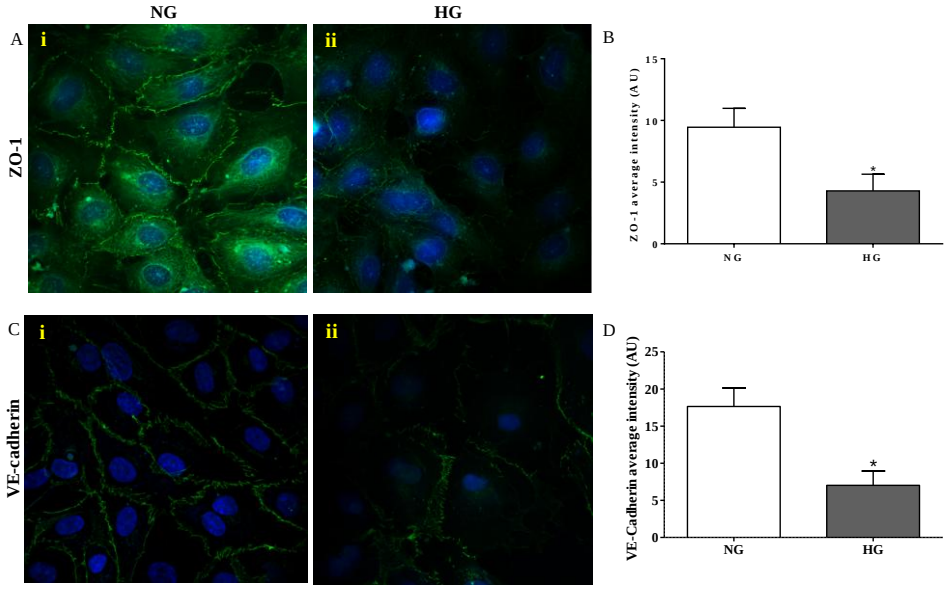

Figure 4. Measurement of A) IL-6 and B) IL-1β mRNA expression levels (qRT-PCR) in astrocytes subjected to normal or high glucose conditions for 48 hours. The abundance of each mRNA of interest was expressed relative to the abundance of 18S rRNA, as an internal control. NG = normal glucose condition (5 mM); HG = high glucose condition (40 mM). Values are means ± SD of three independent experiments. Statistical analysis was performed using Student's t-test. *p < 0.05 vs. NG; **p < 0.01 vs. NG.

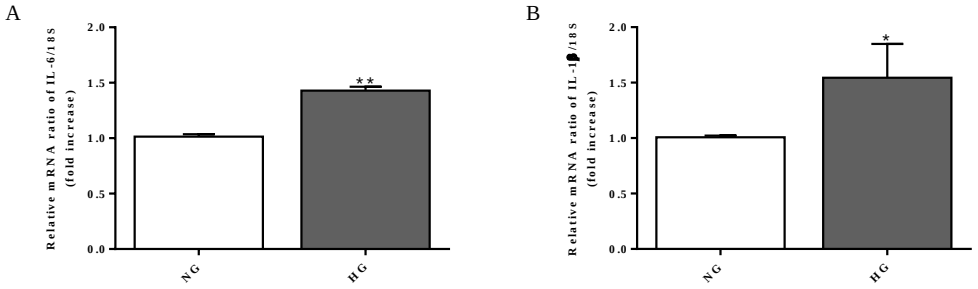

Figure 5. Measurement of A) iNOS and B) Nox2 expression levels (qRT-PCR) in astrocytes subjected to normal or high glucose conditions for 48 hours. The abundance of each mRNA of interest was expressed relative to the abundance of 18S rRNA, as an internal control. C) Intracellular ROS production in astrocytes under normal and high glucose conditions. NG = normal glucose condition (5 mM); HG = high glucose condition (40 mM). Values are means ± SD of three to four independent experiments. Statistical analysis was performed using Student's t-test. **p < 0.01 vs. NG; ***p < 0.001 vs. NG.

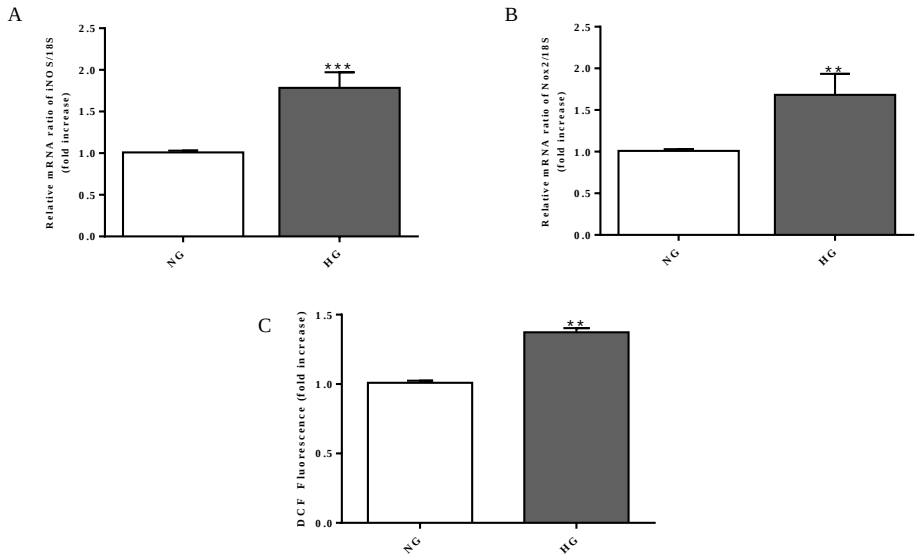

Figure 6. Representative immunoblots of A) cytoplasmic and nuclear pNF-□B, B) cytoplasmic and nuclear Nrf2, and C) total HO-1 in protein extracts from astrocytes subjected to normal or high glucose conditions for 48 hours. NG = normal glucose condition (5 mM); HG = high glucose condition (40 mM). Histograms refer to the means ± SD of three independent experiments. Statistical analysis was performed using Student's t-test. The densitometric values of cytoplasmic and nuclear pNF-□B bands were normalized against total NF-□B. The densitometric values of cytoplasmic Nrf2 and total HO-1 bands were normalized against β-Actin, while densitometric values of nuclear Nrf2 bands were normalized against Lamin B. *$p < 0.05$ vs. NG.

A

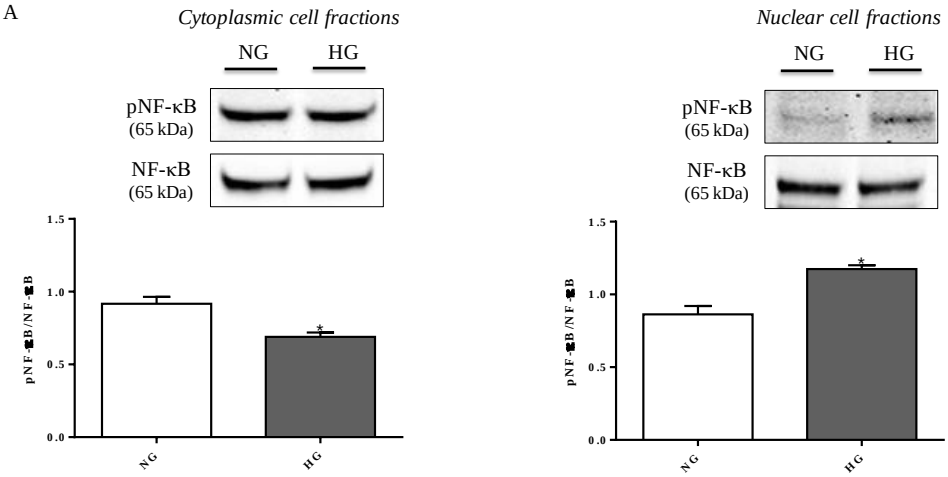
Cytoplasmic cell fractions
NG
HG
pNF-κB
(65 kDa)
NF-κB
(65 kDa)
1.5
1.0
0.5
0.0
*
NG
HG
Nuclear cell fractions
NG
HG
pNF-κB
(65 kDa)
NF-κB
(65 kDa)
1.5
1.0
0.5
0.0
*
NG
HG

B

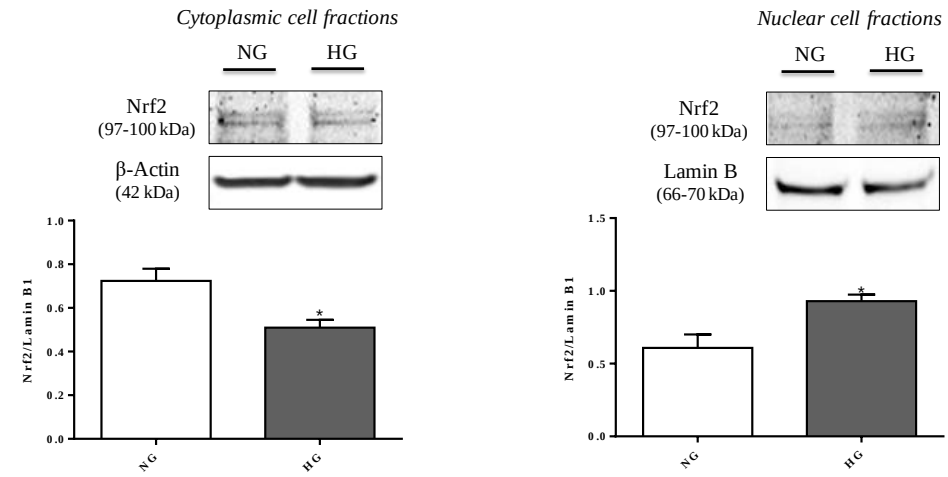
Cytoplasmic cell fractions
NG
HG
Nrf2
(97-100 kDa)
β-Actin
(42 kDa)
1.0
0.8
0.6
0.4
0.2
0.0
*
NG
HG
Nuclear cell fractions
NG
HG
Nrf2
(97-100 kDa)
Lamin B
(66-70 kDa)
1.5
1.0
0.5
0.0
*
NG
HG

C

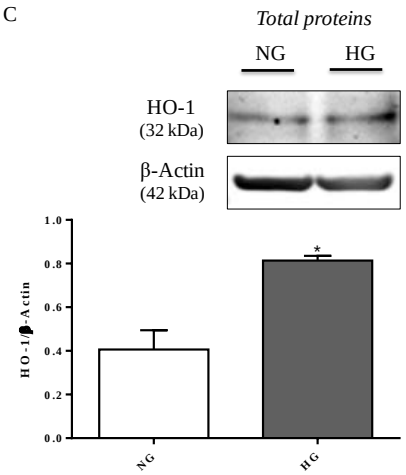
Total proteins
NG
HG
HO-1
(32 kDa)
β-Actin
(42 kDa)
1.0
0.8
0.6
0.4
0.2
0.0
*
NG
HG

Figure 7. Experimental procedure followed to set up the in vitro BRB model. A) PLL coating; B) human retinal pericytes are seeded on the bottom side of the insert; C) inserts are rotated of 180° and inserted into a 12-well plate containing pericytes medium; D) human retinal astrocytes are seeded on a 12-well plate containing astrocytes medium; E) cell incubation and adhesion; F) the insert with pericytes is moved into the 12-well plate holding astrocytes; G) human retinal endothelial cells are seeded on the top side of the insert; H) cells are grown with a medium consisting of a mixture of the three cell lines' media (1:1:1); I) glucose was added in order to obtain high glucose conditions.

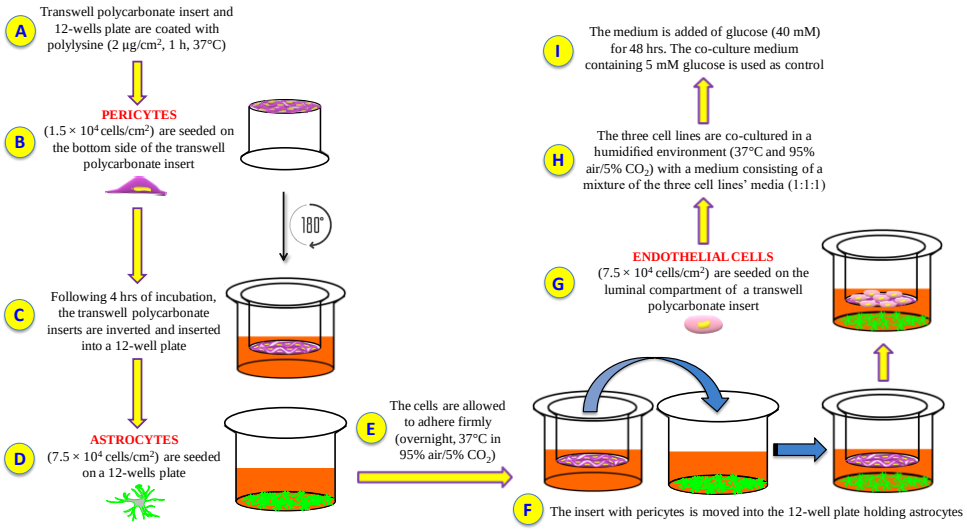

Supplementary Figure 1. The purity of endothelial cells, pericytes, and astrocytes was confirmed by immunofluorescence staining with A) von Willebrand factor, B) α-SMA, and C) GFAP, respectively.

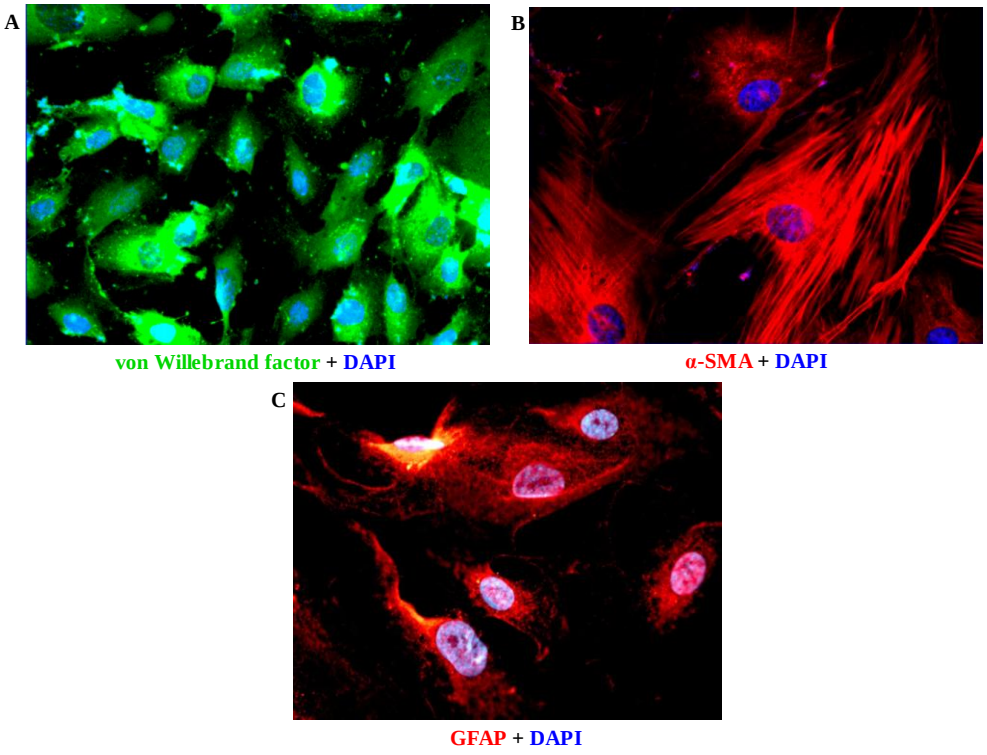

Table 1. Details of primary antibodies used for fluorescence immunohistochemistry.

Primary antibody	Source	Primary antibody dilution in PBS + BSA or NGS (1%)	Protein Function/Characteristics
Mouse anti-human α-SMA	Dako[a] (M0851)	1:120	Expressed by smooth muscle cells of arterioles and venules, myofibroblasts, and pericytes [71]
Rabbit anti-human Von Willebrand Factor	Abcam[b] (ab6994)	1:120	Adhesive and multimeric glycoprotein present in blood plasma and produced constitutively in endothelium, megakaryocytes, and subendothelial connective tissue [72]
Mouse anti-human GFAP	Novus Biologicals[c] (NB120-10062)	1:200	The hallmark intermediate filament (also known as nanofilament) protein in astrocytes [73]
Rabbit anti-human ZO-1	Life Technology[d] (61-7300)	1:100	Scaffold protein located on a cytoplasmic membrane surface of intercellular tight junctions involved in signal transduction at cell-cell junctions [74]
Rabbit anti-human VE-cadherin	Cell Signaling Technology[e] (2500)	1:100	Endothelial specific adhesion molecule located at junctions between endothelial cells [75]

Abbreviations: α-SMA, α-smooth muscle actin; GFAP, Glial fibrillary acidic protein; ZO-1, Zonula occludens-1; VE-cadherin, Vascular endothelial-cadherin. [a]Dako, Santa Clara, California, USA; [b]Abcam, Cambridge, UK; [c]Novus Biologicals, Milan, Italy; [d]Life Technology, Monza, Italy; [e]Cell Signaling Technology, Danvers, MA, USA.

Table 2. The list of primers used for quantitative real-time PCR (qRT-PCR).

Official name[#]	Official symbol	Alternative titles/symbols	Detected transcript	Amplicon Length	Cat. No.[§]
nitric oxide synthase 2, inducible	Nos2	iNOS; Nos-2; Nos2a; i-NOS; NOS-II; MAC-NOS	NM_010927	118 bp	QT00100275
cytochrome b-245, beta polypeptide	Cybb	Cgd; Cyd; Nox2; C88302; gp91-1; gp91phox; CGD91-phox	NM_007807 XM_006527565	146 bp	QT00139797
interleukin 6	Il6	Il-6	NM_031168	128 bp	QT00098875

[#]https://www.ncbi.nlm.nih.gov/gene/; [§]https://www.qiagen.com/it/shop/pcr/real-time-pcr-enzymes-and-kits/two-step-qrt-pcr/quantitect-primer-assays/.

CHAPTER 2

Int J Mol Sci. 2020 Dec 6;21(23):9305. doi: 10.3390/ijms21239305.
PMID: 33291318.

Dihydrotanshinone, a Natural Diterpenoid, Preserves Blood-Retinal Barrier Integrity via P2X7 Receptor

Claudia G. Fresta[1], Giuseppe Caruso[2,3], Annamaria Fidilio[2], Chiara Bianca Maria Platania[1], Nicolò Musso[1], Filippo Caraci[2,3], Filippo Drago[1,4], Claudio Bucolo[1,4]

[1] Department of Biomedical and Biotechnological Sciences, School of Medicine, University of Catania, Italy
[2] Department of Drug Sciences, University of Catania, Catania, Italy
[3] Oasi Research Institute - IRCCS, Troina, Italy
[4] Center for Research in Ocular Pharmacology-CERFO, University of Catania, Catania, Italy

Abstract

Activation of P2X7 signaling, due to high glucose levels, leads to blood retinal barrier (BRB) breakdown, a hallmark of diabetic retinopathy (DR). Furthermore, several studies report that high glucose (HG) conditions and the related activation of the P2X7 receptor (P2X7R) lead to the over-expression of pro-inflammatory markers. In order to identify novel P2X7R antagonists, we carried out virtual screening on a focused compound dataset, including indole derivatives and natural compounds such as caffeic acid phenethyl ester derivatives, flavonoids, and diterpenoids. Molecular-Mechanics Generalized Born Surface Area (MM-GBSA) rescoring and structural fingerprint clustering of docking poses from virtual screening highlighted that the diterpenoid dihydrotanshinone (DHTS) clustered with the well-known P2X7R antagonist JNJ47965567. A human-based in vitro BRB model made of retinal pericytes, astrocytes, and endothelial cells was used to assess the potential protective effect of DHTS against HG and 2'(3')-O-(4-Benzoylbenzoyl)adenosine-5'-triphosphate (BzATP), a P2X7R agonist, insult. We found that HG/BzATP exposure generated BRB breakdown by enhancing barrier permeability (transendothelial electrical resistance (TEER)) and reducing the levels of ZO-1 and VE-cadherin junction proteins as well as of the Cx-43 mRNA expression levels. Furthermore, HG levels and P2X7R agonist treatment led to increased expression of pro-inflammatory mediators (TLR-4, IL-1β, IL-6, TNF-α, and IL-8) and other molecular markers (P2X7R, VEGF-A, and ICAM-1), along with enhanced production of reactive oxygen species. Treatment with DHTS preserved the BRB integrity from HG/BzATP damage. The protective effects of DHTS were also compared to the validated P2X7R antagonist, JNJ47965567. In conclusion, we provided

new findings pointing out the therapeutic potential of DHTS, an inhibitor of P2X7R, preventing and/or counteracting the BRB dysfunctions elicited by HG conditions.

Keywords: diabetic retinopathy; blood-retinal barrier; purinergic P2X7 receptor; endothelial cells; oxidative stress; inflammation.

Introduction

Diabetic retinopathy (DR) is one of the microvascular complications of diabetes. DR is a leading cause of vision impairment among the working-age population [1]. It has been estimated that DR incidence will grow up, affecting 190 million patients by 2030, pointing out the importance of research efforts towards new diagnostic and therapeutic strategies [2]. DR progresses from non-proliferative (NPDR) to proliferative (PDR) stage, this latter is characterized by vitreous hemorrhages and extensive neovascularization [3]. Furthermore, DR in early stages is characterized by pericytes and endothelial cells death [4]; indeed, changes in the vascular endothelial membrane as well as vascular leakage compromise the blood-retinal barrier (BRB)[5], whose structural integrity is essential for retinal homeostasis and function[6]. In fact, the loss of the BRB integrity significantly contributes to the pathophysiology of several retinal disorders including DR [7].The BRB is a tight and limitative barrier that manages the flux of ions, proteins, metabolic waste compounds, and water flow through the retina, and consists of two distinct regions, the inner and outer BRB [8]. The outer BRB (oBRB) is formed by retinal pigmented epithelial cells connected by tight junction proteins, while the inner BRB (iBRB) is established by tight junctions between retinal capillary endothelial cells, surrounded by pericytes and supported by glial cells [9]. Among glial cells, astrocytes provide functional support to the iBRB, playing a crucial role for the maintenance of retinal endothelial capillaries integrity [10].

Zonula occludens-1, -2, and -3 (ZO-1 ZO-2, and ZO-3), occludins, and claudins are tight junctions essential for BRB structural stability [9]. A decrease of the tight junction protein expression levels, and the consequent BRB breakdown, has been shown in experimental models of diabetes [11]. According to Osanai *et al.*, tight junction proteins are involved in many physiological processes including cell proliferation and differentiation; furthermore, they limit the passage of proteins and lipids between apical and basolateral membranes, guiding endothelial cell polarity [12].The maintenance of the BRB integrity is also due to the interactions between tight and adherens junctions, mediated by cell-cell adhesion molecules such as cadherins [13], which represent a family of proteins implicated in maintenance of endothelial cells adhesion to the vasculatures, including VE-cadherin [14]. Since several studies have shown the role played by the inflammatory processes in diabetes-associated retinal alterations, the interest on the link between reactive oxygen species (ROS), inflammatory processes, and endothelial dysfunction has been increasing. The inflammatory processes occurring during the development of DR lead to the activation

of toll-like receptors 4 (TLR-4) that, in turn, trigger the overexpression of pro-inflammatory cytokines and acute phase proteins [15]. In particular, IL-1β and TNF-α are involved in the pathogenesis of DR, concurring to diabetes-induced degeneration of retinal capillaries [16,17]. Still in the context of inflammation, an additional pathophysiological event is the interaction between leucocytes and endothelial cells; indeed, this cell interaction is fundamental for the recruitment of leucocytes at the inflammation site [18]. In particular, intercellular adhesion molecule-1 (ICAM-1), whose expression in the retina is increased in DR [19], has been linked to both leukostasis and inflammatory phenomena [20].

During the last three decades several studies have demonstrated the pivotal role played by ROS in retinal microvascular complications, such as DR [21]. Since the retina is a high energy-demanding organ, it becomes more susceptible to high levels of ROS, that along with a hyperglycemic environment enhance mitochondrial dysfunction, inflammation, and degeneration pathways, leading to vascular, neural, and retinal tissue damage *via* pyroptosis and/or apoptosis [22].

Inside the retina, the combination between hyperglycemic and hypoxic conditions represents a strong stimulus for both astrocytes and endothelial cells, which therefore enhance the expression of vascular endothelial growth factor (VEGF) [23]. When hyperglycemia becomes chronic, VEGF deflects from its physiological functions, leading to the formation of abnormal new blood vessels as observed for PDR [24]. Furthermore, it has been shown that this trophic factor, by interacting with VEGF receptor 2, promotes endothelial tight-junctions alteration and development of endothelial cell fenestration, resulting in a thinning of the blood vessels [25].

Endothelial and pericyte dysfunction represent a key factor for DR progression and increased extracellular ATP (eATP) has been observed at the site of inflammation as a consequence of endothelial cell injury [26]. Moreover, it is well-established that the hyperglycemic environment leads to an enhanced eATP concentration, that triggers a cascade of events culminating in the activation of the purinergic signaling pathway, which includes P2X7 receptor (P2X7R) [27]. In literature, there are numerous evidences highlighting the role of this ATP-gated ion channel in modulating inflammatory responses in the retinal microvasculature [28-30]; indeed, studies conducted in experimental models of DR revealed that the P2X7R mediates the vascular inflammatory reactions due to an overexpression of cytokines, thus contributing to BRB dysfunction, ischemia, and retinal vascular occlusion [29,31]. When considering endothelial cells, it has been recently demonstrated that high glucose conditions led to P2X7R over-activation in these cells,

increased expression pro-inflammatory markers, decreased cell viability, and finally loss of BRB integrity [32].

In the present work we aimed to explore the role played by the P2X7R in a recently established *in vitro* primary culture based triple co-culture BRB model entirely based on human cells (retinal perycites, retinal astrocytes, and retinal endothelial cells) [33]. Along with specific hallmarks of P2X7R activation in the iBRB (barrier permeability and expression of IL-1β, Cx43, tight and adherens junctions), we evaluated the effects of P2X7R inhibition on expression of other inflammatory cytokines, including VEGF, IL-6, IL-8, and TNF-α, along with ROS production in order to estimate an expression network linked to P2X7 signalling.We also investigated the potential protective effect of DHTS, a natural diterpenoid extracted from *Salvia miltiorrhiza*, against the retinal damage elicited by HG and a selective P2X7R agonist [2'(3')-O-(4-Benzoylbenzoyl)adenosine-5'-triphosphate (BzATP)].

Results

Virtual screening at P2X7R

According to the last solved structure of full-length rat P2X7R [34], we built the human full-length P2X7R model and minimized it in an implicit membrane model (Figure 1).

A series of compounds [35] have been screened, the database included known P2X7R allosteric antagonists [36]. Structural fingerprint clustering was carried out and DHTS, along with quercetin, clustered with JNJ47965567, a validated P2X7R allosteric inhibitor (Table 1).

Furthermore, we carried out molecular docking and Molecular-Mechanics Generalized Born Surface Area (MM-GBSA) calculations of DHTS binding at P2X7R allosteric, orthosteric pockets. We included in our analysis a pocket in the cytosolic domain of P2X7R, as identified by the SiteMap® task of Schrodinger Maestro. According to our computational analysis (Table1), DHTS can be an allosteric P2X7R antagonist, given the lowest (more favorable) predicted binding free energy at the allosteric pocket, compared to the orthosteric one. On this perspective we carried out in vitro studies on retinal endothelial cells in order to assess the DHTS activity as P2X7R antagonist, by treating cells with this putative antagonist, HG and the selective P2X7R agonist BzATP.

BRB integrity

Inner BRB integrity was evaluated by performing transendothelial electrical resistance (TEER) measurements and the paracellular permeability assay following an exposure for 24 or 48 h to high glucose (HG) levels and BzATP (200 µM), in the absence or in the presence of JNJ47965567 (100 nM) or DHTS (500 nM) (2 h pre-treatment). Co-stimulus with HG and BzATP led to significant, albeit small, decreased TEER values, -18.5%, at 24 h, that further increased to -25.3% at 48 h, i.e. an increased permeability of our triple co-culture model of iBRB (Figure 2). DHTS and JNJ47965567 (validated, P2X7R antagonist) pre-treatment separately prevented the alterations of iBRB integrity (Figure 2).

These data were also confirmed by measuring the apical-to-basolateral permeability of sodium fluorescein (Na-F). Na-F permeability accounts to paracellular permeability across the endothelial cells/perycites monolayers under our experimental conditions [33] (Figure 3).

HG + BzATP stimuli significantly increased the Na-F fluorescence, indicating that HG and activation of P2X7R led to higher permeability of endothelial cells/perycites monolayers ($p< 0.05$ *vs.* NG), confirming the TEER measurements. The inhibition of P2X7R by pre-treatment with JNJ47965567 significantly decreased the Na-F permeability, counteracting the effects of HG + BzATP. According to virtual screening predictions, DHTS (putative P2X7R antagonist) also decreased the monolayer Na-F permeability, preventing and/or counteracting the damage induced by both HG and P2X7R agonist (BzATP)as already showed in TEER measurements. Therefore, JNJ47965567 and DHTS exerted protective effects on iBRB integrity challenged with the co-stimuli HG and BzATP.

Junctional proteins

Since iBRB integrity is dependent from expression of tight (ZO-1, ZO-2, and ZO-3, occludins, and claudins) and adherens junctions, we carried out immunocytochemistry experiments to assess the expression of ZO-1 and VE-cadherin proteins in endothelial cells monolayer, part of our iBRB model. As shown in Figure 4, ZO-1 expression, measured as fluorescence arbitrary units (AUs), was significantly reduced after an exposure for 48 h to HG in combination with BzATP compared to NG conditions, whereas JNJ47965567 or DHTS pre-treatment protected against the reduction of ZO-1 expression HG/BzATP-induced, preserving and/or counteracting the continuous brush border observed in control levels (Figure 4).

A similar trend was observed for expression of the adherens junction VE-cadherin. Figure 5 shows a significant reduction of VE-cadherin staining at the cell-cell contacts following the exposure to HG/BzATP insult as compared to cells grown in NG conditions. On the other hand, an increased expression of VE-cadherin was observed at endothelial cell-cell interface after the pre-treatment with JNJ47965567 or DHTS compounds (Figure 5).

ROS production

In order to investigate the role played by P2X7R signaling in HG-induced oxidative stress in endothelial cells, part of the *in vitro* tri-culture BRB model, we employed the ROS sensitive dye 2',7'-dichlorofluorescin diacetate (DCFDA). After stimulation for 48 h with HG + BzATP there was a significant ($p< 0.001$) increase in ROS formation compared to control conditions. JNJ47965567 or DHTS pre-treatment significantly prevented the increase in ROS production elicited by HG + BzATP (Figure 6).

Inflammatory biomarkers

It is well-established that endothelial dysfunction is linked to P2X7R over-activation [27] and pro-inflammatory phenomena, culminating in the development of DR [26]. The vascular inflammation P2X7R-mediated is due, among other things, to the unregulated production of cytokines, strongly contributing to BRB dysfunction, ischemia, and retinal vascular occlusion [29,31]. By using an endothelial cell monolayer we have recently demonstrated that HG conditions led to P2X7R over-activation, paralleled by increased expression of pro-inflammatory markers and decreased cell viability [32].

As shown in Figure 7A-D, the combined treatment with HG and BzATP led to the significant over-expression at the mRNA level of IL-1β, IL-6, TNF-α, and IL-8, the major mediators of inflammation-induced damage, in retinal endothelial cells compared to NG conditions ($p< 0.01$ for IL-8; $p< 0.05$ for the remaining cytokines).

Inhibition of P2X7R, through JNJ47965567 pre-treatment, significantly decreased cytokines levels such as IL-1β ($p< 0.05$), TNF-α ($p< 0.05$), and IL-8 ($p< 0.01$), counteracting the inflammatory stimuli exerted by HG + BzATP. The "predicted" P2X7R antagonist DHTS significantly decreased the expression levels of the analyzed pro-inflammatory markers ($p< 0.05$) to values of control cells. Furthermore,HG + BzATP stimulation led to a significant increased expression of TLR-4 expression compared to NG conditions ($p< 0.05$) (Figure 7E). DHTS pre-treatment significantly reduced TLR-4 expression levels compared to HG + BzATP condition ($p< 0.05$ *vs.* HG + BzATP). As observed for IL-6, JNJ47965567 pre-treatment diminished, although not significantly, the

mRNA levels of TLR-4 in endothelial cells challenged with HG + BzATP. The expression at the mRNA level of matrix metallopeptidase 9 (MMP-9), an additional pro-inflammatory marker, NADPH oxidase 2, a pro-oxidant enzyme, and transforming growth factor beta-1 (TGF-β1), an anti-inflammatory cytokine, was measured. We did not detect any significant changes for these three targets under our experimental conditions (data not shown).

P2X7R, Cx-43, VEFG-A, and ICAM-1 expression

In order to assess the effects of HG and P2X7R activation on the expression of connexin-43 (Cx-43) and P2X7R we carried out quantitative real-time PCR (qRT-PCR) experiments. Furthermore, accordingly to pathophysiology markers of DR, we included in our analysis assessment the study of VEGF-A and ICAM-1 mRNA levels under our experimental conditions (Figure 8). The treatment with HG + BzATP significantly raised P2X7R, VEFG-A, and ICAM-1 mRNA expression levels in endothelial cells compared to NG conditions ($p< 0.05$), while an opposite effect was observed for Cx-43 ($p< 0.001$). JNJ47965567 or DHTS pre-treatment significantly counteracted the over-expression of P2X7R, VEGF-A, and ICAM-1 induced by HG + BzATP treatment, and rescued Cx-43 expression levels to values of control cells (NG condition).

Discussion

BRB dysfunction represents a well-known hallmark of DR [37], however the molecular mechanisms underlying this damage are not fully elucidated yet. To shed more light on these mechanism we employed our recently developed BRB triple co-culture model [38]. An alternative BRB triple co-culture model was previously developed byWisniewska-Kruk and colleagues in which bovine endothelial cells and pericytes, and rat astrocytes were used to study the effects of VEGF stimulation [39]. Despite the substantial contribution to the understanding of BRB dysfunction, it is worth of note that the authors employed a mixed (bovine/rat) system, a bit far from human BRB. Our system used only human cells with the same *in vivo cellular numerical ratio, mimicking* the human milieu. However, there are other innovate systems such as BRB-on-chip trying to mimic and control the microenvironment, even though no iBRB-on-chip based on human triple co-culture has been proposed so far [40,41].

During the last decade, the signaling pathway of P2X7R, an ATP gated purinergic channel, has been associated with inflammatory phenomena at retinal level [42].Accordingly to the established liaison between inflammasome NLRP3 and P2X7R, channel activation is linked

to release of mature inflammatory cytokines [43], after inflammatory priming linked to the activation of the receptor for advanced glycation end product (RAGE) and signaling mediated by TLR-4. Therefore, various inflammatory cytokines (e.g., IL-1β and TNF-α) produced by different retinal cell types, such as endothelial cells, have been found to be increased in vitreous and aqueous humor from patients with the early stages of DR [44], strengthening the role of inflammation in disease progression [45]. In fact, before approval of anti-VEGF for treatment of diabetic macular edema, intravitreal steroids were considered the standard of care in DR treatment [46]. Previous preclinical studies highlighted the leading role of P2X7R in modulation of inflammation in *in vitro* and *in vivo* models of DR [36,47-50], along with the modulation of the expression of tight- and adherens junctions in endothelial monolayer [32]. P2X7R antagonists were reported to counteract inflammation in several animal and *in vitro* models of retinal diseases [51-54]. P2X7R antagonists were initially designed as anti-cancer agents, but did not reach the market, due to clinical trial failures [55]. Currently, a selective P2X7 antagonist designed by Janssen is tested in a phase II clinical trial for the treatment of depression [55]. Searching for novel effective P2X7R antagonists, we carried out a virtual screening on a small in-house compound dataset, previously screened for discovery of Elav-1 Hur inhibitors [35,56]. Our virtual screening and MM-GBSA rescoring identified DHTS as a hit P2X7R antagonist. MM-GBSA calculations provide high correlation of binding energy *vs.* experimental activity of congeneric or non-congeneric series of compounds [57-59] and this computational approach was already validated for P2X7R allosteric antagonists. Although, we did not provide single channel electrophysiological studies for characterization of DHTS activity at P2X7R, predicted binding free energy supported the hypothesis that DHTS would be a P2X7R allosteric antagonist. Therefore, we tested in vitro the activity of DHTS as P2X7R antagonist in a triple culture model of iBRB, exposed to the HG and BzATP (selective P2X7R agonist) challenge [32,60,61]. In this experimental paradigm we included as positive P2X7R antagonist control the validated P2X7R antagonist JNJ47965567. Since a well-defined BRB damage can be detected both at both 24 and 48 h [33,62], we challenged the BRB system with a HG/BzATP insult and evaluated the barrier integrity at these time points. As expected, the stimulation with HG/BzATP determined a significant decrease of TEER values after 24 h compared to NG conditions, that further decreased after 48 h challenge (Figure 2). The TEER results are correlated with the significant increased Na-F permeability through the BRB (Figure 3), indicating a dysfunction of the retinal barrier under hyperglycemic conditions, a clinical state often observed in DR patients that are not

under strict glycemic control [63]. These results are also in accordance with previous findings showing a reduced retinal blood flow and disrupted vascular function in the diabetic retina due to P2X7R activation [42]. Of note, the DHTS treatment, similarly to JNJ47965567, during HG/BzATP stimulation preserved the BRB integrity, according to TEER and Na-F data (Figures 2 & 3). The protective potential of both molecules, that antagonized HG/BzATP-induced BRB damage, was also confirmed by the modulation of the expression of endothelial junctional proteins (Figures 4 & 5), according to previous findings on endothelial mono-culture [32]. Reduced ZO-1 and VE-cadherin expression, at membrane cell-cell interface, is one of the causes of BRB permeability in DR pathology, therefore P2X7R activity modulation by selective antagonist would have an important translational impact [64-68].

Along with inflammation, another factor the contributes to DR progression is oxidative stress [69,70]. As shown by El-Remessy *et al.*, increased oxidative stress due to the formation of different reactive species such as nitric oxide, superoxide, and their reaction product peroxynitrite, significantly contributes to the diabetes-induced endothelial dysfunction and death [71]. Furthermore, Shibada *et al.* reported that the activation of P2X7R led to the retinal microvessels toxicity, inducing the overproduction of ROS [49]. It is also well-known that the progressive dysfunction of endothelial cells plays a pivotal role in BRB breakdown and other vascular alterations such as the loss of perivascular cells and dysregulated neovascularization [72]. However, despite that, molecular mechanisms leading to endothelial cells dysfunction during DR development are not completely understood yet and need to be further investigated. In consideration of the results showing the dysregulation of endothelial junction proteins after HG/BzATP insult (Figures 4 & 5) [32], we aimed at exploring the gene-expression network linked to P2X7R signaling in endothelial cells, part of the BRB model. Therefore, we analyzed mRNA levels of inflammatory cytokines, TLR- 4 receptor, VEGF-A, ICAM-1, P2X7R, and Cx-43 in endothelial cells pre-treated with DHTS, a predicted P2X7R antagonist. Regulation of gene expression in our system can be an indirect effect of P2X7R activity regulation, along with inflammasome recruitment and activation [43,73]. This hypothesis is supported by a previous study focused on VEGF expression, which was linked to inflammasome activation and purinergic signaling involving $P2Y_2$ receptor [74]. We included a JNJ47965567 treatment group as positive P2X7R antagonist control.

We also focused on the intracellular production of total ROS in endothelial cells, showing that their levels, significantly increased as a consequence of HG/BzATP treatment, were

significantly decreased by the presence of DHTS and JNJ47965567, that antagonized the BzATP damage (Figure 6). We also examined the expression levels of TLR-4, a receptor linking oxidative stress and inflammatory priming in DR [75], along with the mRNA levels of IL-1β, IL-6, TNF-α, and IL-8 in endothelial cells. As expected, HG/BzATP treatment led to a significant increase in the expression levels of TLR-4 mRNA as well as all the mRNAs of the analyzed pro-inflammatory cytokines (Figure 7); these changes were paralleled by enhanced intracellular levels of ROS compared to control conditions (NG) (Figure 6). Of note, differently by JNJ47965567, the pre-treatment with DHTS significantly decreased the expression levels of TLR-4 and ofIL-1β, IL-6, TNF-α, and IL-8 in endothelial cells induced by HG/BzATP treatment (Figure 7). Worthy of note, JNJ47965567 significantly decreased IL-1β, TNFα and IL-8 expression levels, while decreased, although not significantly, TLR-4 and IL-6 expression levels; therefore, DHTS, bearing a multimodal activity, would affect through other signaling pathways the expression of TLR-4 and IL-6. These data are in accordance with a very recent publication of Yuan *et al.* demonstrating that DHTS exhibits an anti-inflammatory effect both *in vitro* and *in vivo* by acting on TLR-4 [76]. In line with our findings, other studies have shown the potential antioxidant and anti-inflammatory activities of both DHTS and JNJ47965567 in different experimental disease models characterized by oxidative stress and inflammation [36,77-79].

As mentioned before, it has been shown that P2X7R activation leads to increased ROS production in retinal micro-vessels [30] and VEGF release [80], the latter being able to initiate BRB breakdown in early diabetes [81]. VEGF-A is an established target and biomarker of DR [82], and DHTS has been shown to modulate TNF-α and VEGF expression by inhibiting Elav-1 (HuR) protein [35,56]. P2X7R agonist BzATP increased the expression level of VEGF-A mRNA (Figure 8). This enhanced expression was accompanied by the modulation of the expression of other two factors strictly related to BRB damage and DR progression, Cx-43 and ICAM-1. In particular, the junctional endothelial protein Cx-43 was down-regulated by the challenge with HG/BzATP, according with other studies in which its Cx-43 decreased levels are associated with the promotion of retinal vascular lesions typical of DR [83,84]. The present results are also in line with our recent findings obtained by employing an endothelial cell monolayer where the presence of BzATP significantly down-regulated the expression of Cx-43 compared to NG conditions [32]. The pre-treatment with JNJ47965567 or DHTS led to Cx-43 expression levels to values comparable of control cells. The same protective effects were observed by the analyses of ICAM-1 expression; in fact, both JNJ47965567 and DHTS molecules were able

to counteract the ICAM-1 up-regulation induced by HG/BzATP (Figure 8). This is relevant since ICAM-1 over-expression has been associated with diabetic retinal leukostasis and vascular leakage in a rat model of streptozotocin-induced diabetes [19]. Furthermore, a clinical study showed a remarkable association between the genotype distribution or the allele frequency of the ICAM-1 K469E polymorphism and the risk to develop DR in type 2 diabetes mellitus patients [85]. Other findings linked the production of VEGF with the induction of ICAM-1 and retinal leucocyte adhesion, culminating in BRB breakdown and endothelial cell injury along with promotion of neovascularization [82]. Our findings evidenced that DHTS is an intriguing compound with multifunctional activity; because it seems to antagonize HG/BzATP stimuli, at least in our in vitro model, we can speculate that DHTS might inhibit P2X7R activity. Furthermore, we explored the expression network linked to P2X7R signaling, highlighting that modulation of P2X7R activity would impact retinal response through several biochemical pathways, such as angiogenesis and leukostasis. Therefore, P2X7R as pharmacological target for treatment of DR, is worthy of further studies along with the pharmaceutical development of DHTS (hit compound-P2X7R antagonist) for the treatment of DR.

Materials and Methods

Materials and reagents

All materials and reagents were of analytical grade and purchased from Thermo Fisher Scientific (Waltham, MA, USA) or Sigma-Aldrich (St. Louis, MO, USA) unless specified otherwise. The three human retinal cell lines (endothelial cells, pericytes, and astrocytes) along with astrocyte cell medium (AM), pericyte cell medium (PM), endothelial cell medium (ECM), endothelial cell growth supplement (ECGS), fetal bovine serum (FBS), pericyte supplement factor (PGS), astrocytes supplement factor (AGS), polylysine (PLL), and penicillin–streptomycin were purchased from INNOPROT (Derio, Bizkaia, Spain). JNJ47965567 was purchased by Tocris Bioscience (Bristol, UK). Cell culture inserts, 75 cm^2 polystyrene culture flasks, 12- and 96-well plates, and rat-tail collagen type I were obtained from Corning Inc. (Corning, NY, USA). 2',7'-dichlorofluorescin diacetate (DCFDA)—cellular ROS assay kit was purchased from Abcam (Cambridge, UK). Anti-VE-cadherin (2500) primary antibody was supplied by Cell Signaling (Leiden, Netherlands). Sodium fluorescein (Na-F) was obtained from Santa Cruz Biotechnology, Inc. (Dallas, TX, USA).The materials necessary to perform qRT-PCR experiments

(QuantiTect SYBR Green PCR Kit, RNase-free DNase Set, and QuantiTect Primer Assays) were purchased from Qiagen (Hilden, Germany), while 18S rRNA, TLR-4, P2X7R, Cx-43, and ICAM-1 primers were all purchased by Eurofins MWG Synthesis GmbH (Ebersberg, Germany).

Molecular modeling and molecular docking

The human full-length model of P2X7R has been built with the advanced homology modeling task of Schrodinger Maestro, using the following input: primary sequence (uniprot accession# Q99572) and the template full-length rat P2X7 apo structure (PDB:6U9V). The hP2X7 model was minimized with the Prime® Schrodinger Maestro task, using implicit solvation and membrane. The protein model quality check has been carried out and Ramachandran plot calculated. SitMap® identified three druggable pockets, the allosteric, orthosteric and cytosolic cavities at hP2X7 full-length model. Glide® grids were built and grid origin was fixed at the center of mass of the SitMap pockets. The previously published compounds database [35] was modified including validated allosteric P2X7R agonists. The virtual screening was carried out at allosteric P2X7R pocket, according to a previous published protocol [86]. SIFT structural interaction fingerprint analysis [87] was aimed at identification of compounds bearing binding similarity with JNJ47965567, a validated P2X7R allosteric antagonist. Glide® docking was carried out for DHTS at allosteric, orthosteric, and cytosolic pockets. MMGBSA calculation, using implicit solvation and membrane, was carried out according to previous published protocol [36].

Cell culture protocol and treatment

A previous human triple co-culture BRB model [33] was used in the present study. Briefly, after plates and inserts PLL coating, human retinal pericytes were seeded on the bottom side of the insert. After an incubation step, inserts were rotated of 180° and inserted into a 12-well plate containing pericytes medium. Human retinal astrocytes were seeded on a 12-well plate containing astrocytes medium and left to incubate overnight. The day after, the inserts containing pericytes were moved into the 12-well plate holding astrocytes, and human retinal endothelial cells were seeded on the top side of the insert. At this point, the three cell types were maintained in a medium consisting of a mixture of the three cell lines' media (1:1:1). The day of the experiment, the medium was added of glucose (at the final concentration of 40 mM; indicated as HG) + BzATP (200 μM), in the absence or in the presence of JNJ47965567 (100 nM) or DHTS (500 nM) for 48 h, while the co-culture

medium containing a physiological glucose concentration (5 mM; indicated as NG) was used as control [32]. In particular, JNJ47965567 or DHTS were used as a pre-treatment of 2 h. The selection of BzATP (selective P2X7R agonist), JNJ47965567 (selective validated allosteric P2X7R antagonist), and DHTS (putative allosteric P2X7R antagonist) concentrations was made based on preliminary studies (dose response) carried out in our in vitro BRB model (data not shown). BzATP was always used in combination with HG based on previous results obtained by stimulating endothelial cell monolayer with HG, BzATP, or a combination of them (the latter being more effective) [32], as well as in preliminary experiments carried out on our BRB model.

BRB integrity assessment

The activity of DHTS and JNJ47965567 as antagonists of HG + BzATP challenge was evaluated by measurements of TEER by using a Millicel-Electrical Resistance System (ERS2) (Merck, Millipore, Burlington, MA, USA) at different time points: 0 (T0), 1 (T24), and 2 (T48) days after treatment as previously described [33,88]. TEER values were obtained from there independent experiments.

To evaluate the modification of paracellular permeability under the above-mentioned conditions, the luminal-to-abluminal movements of sodium fluorescein (Na-F) across endothelial cell monolayers after 48 h of treatment were measured by using a Varioskan Flash microplate reader (Thermo Fisher Scientific, Waltham, MA, USA) as previously described [33].

Immunocytochemistry

Astrocytes, pericytes and endothelial cells were characterized as previously described [33]. The details regarding the immunocytochemistry analysis of ZO-1 and VE-cadherin on endothelial cells are reported in [33]. Briefly, to evaluate ZO-1 expression levels, endothelial cell monolayers were washed in PBS, fixed with ice-cold acetone (−20 °C for 15 min), and incubated with ice-cold methanol (−20 °C for 20 min). Cells were then permeabilized with a solution containing PBS, NGS (5%), and Triton-X 100 (0.1%) for 10 min at RT and incubated with ZO-1 antibody (1:100) overnight at 4 °C. After PBS washings, endothelial cells were incubated with FITC-conjugated goat anti-rabbit antibody (1:300) for 1 h at RT in the dark, while cell nuclei were marked by using DAPI (1:10000) for 10 min at RT in the dark. To assess VE-cadherin expression levels, endothelial cells were fixed in 4% PFA for 10 min at RT, permeabilized with a solution containing Triton-X 100 (0.3%) at RT for 5 min, washed three times in PBS, and blocked with BSA (1%)/PBS

for 1 h at RT. Cells were then incubated with VE-cadherin (1:100) antibody overnight at 4 °C. Next, endothelial cells were washed in PBS, incubated with FITC-conjugated goat anti-rabbit (1:300) for 1 h at RT in the dark, and incubated with DAPI for 10 min at RT in the dark.

The semi-quantitative evaluation of ZO-1 and VE-cadherin expression levels was carried out as previously described [32,33]. Briefly, coverslips were mounted on glass slides through the use of mounting medium and analyzed by using a Leica TCS SP8 confocal laser scanning microscope (Leica Biosystems, Wetzlar, Germany) or an epifluorescent Zeiss Observer Z1 microscope (Carl Zeiss Microscopy GmbH, Oberkochen, Germany). ZO-1 and VE-cadherin immunostaining images were acquired at 40× magnification and analyzed with ImageJ software [89]. Measurements of average gray scale intensity were carried out at the cell-cell interface in 10 random areas of 10 image rotations [32]. A number of cells higher than 30 was analyzed for each condition.

Measurement of ROS production

The ability of JNJ47965567 and DHTS in counteracting the changes in intracellular ROS due to HG + BzATP treatment for 48 h was carried out in endothelial cells, part of the *in vitro* tri-culture model, using a 2',7'-dichlorofluorescin diacetate (DCFDA) cellular ROS assay kit according to the manufacturer's recommendations. To determine total ROS formation, the fluorescence (485 nm excitation/535 nm emission) was measured by using a Varioskan Flash microplate reader and normalized to the fluorescent intensity of control conditions (NG).

qRT-PCR

The procedure to extract the RNA by TRIzol reagent from the endothelial cells, part of the *in vitro* BRB model, is the same recently described by us [32]. RNA concentrations were determined by measuring the absorbance (260 nm) with a NanoDrop® ND-1000 (Thermo Fisher Scientific) and the RNA quality was tested by Qubit® 3.0 Fluorometer (Thermo Fisher Scientific Inc. (Pittsburgh, PA, USA). For reverse transcription, sample amplification, fluorescence data collection and sample quantification, the same protocol as previously described was used [90,91]. The details regarding QuantiTect Primer Assays employed for the gene expression analysis is reported in Table 2.

The sequences of the primers purchased by Eurofins MWG Synthesis GmbH (Ebersberg, Germany) are the following: 18S rRNA (forward: 5'-AGT CCC TGC CCT TTG TAC ACA-3'; reverse: 5'-GAT CCG AGG GCC TCA CTA AAC-3'), TLR-4 (forward: 5'-ATA

TTG ACA GGA AAC CCC ATC CA-3'; reverse: 5'-AGA GAG ATT GAG TAG GGG CAT TT-3'), P2X7R (forward: 5'-AAG CTG TAC CAG CGG AAA GA-3'; reverse: 5'-GCT CTT GGC CTT CTG TTT TG-3'), Cx-43 (forward: 5'-GAG TTT GCC TAA GGC GCT C-3'; reverse: 5'-AGG AGT TCA ATC ACT TGG CG-3'),ICAM-1 (forward: 5'-ATG CCC AGA CAT CTG TGT CC-3'; reverse: 5'-GGG GTC TCT ATG CCC AAC AA-3'), and MMP-9 (forward: 5'-CTT TGA GTC CGG TGG ACG AT-3'; reverse: 5'-TCG CCA GTA CTT CCC ATC CT-3'. The gene 18 rRNA was selected as internal control gene to normalize the RNA levels of each gene of interest. Fold changes were calculated by relative quantification ($2^{-\Delta\Delta Ct}$) method.

Statistical analysis

Statistical analysis was performed by using GraphPad Prism 7 (GraphPad Software, La Jolla, CA). One-way or two-way analysis of variance (ANOVA), followed by Tukey *post hoc* test, was used for multiple comparisons. Only two-tailed *p*-values < 0.05 were considered statistically significant. All experiments were performed at least in triplicate and reported as means ± standard deviation (SD).

Conclusions

The effects of the combined treatment with high glucose (HG) and the selective P2X7R agonist 2'(3')-O-(4-Benzoylbenzoyl)adenosine-5'-triphosphate (BzATP) were investigated in our recently developed *in vitro*BRB model, more closely mimicking the inner retinal barrier compared to cell monolayer, entirely based on human retinal cells. This stimulation led to significant BRB breakdown (decreased TEER and increased Na-F permeability), along with significant reduction of both ZO-1 and VE-cadherin in endothelial cells. An increased oxidative stress, measured as total intracellular ROS, and an up-regulation of the genes responsible for the formation of P2X7R and pro-inflammatory mediators was also observed in endothelial cells, part of the BRB model.The predicted P2X7R allosteric antagonist DHTS and the validated P2X7R antagonist JNJ47965567 significantly antagonized HG/BzATP-induced damage in our BRB model.. In particular, DHTS mantained the integrity of the BRB and preserved the expression levels of endothelial junction proteins, ZO-1 and VE-cadherin. The increase of the expression of TLR-4 gene as well as of IL-1β, IL-6, TNF-α, and IL-8 pro-inflammatory genes was also significantly counteracted by both compounds, with the DHTS showing a greater protective effect againstHG/BzATP insult. The anti-inflammatory features along with the antioxidant action

of DHTS were also demonstrated by the down-regulation of VEGF-A and ICAM-1 mRNA expression levels, the rescue of Cx-43, and the decrease in total ROS.

In conclusion, we provided new findings pointing out the therapeutic potential of DHTS in preventing and/or counteracting the blood retinal barrier dysfunctions elicited by high glucose and P2X7R activation.

Author Contributions: Conceptualization, C.G.F., G.C., A.F. and C.B.; Validation, C.G.F., G.C. and A.F.; Formal Analysis, C.G.F., G.C., A.F. and C.B.M.P.; Investigation, C.G.F., G.C., A.F., C.B.M.P., and N.M.; Resources, F.C., F.D. and C.B.; Data Curation, C.G.F., G.C., A.F., C.B.M.P., and N.M.; Writing – Original Draft Preparation, C.G.F., G.C. and A.F.; Writing – Review & Editing, C.G.F., G.C., A.F., C.B.M.P., N.M., F.C., F.D. and C.B.; Visualization, C.G.F., G.C. and A.F.; Supervision, C.B.; Project Administration, F.C., F.D. and C.B.; Funding Acquisition, F.C. and C.B..

Funding: This research was funded by National Grant PRIN 2015JXE7E8 from Ministry of Education, University and Research (MIUR); PIACERI 2020/2022– Linea Intervento 2, University of Catania, Italy; Italian Ministry of Economic Development (MISE) PON-Innovative PhD Program XXXIII code E37H18000340006.

Conflicts of Interest: The authors declare no conflict of interest.

References

1. Klein, B.E. Overview of epidemiologic studies of diabetic retinopathy. *Ophthalmic Epidemiol* **2007**, *14*, 179-183.
2. Ting, D.S.; Cheung, G.C.; Wong, T.Y. Diabetic retinopathy: Global prevalence, major risk factors, screening practices and public health challenges: A review. *Clin Exp Ophthalmol* **2016**, *44*, 260-277.
3. Yang, Q.H.; Zhang, Y.; Zhang, X.M.; Li, X.R. Prevalence of diabetic retinopathy, proliferative diabetic retinopathy and non-proliferative diabetic retinopathy in asian t2dm patients: A systematic review and meta-analysis. *Int J Ophthalmol* **2019**, *12*, 302-311.
4. Mizutani, M.; Kern, T.S.; Lorenzi, M. Accelerated death of retinal microvascular cells in human and experimental diabetic retinopathy. *J Clin Invest* **1996**, *97*, 2883-2890.

5. De Vriese, A.S.; Verbeuren, T.J.; Van de Voorde, J.; Lameire, N.H.; Vanhoutte, P.M. Endothelial dysfunction in diabetes. *Br J Pharmacol* **2000**, *130*, 963-974.
6. Ivanova, E.; Alam, N.M.; Prusky, G.T.; Sagdullaev, B.T. Blood-retina barrier failure and vision loss in neuron-specific degeneration. *JCI Insight* **2019**, *5*.
7. Shin, E.S.; Sorenson, C.M.; Sheibani, N. Diabetes and retinal vascular dysfunction. *J Ophthalmic Vis Res* **2014**, *9*, 362-373.
8. Cunha-Vaz, J.; Bernardes, R.; Lobo, C. Blood-retinal barrier. *Eur J Ophthalmol* **2011**, *21 Suppl 6*, S3-9.
9. Runkle, E.A.; Antonetti, D.A. The blood-retinal barrier: Structure and functional significance. *Methods Mol Biol* **2011**, *686*, 133-148.
10. Cholkar, K.; Dasari, S.R.; Pal, D.; Mitra, A.K. Eye: Anatomy, physiology and barriers to drug delivery. In *Ocular transporters and receptors*, Elsevier: 2013; pp 1-36.
11. Thumann, G.; Hoffmann, S.; Hinton, D.R. Cell biology of the retinal pigment epithelium. In *Retina*, Elsevier: 2006; pp 137-152.
12. Osanai, M.; Takasawa, A.; Murata, M.; Sawada, N. Claudins in cancer: Bench to bedside. *Pflügers Archiv-European Journal of Physiology* **2017**, *469*, 55-67.
13. Campbell, H.K.; Maiers, J.L.; DeMali, K.A. Interplay between tight junctions & adherens junctions. *Exp Cell Res* **2017**, *358*, 39-44.
14. Brückner, B.R.; Janshoff, A. Importance of integrity of cell-cell junctions for the mechanics of confluent mdck ii cells. *Scientific reports* **2018**, *8*, 1-11.
15. Rajamani, U.; Jialal, I. Hyperglycemia induces toll-like receptor-2 and -4 expression and activity in human microvascular retinal endothelial cells: Implications for diabetic retinopathy. *J Diabetes Res* **2014**, *2014*, 790902.
16. Vincent, J.A.; Mohr, S. Inhibition of caspase-1/interleukin-1β signaling prevents degeneration of retinal capillaries in diabetes and galactosemia. *Diabetes* **2007**, *56*, 224-230.
17. Joussen, A.M.; Doehmen, S.; Le, M.L.; Koizumi, K.; Radetzky, S.; Krohne, T.U.; Poulaki, V.; Semkova, I.; Kociok, N. Tnf-α mediated apoptosis plays an important role in the development of early diabetic retinopathy and long-term histopathological alterations. *Molecular vision* **2009**, *15*, 1418.
18. Adams, D.H.; Shaw, S. Leucocyte-endothelial interactions and regulation of leucocyte migration. *Lancet* **1994**, *343*, 831-836.

19. Miyamoto, K.; Khosrof, S.; Bursell, S.E.; Rohan, R.; Murata, T.; Clermont, A.C.; Aiello, L.P.; Ogura, Y.; Adamis, A.P. Prevention of leukostasis and vascular leakage in streptozotocin-induced diabetic retinopathy via intercellular adhesion molecule-1 inhibition. *Proc Natl Acad Sci U S A* **1999**, *96*, 10836-10841.
20. Khalfaoui, T.; Lizard, G.; Ouertani-Meddeb, A. Adhesion molecules (icam-1 and vcam-1) and diabetic retinopathy in type 2 diabetes. *J Mol Histol* **2008**, *39*, 243-249.
21. Koopman, W.J.; Nijtmans, L.G.; Dieteren, C.E.; Roestenberg, P.; Valsecchi, F.; Smeitink, J.A.; Willems, P.H. Mammalian mitochondrial complex i: Biogenesis, regulation, and reactive oxygen species generation. *Antioxidants & redox signaling* **2010**, *12*, 1431-1470.
22. Cecilia, O.-M.; José Alberto, C.-G.; José, N.-P.; Ernesto Germán, C.-M.; Ana Karen, L.-C.; Luis Miguel, R.-P.; Ricardo Raúl, R.-R.; Adolfo Daniel, R.-C. Oxidative stress as the main target in diabetic retinopathy pathophysiology. *Journal of diabetes research* **2019**, *2019*.
23. Díaz-Coránguez, M.; Ramos, C.; Antonetti, D.A. The inner blood-retinal barrier: Cellular basis and development. *Vision research* **2017**, *139*, 123-137.
24. Zhao, Y.; Singh, R.P. The role of anti-vascular endothelial growth factor (anti-vegf) in the management of proliferative diabetic retinopathy. *Drugs in context* **2018**, *7*.
25. Shibuya, M. Differential roles of vascular endothelial growth factor receptor-1 and receptor-2 in angiogenesis. *J Biochem Mol Biol* **2006**, *39*, 469-478.
26. Arulkumaran, N.; Unwin, R.J.; Tam, F.W. A potential therapeutic role for p2x7 receptor (p2x7r) antagonists in the treatment of inflammatory diseases. *Expert opinion on investigational drugs* **2011**, *20*, 897-915.
27. Parodi, J.; Flores, C.; Aguayo, C.; Rudolph, M.I.; Casanello, P.; Sobrevia, L. Inhibition of nitrobenzylthioinosine-sensitive adenosine transport by elevated d-glucose involves activation of p2y2 purinoceptors in human umbilical vein endothelial cells. *Circulation research* **2002**, *90*, 570-577.
28. Trueblood, K.E.; Mohr, S.; Dubyak, G.R. Purinergic regulation of high-glucose-induced caspase-1 activation in the rat retinal müller cell line rmc-1. *American Journal of Physiology-Cell Physiology* **2011**, *301*, C1213-C1223.

29. Sathanoori, R.; Swärd, K.; Olde, B.; Erlinge, D. The atp receptors p2x7 and p2x4 modulate high glucose and palmitate-induced inflammatory responses in endothelial cells. *PloS one* **2015**, *10*.
30. Shibata, M.; Ishizaki, E.; Zhang, T.; Fukumoto, M.; Barajas-Espinosa, A.; Li, T.; Puro, D.G. Purinergic vasotoxicity: Role of the pore/oxidant/katp channel/ca2+ pathway in p2x7-induced cell death in retinal capillaries. *Vision* **2018**, *2*, 25.
31. Sugiyama, T. Role of p2x7 receptors in the development of diabetic retinopathy. *World journal of diabetes* **2014**, *5*, 141.
32. Platania, C.B.M.; Lazzara, F.; Fidilio, A.; Fresta, C.G.; Conti, F.; Giurdanella, G.; Leggio, G.M.; Salomone, S.; Drago, F.; Bucolo, C. Blood-retinal barrier protection against high glucose damage: The role of p2x7 receptor. *Biochem Pharmacol* **2019**, *168*, 249-258.
33. Fresta, C.G.; Fidilio, A.; Caruso, G.; Caraci, F.; Giblin, F.J.; Leggio, G.M.; Salomone, S.; Drago, F.; Bucolo, C. A new human blood–retinal barrier model based on endothelial cells, pericytes, and astrocytes. *International Journal of Molecular Sciences* **2020**, *21*, 1636.
34. McCarthy, A.E.; Yoshioka, C.; Mansoor, S.E. Full-length p2x(7) structures reveal how palmitoylation prevents channel desensitization. *Cell* **2019**, *179*, 659-670.e613.
35. Platania, C.B.M.; Pittalà, V.; Pascale, A.; Marchesi, N.; Anfuso, C.D.; Lupo, G.; Cristaldi, M.; Olivieri, M.; Lazzara, F.; Di Paola, L.; Drago, F.; Bucolo, C. Novel indole derivatives targeting hur-mrna complex to counteract high glucose damage in retinal endothelial cells. *Biochem Pharmacol* **2020**, *175*, 113908.
36. Platania, C.B.M.; Giurdanella, G.; Di Paola, L.; Leggio, G.M.; Drago, F.; Salomone, S.; Bucolo, C. P2x7 receptor antagonism: Implications in diabetic retinopathy. *Biochem Pharmacol* **2017**, *138*, 130-139.
37. Eshaq, R.S.; Aldalati, A.M.Z.; Alexander, J.S.; Harris, N.R. Diabetic retinopathy: Breaking the barrier. *Pathophysiology* **2017**, *24*, 229-241.
38. Fresta, C.G.; Fidilio, A.; Caruso, G.; Caraci, F.; Giblin, F.J.; Leggio, G.M.; Salomone, S.; Drago, F.; Bucolo, C. A new human blood-retinal barrier model based on endothelial cells, pericytes, and astrocytes. *Int J Mol Sci* **2020**, *21*.
39. Wisniewska-Kruk, J.; Hoeben, K.A.; Vogels, I.M.; Gaillard, P.J.; Van Noorden, C.J.; Schlingemann, R.O.; Klaassen, I. A novel co-culture model of the blood-

retinal barrier based on primary retinal endothelial cells, pericytes and astrocytes. *Exp Eye Res* **2012**, *96*, 181-190.

40. Ragelle, H.; Goncalves, A.; Kustermann, S.; Antonetti, D.A.; Jayagopal, A. Organ-on-a-chip technologies for advanced blood-retinal barrier models. *J Ocul Pharmacol Ther* **2020**, *36*, 30-41.
41. Caruso, G.; Musso, N. Microfluidics as a novel tool for biological and toxicological assays in drug discovery processes: Focus on microchip electrophoresis. **2020**, *11*.
42. Sugiyama, T. Role of p2x7 receptors in the development of diabetic retinopathy. *World J Diabetes* **2014**, *5*, 141-145.
43. Giuliani, A.L.; Sarti, A.C.; Falzoni, S.; Di Virgilio, F. The p2x7 receptor-interleukin-1 liaison. *Front Pharmacol* **2017**, *8*, 123.
44. Boss, J.D.; Singh, P.K.; Pandya, H.K.; Tosi, J.; Kim, C.; Tewari, A.; Juzych, M.S.; Abrams, G.W.; Kumar, A. Assessment of neurotrophins and inflammatory mediators in vitreous of patients with diabetic retinopathy. *Invest Ophthalmol Vis Sci* **2017**, *58*, 5594-5603.
45. Wu, H.; Hwang, D.K.; Song, X.; Tao, Y. Association between aqueous cytokines and diabetic retinopathy stage. *J Ophthalmol* **2017**, *2017*, 9402198.
46. Bucolo, C.; Gozzo, L.; Longo, L.; Mansueto, S.; Vitale, D.C.; Drago, F. Long-term efficacy and safety profile of multiple injections of intravitreal dexamethasone implant to manage diabetic macular edema: A systematic review of real-world studies. *J Pharmacol Sci* **2018**, *138*, 219-232.
47. Sugiyama, T.; Kawamura, H.; Yamanishi, S.; Kobayashi, M.; Katsumura, K.; Puro, D.G. Regulation of p2x7-induced pore formation and cell death in pericyte-containing retinal microvessels. *Am J Physiol Cell Physiol* **2005**, *288*, C568-576.
48. Kawamura, H.; Sugiyama, T.; Wu, D.M.; Kobayashi, M.; Yamanishi, S.; Katsumura, K.; Puro, D.G. Atp: A vasoactive signal in the pericyte-containing microvasculature of the rat retina. *J Physiol* **2003**, *551*, 787-799.
49. Shibata, M.; Ishizaki, E.; Zhang, T.; Fukumoto, M.; Barajas-Espinosa, A.; Li, T.; Puro, D.G. Purinergic vasotoxicity: Role of the pore/oxidant/k(atp) channel/ca(2+) pathway in p2x(7)-induced cell death in retinal capillaries. *Vision (Basel)* **2018**, *2*.
50. Clapp, C.; Diaz-Lezama, N.; Adan-Castro, E.; Ramirez-Hernandez, G.; Moreno-Carranza, B.; Sarti, A.C.; Falzoni, S.; Solini, A.; Di Virgilio, F. Pharmacological

blockade of the p2x7 receptor reverses retinal damage in a rat model of type 1 diabetes. *Acta Diabetol* **2019**, *56*, 1031-1036.

51. Sanderson, J.; Dartt, D.A.; Trinkaus-Randall, V.; Pintor, J.; Civan, M.M.; Delamere, N.A.; Fletcher, E.L.; Salt, T.E.; Grosche, A.; Mitchell, C.H. Purines in the eye: Recent evidence for the physiological and pathological role of purines in the rpe, retinal neurons, astrocytes, müller cells, lens, trabecular meshwork, cornea and lacrimal gland. *Exp Eye Res* **2014**, *127*, 270-279.
52. Križaj, D.; Ryskamp, D.A.; Tian, N.; Tezel, G.; Mitchell, C.H.; Slepak, V.Z.; Shestopalov, V.I. From mechanosensitivity to inflammatory responses: New players in the pathology of glaucoma. *Curr Eye Res* **2014**, *39*, 105-119.
53. Beckel, J.M.; Argall, A.J.; Lim, J.C.; Xia, J.; Lu, W.; Coffey, E.E.; Macarak, E.J.; Shahidullah, M.; Delamere, N.A.; Zode, G.S.; Sheffield, V.C.; Shestopalov, V.I.; Laties, A.M.; Mitchell, C.H. Mechanosensitive release of adenosine 5'-triphosphate through pannexin channels and mechanosensitive upregulation of pannexin channels in optic nerve head astrocytes: A mechanism for purinergic involvement in chronic strain. *Glia* **2014**, *62*, 1486-1501.
54. Romano, G.L.; Amato, R.; Lazzara, F.; Porciatti, V.; Chou, T.H.; Drago, F.; Bucolo, C. P2x7 receptor antagonism preserves retinal ganglion cells in glaucomatous mice. *Biochem Pharmacol* **2020**, *180*, 114199.
55. Bhattacharya, A. Recent advances in cns p2x7 physiology and pharmacology: Focus on neuropsychiatric disorders. *Front Pharmacol* **2018**, *9*, 30.
56. D'Agostino, V.G.; Lal, P.; Mantelli, B.; Tiedje, C.; Zucal, C.; Thongon, N.; Gaestel, M.; Latorre, E.; Marinelli, L.; Seneci, P.; Amadio, M.; Provenzani, A. Dihydrotanshinone-i interferes with the rna-binding activity of hur affecting its post-transcriptional function. *Sci Rep* **2015**, *5*, 16478.
57. Bharadwaj, S.; Lee, K.E.; Dwivedi, V.D. Discovery of ganoderma lucidum triterpenoids as potential inhibitors against dengue virus ns2b-ns3 protease. **2019**, *9*, 19059.
58. Sakamoto, Y.; Suzuki, Y.; Nakamura, A.; Watanabe, Y.; Sekiya, M.; Roppongi, S.; Kushibiki, C.; Iizuka, I.; Tani, O.; Sakashita, H.; Inaka, K.; Tanaka, H.; Yamada, M.; Ohta, K.; Honma, N.; Shida, Y.; Ogasawara, W.; Nakanishi-Matsui, M.; Nonaka, T.; Gouda, H.; Tanaka, N. Fragment-based discovery of the first nonpeptidyl inhibitor of an s46 family peptidase. **2019**, *9*, 13587.

59. Pittalà, V.; Vanella, L.; Maria Platania, C.B.; Salerno, L.; Raffaele, M.; Amata, E. Synthesis, in vitro and in silico studies of ho-1 inducers and lung antifibrotic agents. **2019**, *11*, 1523-1536.

60. Adamczyk, M.; Griffiths, R.; Dewitt, S.; Knäuper, V.; Aeschlimann, D. P2x7 receptor activation regulates rapid unconventional export of transglutaminase-2. *J Cell Sci* **2015**, *128*, 4615-4628.

61. Di Virgilio, F.; Giuliani, A.L.; Vultaggio-Poma, V.; Falzoni, S.; Sarti, A.C. Non-nucleotide agonists triggering p2x7 receptor activation and pore formation. *Front Pharmacol* **2018**, *9*, 39.

62. Maugeri, G.; D'Amico, A.G.; Gagliano, C.; Saccone, S.; Federico, C.; Cavallaro, S.; D'Agata, V. Vip family members prevent outer blood retinal barrier damage in a model of diabetic macular edema. *J Cell Physiol* **2017**, *232*, 1079-1085.

63. Lobo, C.L.; Bernardes, R.C.; Cunha-Vaz, J.G. Alterations of the blood-retinal barrier and retinal thickness in preclinical retinopathy in subjects with type 2 diabetes. *Arch Ophthalmol* **2000**, *118*, 1364-1369.

64. Umeda, K.; Matsui, T.; Nakayama, M.; Furuse, K.; Sasaki, H.; Furuse, M.; Tsukita, S. Establishment and characterization of cultured epithelial cells lacking expression of zo-1. *J Biol Chem* **2004**, *279*, 44785-44794.

65. McNeil, E.; Capaldo, C.T.; Macara, I.G. Zonula occludens-1 function in the assembly of tight junctions in madin-darby canine kidney epithelial cells. *Mol Biol Cell* **2006**, *17*, 1922-1932.

66. Deissler, H.L.; Deissler, H.; Lang, G.K.; Lang, G.E. Vegf but not plgf disturbs the barrier of retinal endothelial cells. *Exp Eye Res* **2013**, *115*, 162-171.

67. Lee, C.S.; Kim, Y.G.; Cho, H.J.; Park, J.; Jeong, H.; Lee, S.E.; Lee, S.P.; Kang, H.J.; Kim, H.S. Dipeptidyl peptidase-4 inhibitor increases vascular leakage in retina through ve-cadherin phosphorylation. *Sci Rep* **2016**, *6*, 29393.

68. He, J.; Wang, H.; Liu, Y.; Li, W.; Kim, D.; Huang, H. Blockade of vascular endothelial growth factor receptor 1 prevents inflammation and vascular leakage in diabetic retinopathy. *J Ophthalmol* **2015**, *2015*, 605946.

69. Al-Kharashi, A.S. Role of oxidative stress, inflammation, hypoxia and angiogenesis in the development of diabetic retinopathy. *Saudi J Ophthalmol* **2018**, *32*, 318-323.

70. Rivera, J.C.; Dabouz, R.; Noueihed, B.; Omri, S.; Tahiri, H.; Chemtob, S. Ischemic retinopathies: Oxidative stress and inflammation. *Oxid Med Cell Longev* **2017**, *2017*, 3940241.

71. El-Remessy, A.B.; Tawfik, H.E.; Matragoon, S.; Pillai, B.; Caldwell, R.B.; Caldwell, R.W. Peroxynitrite mediates diabetes-induced endothelial dysfunction: Possible role of rho kinase activation. *Exp Diabetes Res* **2010**, *2010*, 247861.

72. Sorrentino, F.S.; Matteini, S.; Bonifazzi, C.; Sebastiani, A.; Parmeggiani, F. Diabetic retinopathy and endothelin system: Microangiopathy versus endothelial dysfunction. *Eye (Lond)* **2018**, *32*, 1157-1163.

73. Karmakar, M.; Katsnelson, M.A.; Dubyak, G.R. Neutrophil p2x7 receptors mediate nlrp3 inflammasome-dependent il-1β secretion in response to atp. **2016**, *7*, 10555.

74. Doktor, F.; Prager, P.; Wiedemann, P.; Kohen, L.; Bringmann, A.; Hollborn, M. Hypoxic expression of nlrp3 and vegf in cultured retinal pigment epithelial cells: Contribution of p2y(2) receptor signaling. *Purinergic Signal* **2018**, *14*, 471-484.

75. Gill, R.; Tsung, A.; Billiar, T. Linking oxidative stress to inflammation: Toll-like receptors. *Free Radic Biol Med* **2010**, *48*, 1121-1132.

76. Yuan, R.; Huang, L.; Du, L.J.; Feng, J.F.; Li, J.; Luo, Y.Y.; Xu, Q.M.; Yang, S.L.; Gao, H.; Feng, Y.L. Dihydrotanshinone exhibits an anti-inflammatory effect in vitro and in vivo through blocking tlr4 dimerization. *Pharmacol Res* **2019**, *142*, 102-114.

77. Bhattacharya, A.; Wang, Q.; Ao, H.; Shoblock, J.R.; Lord, B.; Aluisio, L.; Fraser, I.; Nepomuceno, D.; Neff, R.A.; Welty, N.; Lovenberg, T.W.; Bonaventure, P.; Wickenden, A.D.; Letavic, M.A. Pharmacological characterization of a novel centrally permeable p2x7 receptor antagonist: Jnj-47965567. *Br J Pharmacol* **2013**, *170*, 624-640.

78. Aronica, E.; Bauer, S.; Bozzi, Y.; Caleo, M.; Dingledine, R.; Gorter, J.A.; Henshall, D.C.; Kaufer, D.; Koh, S.; Löscher, W.; Louboutin, J.P.; Mishto, M.; Norwood, B.A.; Palma, E.; Poulter, M.O.; Terrone, G.; Vezzani, A.; Kaminski, R.M. Neuroinflammatory targets and treatments for epilepsy validated in experimental models. *Epilepsia* **2017**, *58 Suppl 3*, 27-38.

79. Yu, L.; Qian, J. Dihydrotanshinone i alleviates spinal cord injury via suppressing inflammatory response, oxidative stress and apoptosis in rats. *Med Sci Monit* **2020**, *26*, e920738.

80. Zhang, Y.; Cheng, H.; Li, W.; Wu, H.; Yang, Y. Highly-expressed p2x7 receptor promotes growth and metastasis of human hos/mnng osteosarcoma cells via pi3k/akt/gsk3β/β-catenin and mtor/hif1α/vegf signaling. *Int J Cancer* **2019**, *145*, 1068-1082.

81. Qaum, T.; Xu, Q.; Joussen, A.M.; Clemens, M.W.; Qin, W.; Miyamoto, K.; Hassessian, H.; Wiegand, S.J.; Rudge, J.; Yancopoulos, G.D.; Adamis, A.P. Vegf-initiated blood-retinal barrier breakdown in early diabetes. *Invest Ophthalmol Vis Sci* **2001**, *42*, 2408-2413.

82. Ahuja, S.; Saxena, S.; Akduman, L.; Meyer, C.H.; Kruzliak, P.; Khanna, V.K. Serum vascular endothelial growth factor is a biomolecular biomarker of severity of diabetic retinopathy. *Int J Retina Vitreous* **2019**, *5*, 29.

83. Bobbie, M.W.; Roy, S.; Trudeau, K.; Munger, S.J.; Simon, A.M.; Roy, S. Reduced connexin 43 expression and its effect on the development of vascular lesions in retinas of diabetic mice. *Invest Ophthalmol Vis Sci* **2010**, *51*, 3758-3763.

84. Tien, T.; Barrette, K.F.; Chronopoulos, A.; Roy, S. Effects of high glucose-induced cx43 downregulation on occludin and zo-1 expression and tight junction barrier function in retinal endothelial cells. *Invest Ophthalmol Vis Sci* **2013**, *54*, 6518-6525.

85. Kamiuchi, K.; Hasegawa, G.; Obayashi, H.; Kitamura, A.; Ishii, M.; Yano, M.; Kanatsuna, T.; Yoshikawa, T.; Nakamura, N. Intercellular adhesion molecule-1 (icam-1) polymorphism is associated with diabetic retinopathy in type 2 diabetes mellitus. *Diabet Med* **2002**, *19*, 371-376.

86. Platania, C.B.M.; Ronchetti, S.; Riccardi, C.; Migliorati, G.; Marchetti, M.C.; Di Paola, L.; Lazzara, F.; Drago, F.; Salomone, S.; Bucolo, C. Effects of protein-protein interface disruptors at the ligand of the glucocorticoid-induced tumor necrosis factor receptor-related gene (gitr). *Biochem Pharmacol* **2020**, *178*, 114110.

87. Deng, Z.; Chuaqui, C.; Singh, J. Structural interaction fingerprint (sift): A novel method for analyzing three-dimensional protein-ligand binding interactions. *J Med Chem* **2004**, *47*, 337-344.

88. Giurdanella, G.; Lazzara, F.; Caporarello, N.; Lupo, G.; Anfuso, C.D.; Eandi, C.M.; Leggio, G.M.; Drago, F.; Bucolo, C.; Salomone, S. Sulodexide prevents activation of the pla2/cox-2/vegf inflammatory pathway in human retinal

endothelial cells by blocking the effect of age/rage. *Biochem Pharmacol* **2017**, *142*, 145-154.

89. Rueden, C.T.; Schindelin, J.; Hiner, M.C.; DeZonia, B.E.; Walter, A.E.; Arena, E.T.; Eliceiri, K.W. Imagej2: Imagej for the next generation of scientific image data. *BMC Bioinformatics* **2017**, *18*, 529.

90. Caruso, G.; Fresta, C.G.; Fidilio, A.; O'Donnell, F.; Musso, N.; Lazzarino, G.; Grasso, M.; Amorini, A.M.; Tascedda, F.; Bucolo, C.; Drago, F.; Tavazzi, B.; Lazzarino, G.; Lunte, S.M.; Caraci, F. Carnosine decreases pma-induced oxidative stress and inflammation in murine macrophages. *Antioxidants (Basel)* **2019**, *8*.

91. Torrisi, S.A.; Geraci, F.; Tropea, M.R.; Grasso, M.; Caruso, G.; Fidilio, A.; Musso, N.; Sanfilippo, G.; Tascedda, F.; Palmeri, A.; Salomone, S.; Drago, F.; Puzzo, D.; Leggio, G.M.; Caraci, F. Fluoxetine and vortioxetine reverse depressive-like phenotype and memory deficits induced by abeta1-42 oligomers in mice: A key role of transforming growth factor-beta1. *Front Pharmacol* **2019**, *10*, 693.

Figure 1. DHTS is predicted to bind the allosteric site of human P2X7 receptor. A) Ramachandran plot of full-length hP2X7R model, after energy minimization in implicit solvent and membrane. B) Representation of DHTS poses in the orthosteric (magenta Van der Waals spheres) and the allosteric (blue Van der Waals spheres) pockets of P2X7R. C) ligand interaction 2D diagram of DHTS in the orthosteric pocket of P2X7R. D) ligand interaction 2D diagram of DHTS in the allosteric pocket of P2X7R.

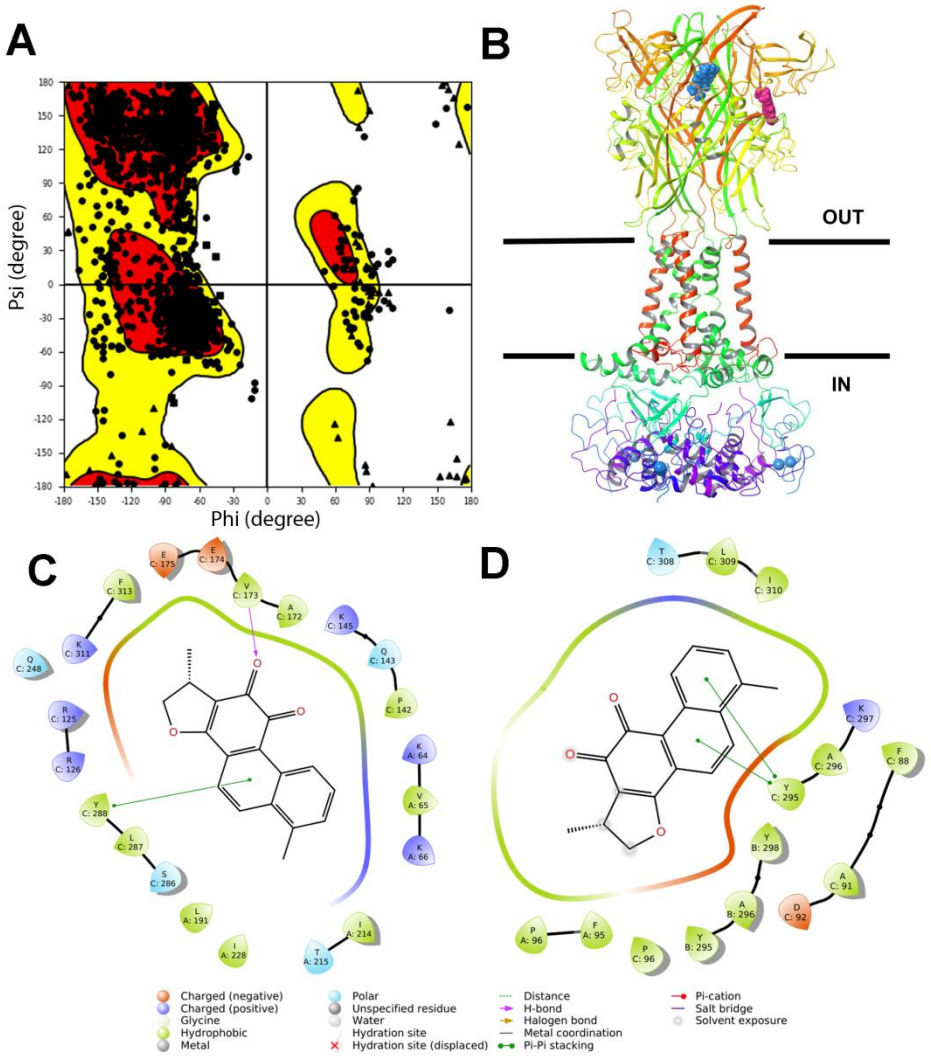

Figure 2. Assessment of barrier integrity in the in vitro human primary culture based triple co-culture iBRB model by TEER under our experimental conditions. TEER values were measured at time 0 (T0), and after 24 (T24) and 48 (T48) h. NG = normal glucose condition (5 mM); HG = high glucose condition (40 mM); BzATP = 200 µM; JNJ47965567 = 100 nM; DHTS = 500 nM. Values are reported as means ± SD of three independent experiments. Statistical analysis was performed using two-way ANOVA with Tukey's post-hoc analysis. *p < 0.05 vs. NG; ***p < 0.001 vs. NG; #p < 0.05 vs. HG + BzATP; $^{###}$p < 0.001 vs. HG + BzATP; ns = not significant.

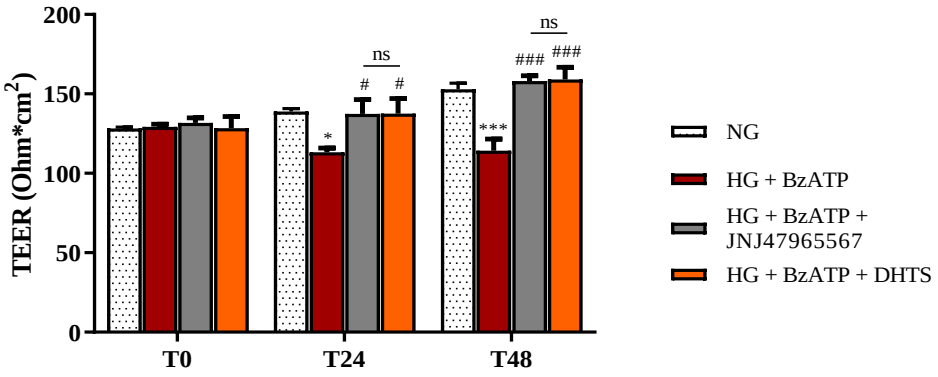

Figure 3. Measurement of apical-to-basolateral Na-F permeability in our iBRB model (in vitro human primary culture based triple co-culture) . Na-F permeability was measured after 5, 15, and 30 min. NG = normal glucose condition (5 mM); HG = high glucose condition (40 mM); RFUs = relative fluorescence units; BzATP = 200 µM; JNJ47965567 = 100 nM; DHTS = 500 nM. Values are reported as means ± SD of three independent experiments. Statistical analysis was performed using two-way ANOVA with Tukey's post-hoc analysis. **p < 0.01 vs. NG; $^{##}$p < 0.01 vs. HG + BzATP; ns = not significant.

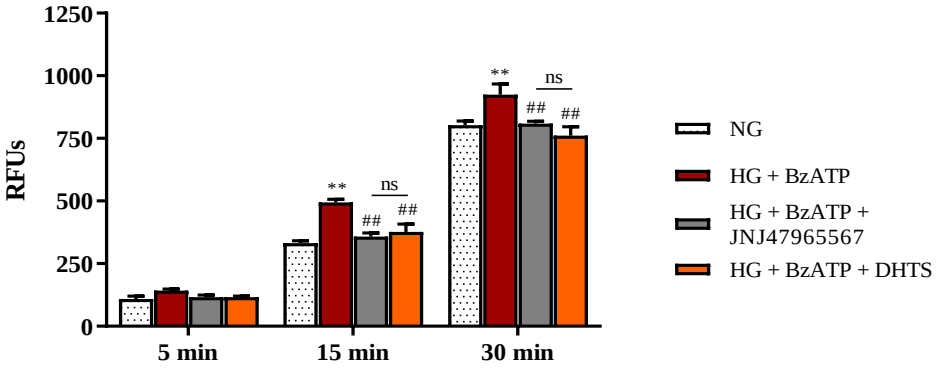

Figure 4. Immunocytochemistry evaluation of ZO-1 staining in endothelial cells subjected to normal or high glucose conditions + BzATP, in the absence or in the presence of JNJ47965567 or DHTS, for 48 h. ZO-1 was labeled with FITC (green) while nuclei were labeled with DAPI (blue). Images for ZO-1 immunostaining were acquired at 40× magnification. NG = normal glucose condition (5 mM); HG = high glucose condition (40 mM); BzATP = 200 µM; JNJ47965567 = 100 nM; DHTS = 500 nM. The average intensity (AU) of the data from more than 30 cells per coverslip for ZO-1 under our experimental conditions are shown. Values are reported as means ± SD of three independent experiments. Statistical analysis was performed using one-way ANOVA with Tukey's post-hoc analysis. ***$p < 0.0001$ vs. NG; $^{###}p < 0.0001$ vs. HG + BzATP; ns = not significant.

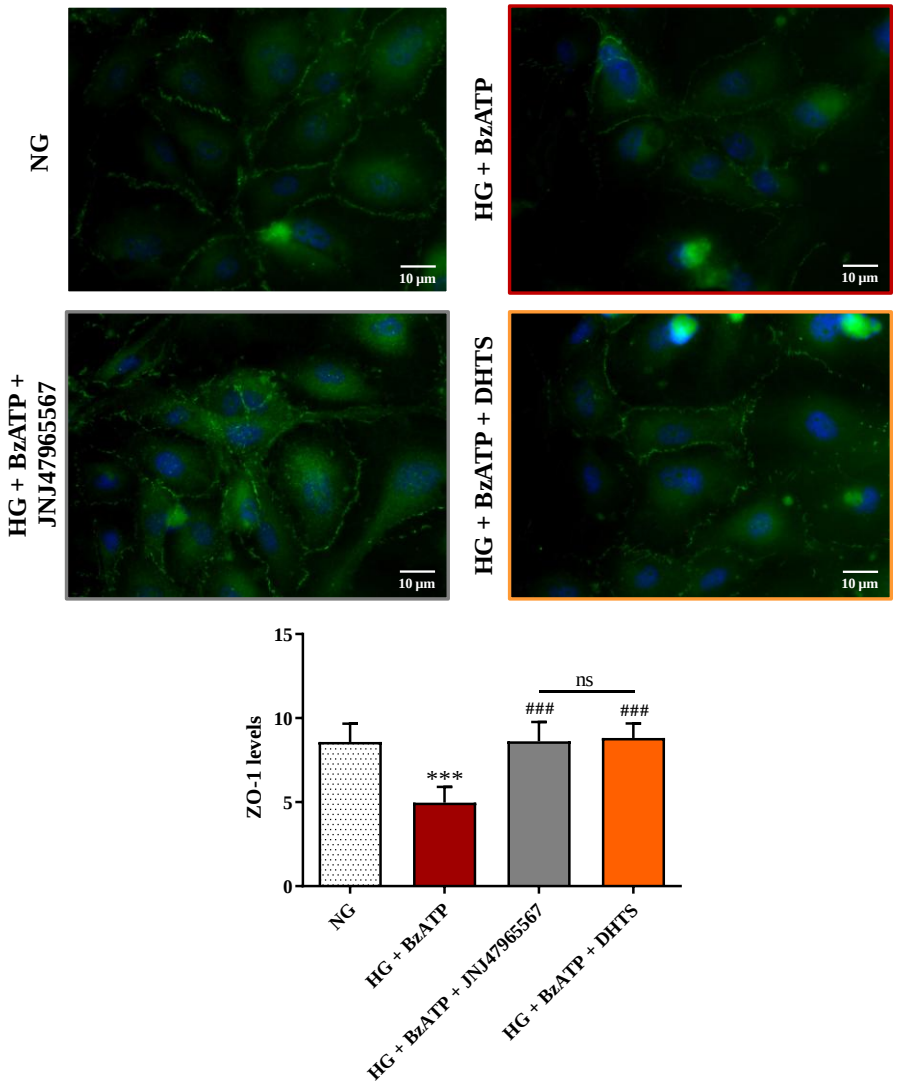

Figure 5. Confocal analysis of VE-cadherin in endothelial cells subjected to normal or high glucose conditions + BzATP, in the absence or in the presence of JNJ47965567 or DHTS, for 48 h. VE-cadherin was labeled with FITC (green) while nuclei were labeled with DAPI (blue). Images for VE-cadherin immunostaining were acquired at 20× magnification. NG = normal glucose condition (5 mM); HG = high glucose condition (40 mM); BzATP = 200 µM; JNJ47965567 = 100 nM; DHTS = 500 nM. The average intensity (AU) of the data from more than 30 cells per coverslip for VE-cadherin under our experimental conditions are shown. Values are reported as means ± SD of three independent experiments. Statistical analysis was performed using one-way ANOVA with Tukey's post-hoc analysis. ***$p < 0.0001$ vs. NG; $^{###}p < 0.0001$ vs. HG + BzATP; ns = not significant.

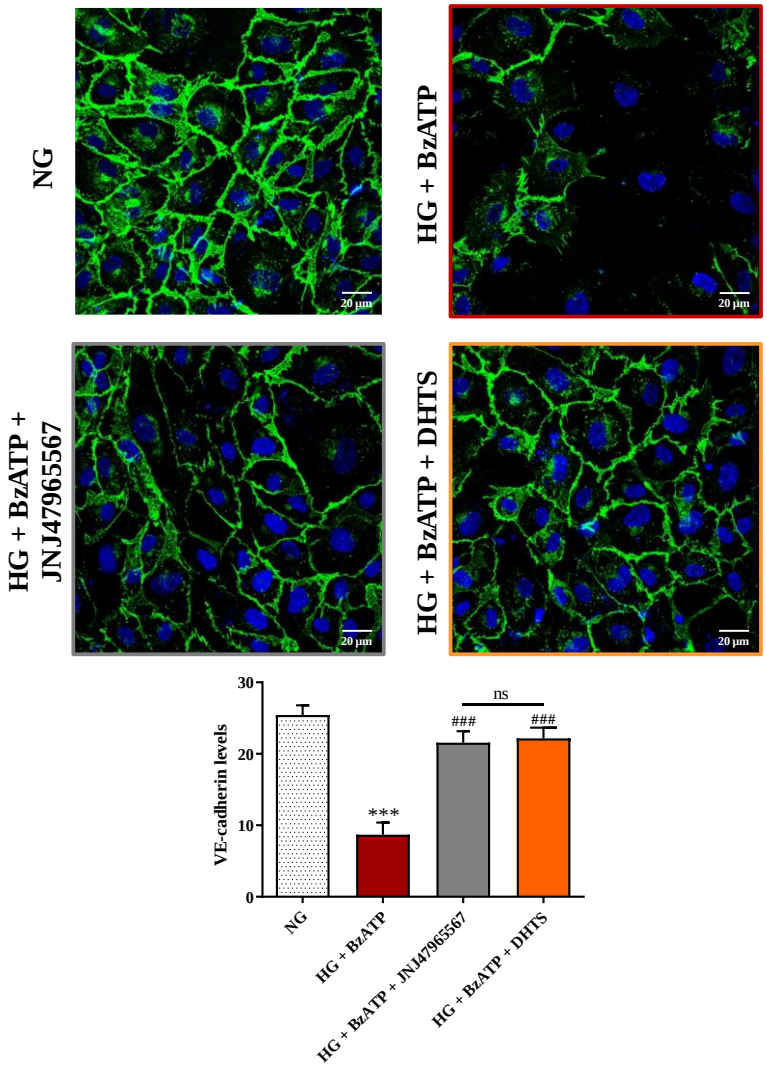

Figure 6. Intracellular ROS production in endothelial cells under our experimental conditions. NG = normal glucose condition (5 mM); HG = high glucose condition (40 mM); BzATP = 200 µM; JNJ47965567 = 100 nM; DHTS = 500 nM. Values are reported as means ± SD of three independent experiments. Two-way ANOVA with Tukey's post-hoc analysis. ***$p < 0.001$ vs. NG; $^{\#\#}p < 0.01$ vs. HG + BzATP; $^{\#\#\#}p < 0.001$ vs. HG + BzATP; ns = not significant.

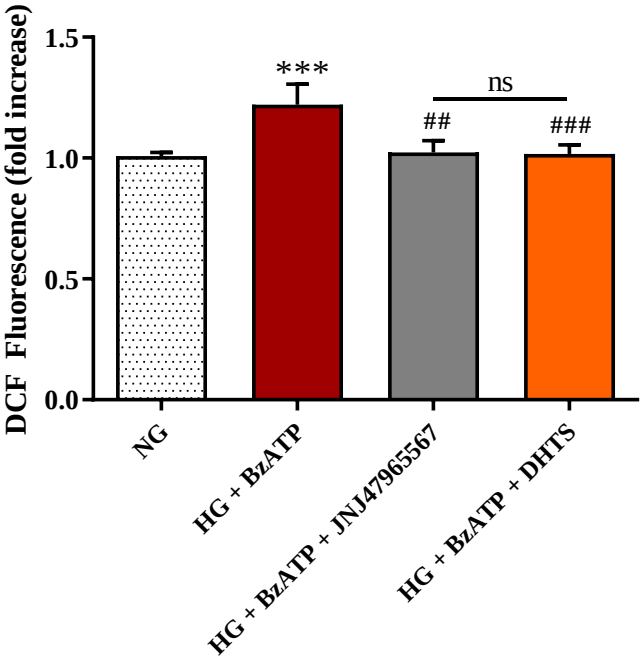

Figure 7. Measurement of A) IL-1β, B) IL-6, C) TNF-α, D) IL-8, and E) TLR-4 mRNA levels (qRT-PCR) in endothelial cells under our experimental conditions. NG = normal glucose condition (5 mM); HG = high glucose condition (40 mM); BzATP = 200 µM; JNJ47965567 = 100 nM; DHTS = 500 nM. The abundance of each mRNA of interest was expressed relatively to the abundance of 18S rRNA, as an internal control. Values are reported as means ± SD of three independent experiments. **p < 0.01 vs. NG; *p < 0.05 vs. NG; ##p < 0.01 vs. HG + BzATP; #p < 0.05 vs. HG + BzATP; ns = not significant.

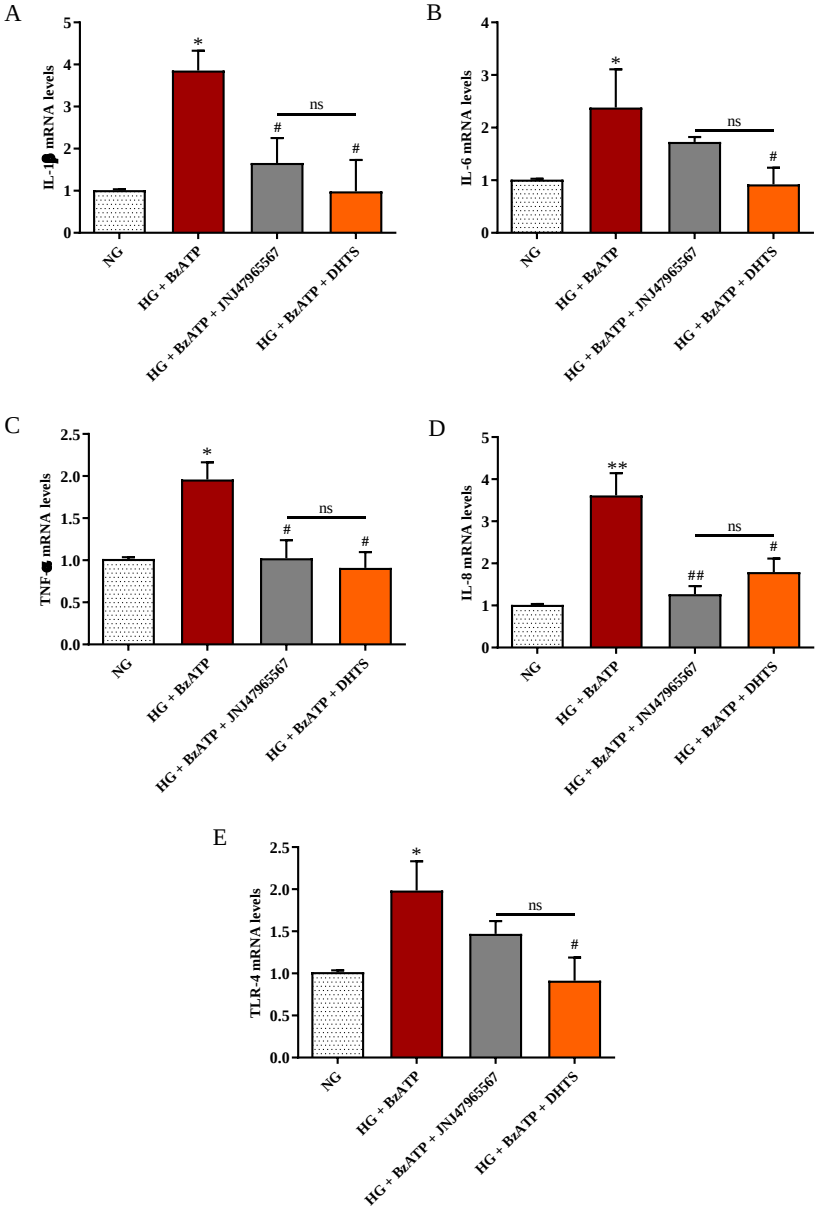

Figure 8. Measurement of A) P2X7R, B) Cx-43, C) VEGF-A, and D) ICAM-1 mRNA expression levels (qRT-PCR) in endothelial cells under our experimental conditions. NG = normal glucose condition (5 mM); HG = high glucose condition (40 mM); BzATP = 200 µM; JNJ47965567 = 100 nM; DHTS = 500 nM. The abundance of each mRNA of interest was expressed relatively to the abundance of 18S rRNA, as an internal control. Values are means ± SD of three independent experiments. *$p < 0.05$ vs. NG; $^{\#\#}p < 0.01$ vs. HG + BzATP; $^{\#}p < 0.05$ vs. HG + BzATP; ns = not significant.

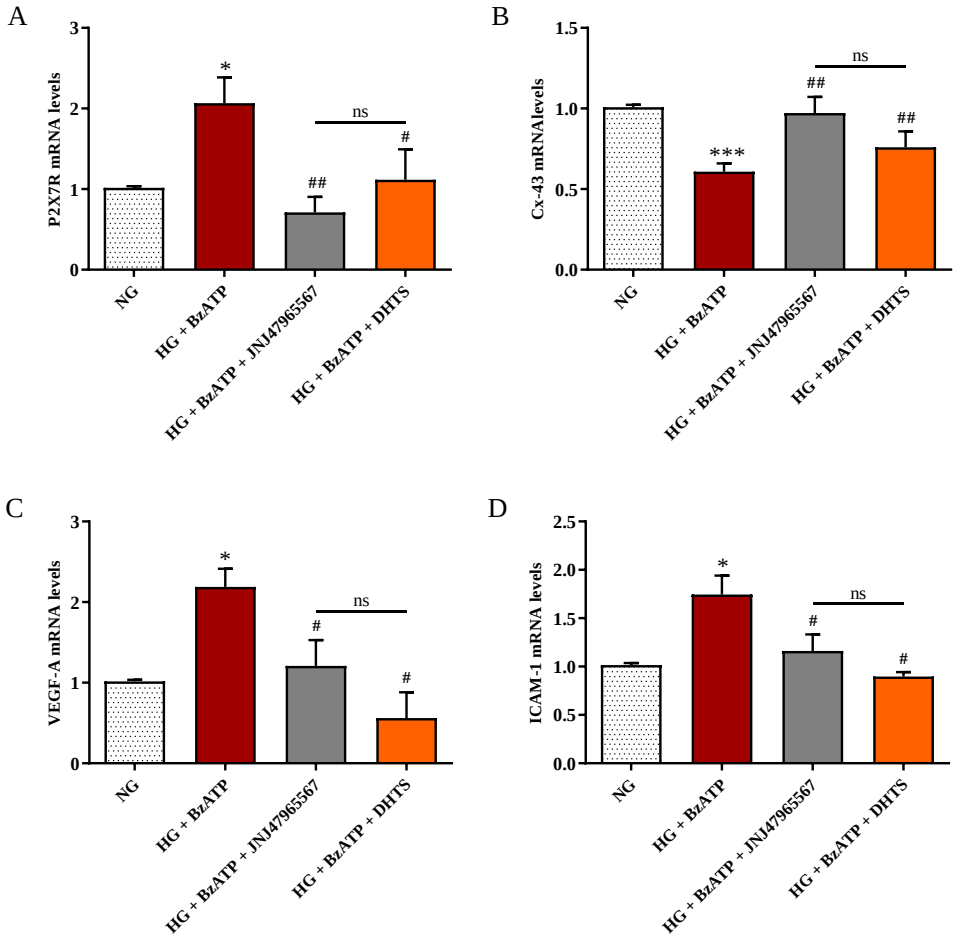

Table 1. Predicted score of P2X7R inhibitors binding. DHTS structural interaction fingerprints clustered with JNJ47965567, validated P2X7R inhibitor. A438079 is another selective P2X7R inhibitor [36], that did not cluster with DHTS or JNJ47965567**.**

	Docking Score	**$\Delta G_{binding}$ allosteric (kcal/mol)**	**$\Delta G_{binding}$ orthosteric (kcal/mol)**	**$\Delta G_{binding}$ cytosolic (kcal/mol)**
DHTS	-7.0	-59	-49	-30
JNJ47965567	-8.0	-86	N.A.	N.A.
A438079	-7.5	-56	N.A.	N.A.
Quercetin	-6.0	-30	-20	-30

Table 2. The list of primers used for qRT-PCR**.**

Official name[#]	Official symbol	Alternative titles/symbols	Detected transcript	Amplicon Length	Cat. No.[§]
interleukin 1, beta	IL1B	IL-1; IL1F2; IL1beta; IL1-BETA	NM_000576; XM_006712496	117 bp 117 bp	QT00021385
interleukin 6	IL6	CDF; HGF; HSF; BSF2; IL-6; BSF-2; IFNB2; IFN-beta-2	NM_000600; XM_005249745	107 bp 107 bp	QT00083720
tumor necrosis factor	TNF	DIF; TNFA; TNFSF2; TNLG1F; TNF-alpha	NM_000594	98 bp	QT00029162
vascular endothelial growth factor A	VEGFA	VPF; VEGF; MVCD1	NM_001025366; NM_001025367; NM_001025368; NM_001033756; NM_001171623; NM_001171624; NM_001171625; NM_001171626; NM_001171629; NM_003376; NM_001287044	273 204 150 150 273 222 204 150 150 222 150	QT01010184
chemokine (C-X-C motif) ligand 8	CXCL8	GCP-1, GCP1, IL8, LECT, LUCT, LYNAP, MDNCF, MONAP, NAF, NAP-1, NAP1, SCYB8	NM_000584	102 bp	QT00000322
cytochrome b-245 beta chain	CYBB	CGD; NOX2; IMD34; AMCBX2; GP91-1; GP91PHOX; p91-PHOX; GP91-PHOX	NM_000397	124 bp	QT00029533
transforming growth factor beta 1	TGFB1	CED; LAP; DPD1; TGFB; IBDIMDE; TGFbeta; TGF-beta1	NM_000660	108 bp	QT00000728

[#]https://www.ncbi.nlm.nih.gov/gene/; [§]https://www.qiagen.com/it/shop/pcr/real-time-pcr-enzymes-and-kits/two-step-qrt-pcr/quantitect-primer-assays/.

DISCUSSION AND CONCLUSIONS

Diabetic retinopathy can be considered a serious complication of diabetes and the leading cause of irreversible vision loss in working-age adults worldwide. DR affects both type I and type II diabetic subjects at any stage of the disease [166]. Despite its first definition as “a purely microvascular disease”, there are now plenty of studies suggesting that DR is a complex neurovascular complication [167]. Indeed, the retinal neural tissue dysfunction leads to microvascular abnormalities. Moreover, the alteration of the interactions between the different cell types forming the neurovascular unit in the retina is associated with the progression of early DR. The vascular pathology of DR has been mainly attributed to hyperglycemia that leads to a complex interaction between cytokines, chemokines and ROS, all factors contributing to the endothelial cell surface changes and BRB breakdown. Therefore, the development of novel therapeutic strategies allowing a deeper understanding of the mechanisms underlying BRB dysfunction are mandatory in order to limit the progression of DR. *In vitro* models of biological barriers are particularly suitable for the investigation of different aspects of BRB function and are useful tools for testing potential drug candidates [40]. The availability of *in vitro* models closely mimicking the iBRB observed *in vivo* are currently missing, making the pre-clinical prediction of the effectiveness of a potential drug complicated. To this end, as reported in Chapter I, the main goal of our studies was the development of the first, high-reproducible *in vitro* iBRB triple co-culture model entirely formed by human retinal endothelial cells, retinal pericytes, and retinal astrocytes closely mimicking the human BRB environment. In order to reproduce a condition very similar to that observed in human beings, we respected and maintained the same cellular layers order and position during the building of the model. More in details, our iBRB

system was assembled by placing endothelial cells in the luminal chamber of a transwell insert, having pericytes on the other side, while the astrocytes were positioned in the luminal compartment of the well. Furthermore, with the aim to mimic the hyperglycemic environment typical of the early phase of DR, we stimulated all cell types forming the iBRB *in vitro* model with high concentrations of glucose (40 mM) for 48 hours.

The HG-induced damage was evaluated by the analysis of several parameters indicative of BRB alteration along with the variation of the expression of oxidative-stress and inflammatory-related mediators. Our results showed a significant decrease of TEER values following HG exposure paralleled by a significant increase in Na-F permeability, both indicating as the hyperglycemic conditions provoked several alterations affecting the structural integrity of the BRB. These finding are in accordance with literature data showing the deleterious effects of HG-induced damage on BRB stability in patients with DR [7].

The disruption of junctional protein complexes, due to a hyperglycemic environment, has been associated with an increased endothelial barrier permeability [168]; in fact the alteration of the distribution of tight and adherents junctions has been identified as a possible mechanism of BRB breakdown in several ocular pathologies, including DR [169]. Taking into consideration the above, we carried out immunofluorescence staining analysis to measure the integrity and the abundance of ZO-1 and VE-cadherin following the exposure of our system to HG. The obtained results showed a significant reduction of the organization pattern of both proteins on endothelial cells, part of our iBRB model, as depicted by discontinuous fluorescence lines at the cell–cell contact with respect to cells maintained under normal glucose conditions (5 mM). Our findings clearly highlight that HG exposure is linked to junctional complexes alteration in the context of

the BRB system; furthermore, our data strengthen the thesis that tight and adherens junction disruption plays a crucial role in chronic BRB dysfunction [7,170].

Diabetic conditions also affect retinal astrocytes function through the alterations of pro-inflammatory and oxidative stress-related mediators production, both playing a crucial role in HG-mediated vascular cell dysfunction [171]. Retinal astrocytes are known to be involved in the regulation of blood vessels as well as in the maintenance of BRB integrity; thus their alteration greatly contributes to the development of neuronal and barrier dysfunction in DR [172]. Since the exact mechanisms underlying astrocytes dysfunction have not been fully elucidated, we aimed to better investigate the role played by this cell type in our iBRB model. We then analyzed the expression of genes related to pro-oxidant enzymes and pro-inflammatory mediators along with the production of total ROS following HG exposure. There was a significant up-regulation of all the genes considered (iNOS, Nox2, IL-1β, IL-6) as well as an increased intracellular ROS production in human retinal astrocytes compared to control cells. These data are in line with other finding showing the involvement of hyperglycaemia-induced inflammatory mediators and ROS over-production in several ocular disorders, such as DR [173].

Under pathological conditions, the negative regulation of the redox homeostasis at cellular level occurs mainly at the transcriptional levels, with nuclear factor (erythroid-derived 2)-like 2 (Nrf2)/heme-oxigenase-1 (HO-1) and NF-κB pathways being strongly activate by hyperglycemic conditions [174]. With this in mind, we investigate the variation on protein expression levels of the above mentioned factors in retinal astrocytes under our experimental condition. We found that HG treatment induced the phosphorylation and then the nuclear translocation of both Nrf2 and NF-κB

as well as an increased expression of HO-1. These data are in agreement with previously findings showing the involvement of both Nrf2/HO-1 axis and NF-κB pathway in the pathogenesis of DR [174].

Once the model was established, we explored new possible pharmacological targets for BRB-related disorders. In particular, we focused our attention on ATP-gated ion channel P2X7R, the activation of which is linked to an increased pro-inflammatory cytokines expression in the retina, mainly through the activation of NLRP3 inflammasome [175]. For this reason, the inhibition of P2X7R could represent an encouraging strategy to limit the microvascular alterations observed in the early phase of DR. In accordance with the aforementioned, we identified, through a bioinformatic approach (already validated for another P2X7R allosteric antagonist, JNJ47965567), the diterpenoid dihydrotanshinone (DHTS) as a possible novel effective P2X7R antagonist. As reported in Chapter II, the ability of DHTS to inhibit P2X7R was tested in the iBRB *in vitro* system exposed to HG and BzATP (selective P2X7R agonist). According to our TEER and Na-F data, the DHTS pre-treatment preserved BRB integrity by the damage HG/BzATP-induced. DHTS was also able to preserve the expression of junctional proteins in endothelial cells, part of the iBRB model. These results point out the important role played by this promising P2X7R antagonist in protecting the structural integrity of the BRB since the dysregulation of endothelial junction proteins represents one of the cause of BRB dysfunction in the progression of DR [37].

Since the activation of P2X7R has been associated with oxidative stress and inflammatory processes, primarily due to the NLRP3 pathway [176], we investigated the gene expression network linked to P2X7R signaling in endothelial cells. In particular, we focused our attention on the pro-inflammatory cytokines IL-1β, IL-6, IL-8, and TNF-α along with toll-like

receptor 4 (TLR-4), a receptor whose activation is linked to inflammation and oxidative stress phenomena [177], at the mRNA level. We found that DHTS was able to significantly reduce the expression levels of all the above pro-inflammatory mediators as well as the intracellular levels of ROS, counteracting the damage caused by the combined HG + BzATP challenge. These results are in line with literature data showing the ability of DHTS in reducing the inflammatory processes by acting on TLR-4 [178]; furthermore, our results are in line with other findings highlighting the anti-inflammatory and anti-oxidant abilities of DHTS in several disorders characterized by oxidative stress and inflammation [179-181].

The activation of the P2X7R signaling by its agonist BzATP leads to the release of VEGF-A, an established DR biomarker involved in the BRB dysfunction observed during the early phase of DR [182]. In our study, DHTS was able to significantly decrease VEGF-A expression levels HG/BzATP-induced as well as the expression of an additional factor involved in BRB breakdown, ICAM-1. Indeed, the up-regulation of ICAM-1, a key factor for leukostasis, is increased in diabetic retina and it is closely related to the pathogenesis of DR [183]. We also demonstrated DHTS ability to counteract the damage exerted by the activation of P2X7R under hyperglycemic condition by restoring connexin 43 (Cx-43) expression levels, the down-regulation of which has been linked to vascular cell loss in DR pathology [184]. These results reinforce our previous findings proving the ability of BzATP to reduce Cx-43 expression levels under hyperglycemic condition [185].

In conclusion, we were able to develop the first high-reproducible *in vitro* human inner BRB system, closely mimicking the *in vivo milieu*, that was used to investigate the therapeutic potential of DHTS in counteracting the BRB dysfunction due to the combination of hyperglycemic conditions and

P2X7R activation. Since DR current treatments are entirely focused on the advanced stages of this pathology, our results contribute, albeit to a small extent, to prompt the scientific community towards the search of therapies targeting the early phase of DR.

References

1. Wong, T.Y.; Cheung, C.M.; Larsen, M.; Sharma, S.; Simó, R. Diabetic retinopathy. *Nat Rev Dis Primers* **2016**, *2*, 16012.
2. Solomon, S.D.; Chew, E.; Duh, E.J.; Sobrin, L.; Sun, J.K.; VanderBeek, B.L.; Wykoff, C.C.; Gardner, T.W. Diabetic retinopathy: A position statement by the american diabetes association. *Diabetes Care* **2017**, *40*, 412-418.
3. Simó, R.; Stitt, A.W.; Gardner, T.W. Neurodegeneration in diabetic retinopathy: Does it really matter? *Diabetologia* **2018**, *61*, 1902-1912.
4. Heintz, E.; Wiréhn, A.B.; Peebo, B.B.; Rosenqvist, U.; Levin, L.A. Prevalence and healthcare costs of diabetic retinopathy: A population-based register study in sweden. *Diabetologia* **2010**, *53*, 2147-2154.
5. Wong, T.Y.; Sabanayagam, C. Strategies to tackle the global burden of diabetic retinopathy: From epidemiology to artificial intelligence. *Ophthalmologica* **2020**, *243*, 9-20.
6. Wang, W.; Lo, A.C.Y. Diabetic retinopathy: Pathophysiology and treatments. *Int J Mol Sci* **2018**, *19*.
7. Eshaq, R.S.; Aldalati, A.M.Z.; Alexander, J.S.; Harris, N.R. Diabetic retinopathy: Breaking the barrier. *Pathophysiology* **2017**, *24*, 229-241.
8. Stitt, A.W.; Curtis, T.M.; Chen, M.; Medina, R.J.; McKay, G.J.; Jenkins, A.; Gardiner, T.A.; Lyons, T.J.; Hammes, H.P.; Simó, R.; Lois, N. The progress in understanding and treatment of diabetic retinopathy. *Prog Retin Eye Res* **2016**, *51*, 156-186.
9. Lechner, J.; O'Leary, O.E.; Stitt, A.W. The pathology associated with diabetic retinopathy. *Vision Res* **2017**, *139*, 7-14.

10. Mishra, C.; Tripathy, K. Retinal traction detachment. In *Statpearls*, StatPearls PublishingCopyright © 2021, StatPearls Publishing LLC.: Treasure Island (FL), 2021.
11. Vaz-Pereira, S.; Morais-Sarmento, T.; Esteves Marques, R. Optical coherence tomography features of neovascularization in proliferative diabetic retinopathy: A systematic review. *Int J Retina Vitreous* **2020**, *6*, 26.
12. Kuiper, E.J.; Van Nieuwenhoven, F.A.; de Smet, M.D.; van Meurs, J.C.; Tanck, M.W.; Oliver, N.; Klaassen, I.; Van Noorden, C.J.; Goldschmeding, R.; Schlingemann, R.O. The angio-fibrotic switch of vegf and ctgf in proliferative diabetic retinopathy. *PLoS One* **2008**, *3*, e2675.
13. Wang, J.; Chen, S.; Jiang, F.; You, C.; Mao, C.; Yu, J.; Han, J.; Zhang, Z.; Yan, H. Vitreous and plasma vegf levels as predictive factors in the progression of proliferative diabetic retinopathy after vitrectomy. *PLoS One* **2014**, *9*, e110531.
14. Santiago, A.R.; Boia, R.; Aires, I.D.; Ambrósio, A.F.; Fernandes, R. Sweet stress: Coping with vascular dysfunction in diabetic retinopathy. *Front Physiol* **2018**, *9*, 820.
15. Gupta, M.P.; Herzlich, A.A.; Sauer, T.; Chan, C.C. Retinal anatomy and pathology. *Dev Ophthalmol* **2016**, *55*, 7-17.
16. Nian, S.; Lo, A.C.Y.; Mi, Y.; Ren, K.; Yang, D. Neurovascular unit in diabetic retinopathy: Pathophysiological roles and potential therapeutical targets. *Eye Vis (Lond)* **2021**, *8*, 15.
17. Masland, R.H. The fundamental plan of the retina. *Nat Neurosci* **2001**, *4*, 877-886.
18. Moran, E.P.; Wang, Z.; Chen, J.; Sapieha, P.; Smith, L.E.; Ma, J.X. Neurovascular cross talk in diabetic retinopathy: Pathophysiological roles and therapeutic implications. *Am J Physiol Heart Circ Physiol* **2016**, *311*, H738-749.

19. Nakahara, T.; Mori, A.; Kurauchi, Y.; Sakamoto, K.; Ishii, K. Neurovascular interactions in the retina: Physiological and pathological roles. *Journal of pharmacological sciences* **2013**, *123*, 79-84.
20. Gu, X.; Neric, N.J.; Crabb, J.S.; Crabb, J.W.; Bhattacharya, S.K.; Rayborn, M.E.; Hollyfield, J.G.; Bonilha, V.L. Age-related changes in the retinal pigment epithelium (rpe). *PLoS One* **2012**, *7*, e38673.
21. Sun, Y.; Smith, L.E.H. Retinal vasculature in development and diseases. *Annu Rev Vis Sci* **2018**, *4*, 101-122.
22. Yu, D.Y.; Cringle, S.J.; Yu, P.K.; Balaratnasingam, C.; Mehnert, A.; Sarunic, M.V.; An, D.; Su, E.N. Retinal capillary perfusion: Spatial and temporal heterogeneity. *Prog Retin Eye Res* **2019**, *70*, 23-54.
23. Metea, M.R.; Newman, E.A. Signalling within the neurovascular unit in the mammalian retina. *Exp Physiol* **2007**, *92*, 635-640.
24. Lott, M.E.; Slocomb, J.E.; Shivkumar, V.; Smith, B.; Gabbay, R.A.; Quillen, D.; Gardner, T.W.; Bettermann, K. Comparison of retinal vasodilator and constrictor responses in type 2 diabetes. *Acta Ophthalmol* **2012**, *90*, e434-441.
25. Pemp, B.; Garhofer, G.; Weigert, G.; Karl, K.; Resch, H.; Wolzt, M.; Schmetterer, L. Reduced retinal vessel response to flicker stimulation but not to exogenous nitric oxide in type 1 diabetes. *Invest Ophthalmol Vis Sci* **2009**, *50*, 4029-4032.
26. Newman, E.A. Glial cell regulation of neuronal activity and blood flow in the retina by release of gliotransmitters. *Philos Trans R Soc Lond B Biol Sci* **2015**, *370*.
27. Ruan, Y.; Jiang, S.; Musayeva, A.; Gericke, A. Oxidative stress and vascular dysfunction in the retina: Therapeutic strategies. *Antioxidants (Basel)* **2020**, *9*.
28. Ihezie, S.A.; Mathew, I.E.; McBride, D.W.; Dienel, A.; Blackburn, S.L.; Thankamani Pandit, P.K. Epigenetics in blood-brain barrier disruption. *Fluids Barriers CNS* **2021**, *18*, 17.

29. Rudraraju, M.; Narayanan, S.P.; Somanath, P.R. Regulation of blood-retinal barrier cell-junctions in diabetic retinopathy. *Pharmacol Res* **2020**, *161*, 105115.
30. Díaz-Coránguez, M.; Ramos, C.; Antonetti, D.A. The inner blood-retinal barrier: Cellular basis and development. *Vision Res* **2017**, *139*, 123-137.
31. Toda, R.; Kawazu, K.; Oyabu, M.; Miyazaki, T.; Kiuchi, Y. Comparison of drug permeabilities across the blood-retinal barrier, blood-aqueous humor barrier, and blood-brain barrier. *J Pharm Sci* **2011**, *100*, 3904-3911.
32. Ragelle, H.; Goncalves, A.; Kustermann, S.; Antonetti, D.A.; Jayagopal, A. Organ-on-a-chip technologies for advanced blood-retinal barrier models. *J Ocul Pharmacol Ther* **2020**, *36*, 30-41.
33. Liu, L.; Liu, X. Roles of drug transporters in blood-retinal barrier. *Adv Exp Med Biol* **2019**, *1141*, 467-504.
34. Hosoya, K.; Tachikawa, M. The inner blood-retinal barrier: Molecular structure and transport biology. *Adv Exp Med Biol* **2012**, *763*, 85-104.
35. Klaassen, I.; Van Noorden, C.J.; Schlingemann, R.O. Molecular basis of the inner blood-retinal barrier and its breakdown in diabetic macular edema and other pathological conditions. *Prog Retin Eye Res* **2013**, *34*, 19-48.
36. Cunha-Vaz, J. The blood–retinal barrier in retinal disease. *Journal-The Blood–Retinal Barrier in Retinal Disease* **2009**.
37. Gui, F.; You, Z.; Fu, S.; Wu, H.; Zhang, Y. Endothelial dysfunction in diabetic retinopathy. *Front Endocrinol (Lausanne)* **2020**, *11*, 591.
38. Curtis, T.M.; Gardiner, T.A.; Stitt, A.W. Microvascular lesions of diabetic retinopathy: Clues towards understanding pathogenesis? *Eye (Lond)* **2009**, *23*, 1496-1508.
39. Meza, C.A.; La Favor, J.D.; Kim, D.H.; Hickner, R.C. Endothelial dysfunction: Is there a hyperglycemia-induced imbalance of nox and nos? *Int J Mol Sci* **2019**, *20*.
40. Yeste, J.; Illa, X.; Alvarez, M.; Villa, R. Engineering and monitoring cellular barrier models. *J Biol Eng* **2018**, *12*, 18.

41. Niessen, C.M.; Gottardi, C.J. Molecular components of the adherens junction. *Biochim Biophys Acta* **2008**, *1778*, 562-571.
42. Fathi, F.; Rezabakhsh, A.; Rahbarghazi, R.; Rashidi, M.R. Early-stage detection of ve-cadherin during endothelial differentiation of human mesenchymal stem cells using spr biosensor. *Biosens Bioelectron* **2017**, *96*, 358-366.
43. Gavard, J.; Gutkind, J.S. Ve-cadherin and claudin-5: It takes two to tango. *Nat Cell Biol* **2008**, *10*, 883-885.
44. Xu, K.; Cleaver, O. Tubulogenesis during blood vessel formation. *Semin Cell Dev Biol* **2011**, *22*, 993-1004.
45. Bellot-Saez, A.; Kékesi, O.; Morley, J.W.; Buskila, Y. Astrocytic modulation of neuronal excitability through k(+) spatial buffering. *Neurosci Biobehav Rev* **2017**, *77*, 87-97.
46. Tien, T.; Barrette, K.F.; Chronopoulos, A.; Roy, S. Effects of high glucose-induced cx43 downregulation on occludin and zo-1 expression and tight junction barrier function in retinal endothelial cells. *Invest Ophthalmol Vis Sci* **2013**, *54*, 6518-6525.
47. Armulik, A.; Abramsson, A.; Betsholtz, C. Endothelial/pericyte interactions. *Circ Res* **2005**, *97*, 512-523.
48. Bobbie, M.W.; Roy, S.; Trudeau, K.; Munger, S.J.; Simon, A.M.; Roy, S. Reduced connexin 43 expression and its effect on the development of vascular lesions in retinas of diabetic mice. *Invest Ophthalmol Vis Sci* **2010**, *51*, 3758-3763.
49. Bergers, G.; Song, S. The role of pericytes in blood-vessel formation and maintenance. *Neuro Oncol* **2005**, *7*, 452-464.
50. Thomas, M.; Augustin, H.G. The role of the angiopoietins in vascular morphogenesis. *Angiogenesis* **2009**, *12*, 125-137.
51. Cabral, T.; Mello, L.G.M.; Lima, L.H.; Polido, J.; Regatieri, C.V.; Belfort, R., Jr.; Mahajan, V.B. Retinal and choroidal angiogenesis: A review of new targets. *Int J Retina Vitreous* **2017**, *3*, 31.

52. Fallah, A.; Sadeghinia, A.; Kahroba, H.; Samadi, A.; Heidari, H.R.; Bradaran, B.; Zeinali, S.; Molavi, O. Therapeutic targeting of angiogenesis molecular pathways in angiogenesis-dependent diseases. *Biomed Pharmacother* **2019**, *110*, 775-785.
53. Geranmayeh, M.H.; Rahbarghazi, R.; Farhoudi, M. Targeting pericytes for neurovascular regeneration. *Cell Commun Signal* **2019**, *17*, 26.
54. Fernández-Sánchez, L.; Lax, P.; Campello, L.; Pinilla, I.; Cuenca, N. Astrocytes and müller cell alterations during retinal degeneration in a transgenic rat model of retinitis pigmentosa. *Front Cell Neurosci* **2015**, *9*, 484.
55. de Hoz, R.; Rojas, B.; Ramírez, A.I.; Salazar, J.J.; Gallego, B.I.; Triviño, A.; Ramírez, J.M. Retinal macroglial responses in health and disease. *Biomed Res Int* **2016**, *2016*, 2954721.
56. Shen, W.; Li, S.; Chung, S.H.; Gillies, M.C. Retinal vascular changes after glial disruption in rats. *J Neurosci Res* **2010**, *88*, 1485-1499.
57. Falero-Perez, J.; Sorenson, C.M.; Sheibani, N. Cyp1b1-deficient retinal astrocytes are more proliferative and migratory and are protected from oxidative stress and inflammation. *Am J Physiol Cell Physiol* **2019**, *316*, C767-c781.
58. Ding, X.; Zhang, M.; Gu, R.; Xu, G.; Wu, H. Activated microglia induce the production of reactive oxygen species and promote apoptosis of co-cultured retinal microvascular pericytes. *Graefes Arch Clin Exp Ophthalmol* **2017**, *255*, 777-788.
59. Fu, D.; Yu, J.Y.; Connell, A.R.; Yang, S.; Hookham, M.B.; McLeese, R.; Lyons, T.J. Beneficial effects of berberine on oxidized ldl-induced cytotoxicity to human retinal müller cells. *Invest Ophthalmol Vis Sci* **2016**, *57*, 3369-3379.
60. Cai, J.; Boulton, M. The pathogenesis of diabetic retinopathy: Old concepts and new questions. *Eye (Lond)* **2002**, *16*, 242-260.
61. Bek, T. Diameter changes of retinal vessels in diabetic retinopathy. *Curr Diab Rep* **2017**, *17*, 82.

62. Lorenzi, M. The polyol pathway as a mechanism for diabetic retinopathy: Attractive, elusive, and resilient. *Exp Diabetes Res* **2007**, *2007*, 61038.
63. Miller, D.J.; Cascio, M.A.; Rosca, M.G. Diabetic retinopathy: The role of mitochondria in the neural retina and microvascular disease. *Antioxidants (Basel)* **2020**, *9*.
64. Singh, V.P.; Bali, A.; Singh, N.; Jaggi, A.S. Advanced glycation end products and diabetic complications. *Korean J Physiol Pharmacol* **2014**, *18*, 1-14.
65. Melincovici, C.S.; Boşca, A.B.; Şuşman, S.; Mărginean, M.; Mihu, C.; Istrate, M.; Moldovan, I.M.; Roman, A.L.; Mihu, C.M. Vascular endothelial growth factor (vegf) - key factor in normal and pathological angiogenesis. *Rom J Morphol Embryol* **2018**, *59*, 455-467.
66. Cornel, S.; Adriana, I.D.; Mihaela, T.C.; Speranta, S.; Algerino, S.; Mehdi, B.; Jalaladin, H.R. Anti-vascular endothelial growth factor indications in ocular disease. *Rom J Ophthalmol* **2015**, *59*, 235-242.
67. Semeraro, F.; Morescalchi, F.; Cancarini, A.; Russo, A.; Rezzola, S.; Costagliola, C. Diabetic retinopathy, a vascular and inflammatory disease: Therapeutic implications. *Diabetes Metab* **2019**, *45*, 517-527.
68. Rübsam, A.; Parikh, S.; Fort, P.E. Role of inflammation in diabetic retinopathy. *Int J Mol Sci* **2018**, *19*.
69. Grigsby, J.G.; Cardona, S.M.; Pouw, C.E.; Muniz, A.; Mendiola, A.S.; Tsin, A.T.; Allen, D.M.; Cardona, A.E. The role of microglia in diabetic retinopathy. *J Ophthalmol* **2014**, *2014*, 705783.
70. Liu, Y.; Biarnés Costa, M.; Gerhardinger, C. Il-1β is upregulated in the diabetic retina and retinal vessels: Cell-specific effect of high glucose and il-1β autostimulation. *PLoS One* **2012**, *7*, e36949.
71. Crane, I.J.; Liversidge, J. Mechanisms of leukocyte migration across the blood-retina barrier. *Semin Immunopathol* **2008**, *30*, 165-177.
72. Huang, H.; Gandhi, J.K.; Zhong, X.; Wei, Y.; Gong, J.; Duh, E.J.; Vinores, S.A. Tnfalpha is required for late brb breakdown in diabetic retinopathy,

and its inhibition prevents leukostasis and protects vessels and neurons from apoptosis. *Invest Ophthalmol Vis Sci* **2011**, *52*, 1336-1344.

73. Kern, T.S. Contributions of inflammatory processes to the development of the early stages of diabetic retinopathy. *Exp Diabetes Res* **2007**, *2007*, 95103.
74. Noda, K.; Nakao, S.; Ishida, S.; Ishibashi, T. Leukocyte adhesion molecules in diabetic retinopathy. *J Ophthalmol* **2012**, *2012*, 279037.
75. van der Wijk, A.E.; Hughes, J.M.; Klaassen, I.; Van Noorden, C.J.F.; Schlingemann, R.O. Is leukostasis a crucial step or epiphenomenon in the pathogenesis of diabetic retinopathy? *J Leukoc Biol* **2017**, *102*, 993-1001.
76. Rangasamy, S.; McGuire, P.G.; Franco Nitta, C.; Monickaraj, F.; Oruganti, S.R.; Das, A. Chemokine mediated monocyte trafficking into the retina: Role of inflammation in alteration of the blood-retinal barrier in diabetic retinopathy. *PLoS One* **2014**, *9*, e108508.
77. Taghavi, Y.; Hassanshahi, G.; Kounis, N.G.; Koniari, I.; Khorramdelazad, H. Monocyte chemoattractant protein-1 (mcp-1/ccl2) in diabetic retinopathy: Latest evidence and clinical considerations. *J Cell Commun Signal* **2019**, *13*, 451-462.
78. Bartels, C.M.; Wong, J.C.; Johnson, S.L.; Thorpe, C.T.; Barney, N.P.; Sheibani, N.; Smith, M.A. Rheumatoid arthritis and the prevalence of diabetic retinopathy. *Rheumatology (Oxford)* **2015**, *54*, 1415-1419.
79. Romeo, G.; Liu, W.H.; Asnaghi, V.; Kern, T.S.; Lorenzi, M. Activation of nuclear factor-kappab induced by diabetes and high glucose regulates a proapoptotic program in retinal pericytes. *Diabetes* **2002**, *51*, 2241-2248.
80. Mizutani, M.; Kern, T.S.; Lorenzi, M. Accelerated death of retinal microvascular cells in human and experimental diabetic retinopathy. *J Clin Invest* **1996**, *97*, 2883-2890.
81. Corliss, B.A.; Ray, H.C.; Doty, R.W.; Mathews, C.; Sheybani, N.; Fitzgerald, K.; Prince, R.; Kelly-Goss, M.R.; Murfee, W.L.; Chappell, J.; Owens, G.K.; Yates, P.A.; Peirce, S.M. Pericyte bridges in homeostasis and hyperglycemia. *Diabetes* **2020**, *69*, 1503-1517.

82. Ferland-McCollough, D.; Slater, S.; Richard, J.; Reni, C.; Mangialardi, G. Pericytes, an overlooked player in vascular pathobiology. *Pharmacol Ther* **2017**, *171*, 30-42.
83. Cai, J.; Kehoe, O.; Smith, G.M.; Hykin, P.; Boulton, M.E. The angiopoietin/tie-2 system regulates pericyte survival and recruitment in diabetic retinopathy. *Invest Ophthalmol Vis Sci* **2008**, *49*, 2163-2171.
84. Pfister, F.; Feng, Y.; vom Hagen, F.; Hoffmann, S.; Molema, G.; Hillebrands, J.L.; Shani, M.; Deutsch, U.; Hammes, H.P. Pericyte migration: A novel mechanism of pericyte loss in experimental diabetic retinopathy. *Diabetes* **2008**, *57*, 2495-2502.
85. Enge, M.; Bjarnegård, M.; Gerhardt, H.; Gustafsson, E.; Kalén, M.; Asker, N.; Hammes, H.P.; Shani, M.; Fässler, R.; Betsholtz, C. Endothelium-specific platelet-derived growth factor-b ablation mimics diabetic retinopathy. *Embo j* **2002**, *21*, 4307-4316.
86. Arboleda-Velasquez, J.F.; Valdez, C.N.; Marko, C.K.; D'Amore, P.A. From pathobiology to the targeting of pericytes for the treatment of diabetic retinopathy. *Curr Diab Rep* **2015**, *15*, 573.
87. Betteridge, D.J. What is oxidative stress? *Metabolism* **2000**, *49*, 3-8.
88. Kaludercic, N.; Di Lisa, F. Mitochondrial ros formation in the pathogenesis of diabetic cardiomyopathy. *Front Cardiovasc Med* **2020**, *7*, 12.
89. Drummond, G.R.; Sobey, C.G. Endothelial nadph oxidases: Which nox to target in vascular disease? *Trends Endocrinol Metab* **2014**, *25*, 452-463.
90. De Gara, L.; Foyer, C.H. Ying and yang interplay between reactive oxygen and reactive nitrogen species controls cell functions. *Plant Cell Environ* **2017**, *40*, 459-461.
91. Li, R.; Jia, Z.; Trush, M.A. Defining ros in biology and medicine. *React Oxyg Species (Apex)* **2016**, *1*, 9-21.
92. Benzie, I.F. Evolution of antioxidant defence mechanisms. *Eur J Nutr* **2000**, *39*, 53-61.

93. Dinh, Q.N.; Drummond, G.R.; Sobey, C.G.; Chrissobolis, S. Roles of inflammation, oxidative stress, and vascular dysfunction in hypertension. *Biomed Res Int* **2014**, *2014*, 406960.
94. Schroder, K.; Tschopp, J. The inflammasomes. *Cell* **2010**, *140*, 821-832.
95. Lu, L.; Lu, Q.; Chen, W.; Li, J.; Li, C.; Zheng, Z. Vitamin d(3) protects against diabetic retinopathy by inhibiting high-glucose-induced activation of the ros/txnip/nlrp3 inflammasome pathway. *J Diabetes Res* **2018**, *2018*, 8193523.
96. Devi, T.S.; Lee, I.; Hüttemann, M.; Kumar, A.; Nantwi, K.D.; Singh, L.P. Txnip links innate host defense mechanisms to oxidative stress and inflammation in retinal muller glia under chronic hyperglycemia: Implications for diabetic retinopathy. *Exp Diabetes Res* **2012**, *2012*, 438238.
97. Singh, L.P. Thioredoxin interacting protein (txnip) and pathogenesis of diabetic retinopathy. *J Clin Exp Ophthalmol* **2013**, *4*.
98. Mahajan, N.; Arora, P.; Sandhir, R. Perturbed biochemical pathways and associated oxidative stress lead to vascular dysfunctions in diabetic retinopathy. *Oxid Med Cell Longev* **2019**, *2019*, 8458472.
99. Du, Y.; Miller, C.M.; Kern, T.S. Hyperglycemia increases mitochondrial superoxide in retina and retinal cells. *Free Radic Biol Med* **2003**, *35*, 1491-1499.
100. Yu-Wai-Man, P.; Newman, N.J. Inherited eye-related disorders due to mitochondrial dysfunction. *Hum Mol Genet* **2017**, *26*, R12-r20.
101. Hoegger, M.J.; Lieven, C.J.; Levin, L.A. Differential production of superoxide by neuronal mitochondria. *BMC Neurosci* **2008**, *9*, 4.
102. Remor, A.P.; de Matos, F.J.; Ghisoni, K.; da Silva, T.L.; Eidt, G.; Búrigo, M.; de Bem, A.F.; Silveira, P.C.; de León, A.; Sanchez, M.C.; Hohl, A.; Glaser, V.; Gonçalves, C.A.; Quincozes-Santos, A.; Borba Rosa, R.; Latini, A. Differential effects of insulin on peripheral diabetes-related changes in mitochondrial bioenergetics: Involvement of advanced glycosylated end products. *Biochim Biophys Acta* **2011**, *1812*, 1460-1471.

103. Chen, J.F.; Eltzschig, H.K.; Fredholm, B.B. Adenosine receptors as drug targets--what are the challenges? *Nat Rev Drug Discov* **2013**, *12*, 265-286.
104. Burnstock, G. Purine and purinergic receptors. *Brain Neurosci Adv* **2018**, *2*, 2398212818817494.
105. Jacobson, K.A.; Jarvis, M.F.; Williams, M. Purine and pyrimidine (p2) receptors as drug targets. *J Med Chem* **2002**, *45*, 4057-4093.
106. Burnstock, G.; Fredholm, B.B.; North, R.A.; Verkhratsky, A. The birth and postnatal development of purinergic signalling. *Acta Physiol (Oxf)* **2010**, *199*, 93-147.
107. Burnstock, G.; Kennedy, C. P2x receptors in health and disease. *Adv Pharmacol* **2011**, *61*, 333-372.
108. Kawamura, H.; Sugiyama, T.; Wu, D.M.; Kobayashi, M.; Yamanishi, S.; Katsumura, K.; Puro, D.G. Atp: A vasoactive signal in the pericyte-containing microvasculature of the rat retina. *J Physiol* **2003**, *551*, 787-799.
109. Brändle, U.; Kohler, K.; Wheeler-Schilling, T.H. Expression of the p2x7-receptor subunit in neurons of the rat retina. *Brain Res Mol Brain Res* **1998**, *62*, 106-109.
110. Puthussery, T.; Fletcher, E.L. Synaptic localization of p2x7 receptors in the rat retina. *J Comp Neurol* **2004**, *472*, 13-23.
111. Hattori, M.; Gouaux, E. Molecular mechanism of atp binding and ion channel activation in p2x receptors. *Nature* **2012**, *485*, 207-212.
112. Karasawa, A.; Kawate, T. Structural basis for subtype-specific inhibition of the p2x7 receptor. *Elife* **2016**, *5*.
113. Le Feuvre, R.; Brough, D.; Rothwell, N. Extracellular atp and p2x7 receptors in neurodegeneration. *Eur J Pharmacol* **2002**, *447*, 261-269.
114. Di Virgilio, F. Liaisons dangereuses: P2x(7) and the inflammasome. *Trends Pharmacol Sci* **2007**, *28*, 465-472.
115. Nagy, J. Recent patents on novel p2x7 receptor antagonists potentially effective for treatment of inflammatory diseases. *Recent Patents on Biomarkers* **2013**, *3*, 1-24.

116. Dubyak, G.R.; el-Moatassim, C. Signal transduction via p2-purinergic receptors for extracellular atp and other nucleotides. *Am J Physiol* **1993**, *265*, C577-606.
117. Sugiyama, T.; Oku, H.; Komori, A.; Ikeda, T. Effect of p2x7 receptor activation on the retinal blood velocity of diabetic rabbits. *Arch Ophthalmol* **2006**, *124*, 1143-1149.
118. Sugiyama, T.; Kawamura, H.; Yamanishi, S.; Kobayashi, M.; Katsumura, K.; Puro, D.G. Regulation of p2x7-induced pore formation and cell death in pericyte-containing retinal microvessels. *Am J Physiol Cell Physiol* **2005**, *288*, C568-576.
119. Liao, S.D.; Puro, D.G. Nad+-induced vasotoxicity in the pericyte-containing microvasculature of the rat retina: Effect of diabetes. *Invest Ophthalmol Vis Sci* **2006**, *47*, 5032-5038.
120. Mitchell, C.H.; Lu, W.; Hu, H.; Zhang, X.; Reigada, D.; Zhang, M. The p2x(7) receptor in retinal ganglion cells: A neuronal model of pressure-induced damage and protection by a shifting purinergic balance. *Purinergic Signal* **2009**, *5*, 241-249.
121. Sugiyama, T. Role of p2x7 receptors in the development of diabetic retinopathy. *World J Diabetes* **2014**, *5*, 141-145.
122. Frey, T.; Antonetti, D.A. Alterations to the blood-retinal barrier in diabetes: Cytokines and reactive oxygen species. *Antioxid Redox Signal* **2011**, *15*, 1271-1284.
123. Cunha-Vaz, J.; Bernardes, R.; Lobo, C. Blood-retinal barrier. *Eur J Ophthalmol* **2011**, *21 Suppl 6*, S3-9.
124. Zhang, T.; Mei, X.; Ouyang, H.; Lu, B.; Yu, Z.; Wang, Z.; Ji, L. Natural flavonoid galangin alleviates microglia-trigged blood-retinal barrier dysfunction during the development of diabetic retinopathy. *J Nutr Biochem* **2019**, *65*, 1-14.
125. Santaguida, S.; Janigro, D.; Hossain, M.; Oby, E.; Rapp, E.; Cucullo, L. Side by side comparison between dynamic versus static models of blood-brain barrier in vitro: A permeability study. *Brain Res* **2006**, *1109*, 1-13.

126. Moraes, C.; Mehta, G.; Lesher-Perez, S.C.; Takayama, S. Organs-on-a-chip: A focus on compartmentalized microdevices. *Ann Biomed Eng* **2012**, *40*, 1211-1227.
127. Matteucci, A.; Varano, M.; Mallozzi, C.; Gaddini, L.; Villa, M.; Gabrielli, S.; Formisano, G.; Pricci, F.; Malchiodi-Albedi, F. Primary retinal cultures as a tool for modeling diabetic retinopathy: An overview. *Biomed Res Int* **2015**, *2015*, 364924.
128. Stone, N.L.; England, T.J.; O'Sullivan, S.E. A novel transwell blood brain barrier model using primary human cells. *Front Cell Neurosci* **2019**, *13*, 230.
129. Wisniewska-Kruk, J.; Hoeben, K.A.; Vogels, I.M.; Gaillard, P.J.; Van Noorden, C.J.; Schlingemann, R.O.; Klaassen, I. A novel co-culture model of the blood-retinal barrier based on primary retinal endothelial cells, pericytes and astrocytes. *Exp Eye Res* **2012**, *96*, 181-190.
130. Hamilton, R.D.; Foss, A.J.; Leach, L. Establishment of a human in vitro model of the outer blood-retinal barrier. *J Anat* **2007**, *211*, 707-716.
131. Moyer, A.L.; Ramadan, R.T.; Thurman, J.; Burroughs, A.; Callegan, M.C. Bacillus cereus induces permeability of an in vitro blood-retina barrier. *Infect Immun* **2008**, *76*, 1358-1367.
132. Srinivasan, B.; Kolli, A.R.; Esch, M.B.; Abaci, H.E.; Shuler, M.L.; Hickman, J.J. Teer measurement techniques for in vitro barrier model systems. *J Lab Autom* **2015**, *20*, 107-126.
133. Fu, B.M.; Zhao, Z.; Zhu, D. Blood-brain barrier (bbb) permeability and transport measurement in vitro and in vivo. *Methods Mol Biol* **2021**, *2367*, 105-122.
134. Bhatia, S.N.; Ingber, D.E. Microfluidic organs-on-chips. *Nat Biotechnol* **2014**, *32*, 760-772.
135. Park, T.E.; Mustafaoglu, N.; Herland, A.; Hasselkus, R.; Mannix, R.; FitzGerald, E.A.; Prantil-Baun, R.; Watters, A.; Henry, O.; Benz, M.; Sanchez, H.; McCrea, H.J.; Goumnerova, L.C.; Song, H.W.; Palecek, S.P.; Shusta, E.; Ingber, D.E. Hypoxia-enhanced blood-brain barrier chip

recapitulates human barrier function and shuttling of drugs and antibodies. *Nat Commun* **2019**, *10*, 2621.

136. Grifno, G.N.; Farrell, A.M.; Linville, R.M.; Arevalo, D.; Kim, J.H.; Gu, L.; Searson, P.C. Tissue-engineered blood-brain barrier models via directed differentiation of human induced pluripotent stem cells. *Sci Rep* **2019**, *9*, 13957.

137. Lelièvre, S.A.; Kwok, T.; Chittiboyina, S. Architecture in 3d cell culture: An essential feature for in vitro toxicology. *Toxicol In Vitro* **2017**, *45*, 287-295.

138. Peptu, C.A.; Popa, M.; Savin, C.; Popa, R.F.; Ochiuz, L. Modern drug delivery systems for targeting the posterior segment of the eye. *Curr Pharm Des* **2015**, *21*, 6055-6069.

139. Bogdanov, P.; Simó-Servat, O.; Sampedro, J.; Solà-Adell, C.; Garcia-Ramírez, M.; Ramos, H.; Guerrero, M.; Suñé-Negre, J.M.; Ticó, J.R.; Montoro, B. Topical administration of bosentan prevents retinal neurodegeneration in experimental diabetes. *International journal of molecular sciences* **2018**, *19*, 3578.

140. Sampedro, J.; Bogdanov, P.; Ramos, H.; Solà-Adell, C.; Turch, M.; Valeri, M.; Simó-Servat, O.; Lagunas, C.; Simó, R.; Hernández, C. New insights into the mechanisms of action of topical administration of glp-1 in an experimental model of diabetic retinopathy. *Journal of clinical medicine* **2019**, *8*, 339.

141. Hernández, C.; Bogdanov, P.; Solà-Adell, C.; Sampedro, J.; Valeri, M.; Genís, X.; Simó-Servat, O.; García-Ramírez, M.; Simó, R. Topical administration of dpp-iv inhibitors prevents retinal neurodegeneration in experimental diabetes. *Diabetologia* **2017**, *60*, 2285-2298.

142. Schopf, L.R.; Popov, A.M.; Enlow, E.M.; Bourassa, J.L.; Ong, W.Z.; Nowak, P.; Chen, H. Topical ocular drug delivery to the back of the eye by mucus-penetrating particles. *Translational vision science & technology* **2015**, *4*, 11-11.

143. Popov, A.; Enlow, E.; Bourassa, J.; Chen, H. Mucus-penetrating nanoparticles made with "mucoadhesive" poly(vinyl alcohol). *Nanomedicine* **2016**, *12*, 1863-1871.
144. de Cogan, F.; Hill, L.J.; Lynch, A.; Morgan-Warren, P.J.; Lechner, J.; Berwick, M.R.; Peacock, A.F.A.; Chen, M.; Scott, R.A.H.; Xu, H.; Logan, A. Topical delivery of anti-vegf drugs to the ocular posterior segment using cell-penetrating peptides. *Invest Ophthalmol Vis Sci* **2017**, *58*, 2578-2590.
145. Shikamura, Y.; Yamazaki, Y.; Matsunaga, T.; Sato, T.; Ohtori, A.; Tojo, K. Hydrogel ring for topical drug delivery to the ocular posterior segment. *Curr Eye Res* **2016**, *41*, 653-661.
146. Cabrera, F.J.; Wang, D.C.; Reddy, K.; Acharya, G.; Shin, C.S. Challenges and opportunities for drug delivery to the posterior of the eye. *Drug discovery today* **2019**, *24*, 1679-1684.
147. Early photocoagulation for diabetic retinopathy. Etdrs report number 9. Early treatment diabetic retinopathy study research group. *Ophthalmology* **1991**, *98*, 766-785.
148. Photocoagulation treatment of proliferative diabetic retinopathy: The second report of diabetic retinopathy study findings. *Ophthalmology* **1978**, *85*, 82-106.
149. Fong, D.S.; Girach, A.; Boney, A. Visual side effects of successful scatter laser photocoagulation surgery for proliferative diabetic retinopathy: A literature review. *Retina* **2007**, *27*, 816-824.
150. Distefano, L.N.; Garcia-Arumi, J.; Martinez-Castillo, V.; Boixadera, A. Combination of anti-vegf and laser photocoagulation for diabetic macular edema: A review. *J Ophthalmol* **2017**, *2017*, 2407037.
151. Keil, J.M.; Liu, X.; Antonetti, D.A. Glucocorticoid induction of occludin expression and endothelial barrier requires transcription factor p54 nono. *Invest Ophthalmol Vis Sci* **2013**, *54*, 4007-4015.
152. Elman, M.J.; Aiello, L.P.; Beck, R.W.; Bressler, N.M.; Bressler, S.B.; Edwards, A.R.; Ferris, F.L., 3rd; Friedman, S.M.; Glassman, A.R.; Miller,

K.M.; Scott, I.U.; Stockdale, C.R.; Sun, J.K. Randomized trial evaluating ranibizumab plus prompt or deferred laser or triamcinolone plus prompt laser for diabetic macular edema. *Ophthalmology* **2010**, *117*, 1064-1077.e1035.

153. Bressler, S.B.; Qin, H.; Melia, M.; Bressler, N.M.; Beck, R.W.; Chan, C.K.; Grover, S.; Miller, D.G. Exploratory analysis of the effect of intravitreal ranibizumab or triamcinolone on worsening of diabetic retinopathy in a randomized clinical trial. *JAMA Ophthalmol* **2013**, *131*, 1033-1040.

154. Iyer, S.S.; Lagrew, M.K.; Tillit, S.M.; Roohipourmoallai, R.; Korntner, S. The vitreous ecosystem in diabetic retinopathy: Insight into the patho-mechanisms of disease. *International Journal of Molecular Sciences* **2021**, *22*, 7142.

155. Penn, J.S.; Madan, A.; Caldwell, R.B.; Bartoli, M.; Caldwell, R.W.; Hartnett, M.E. Vascular endothelial growth factor in eye disease. *Prog Retin Eye Res* **2008**, *27*, 331-371.

156. Miller, J.W.; Le Couter, J.; Strauss, E.C.; Ferrara, N. Vascular endothelial growth factor a in intraocular vascular disease. *Ophthalmology* **2013**, *120*, 106-114.

157. Zucchiatti, I.; Bandello, F. Intravitreal ranibizumab in diabetic macular edema: Long-term outcomes. *Dev Ophthalmol* **2017**, *60*, 63-70.

158. Do, D.V.; Nguyen, Q.D.; Khwaja, A.A.; Channa, R.; Sepah, Y.J.; Sophie, R.; Hafiz, G.; Campochiaro, P.A. Ranibizumab for edema of the macula in diabetes study: 3-year outcomes and the need for prolonged frequent treatment. *JAMA Ophthalmol* **2013**, *131*, 139-145.

159. Elman, M.J.; Bressler, N.M.; Qin, H.; Beck, R.W.; Ferris III, F.L.; Friedman, S.M.; Glassman, A.R.; Scott, I.U.; Stockdale, C.R.; Sun, J.K. Expanded 2-year follow-up of ranibizumab plus prompt or deferred laser or triamcinolone plus prompt laser for diabetic macular edema. *Ophthalmology* **2011**, *118*, 609-614.

160. Lang, G.E. Diabetic macular edema. *Ophthalmologica* **2012**, *227*, 21-29.

161. Papadopoulos, N.; Martin, J.; Ruan, Q.; Rafique, A.; Rosconi, M.P.; Shi, E.; Pyles, E.A.; Yancopoulos, G.D.; Stahl, N.; Wiegand, S.J. Binding and neutralization of vascular endothelial growth factor (vegf) and related ligands by vegf trap, ranibizumab and bevacizumab. *Angiogenesis* **2012**, *15*, 171-185.

162. Moradi, A.; Sepah, Y.J.; Sadiq, M.A.; Nasir, H.; Kherani, S.; Sophie, R.; Do, D.V.; Nguyen, Q.D. Vascular endothelial growth factor trap-eye (aflibercept) for the management of diabetic macular edema. *World J Diabetes* **2013**, *4*, 303-309.

163. Takahashi, S. Vascular endothelial growth factor (vegf), vegf receptors and their inhibitors for antiangiogenic tumor therapy. *Biol Pharm Bull* **2011**, *34*, 1785-1788.

164. Wells, J.A.; Glassman, A.R.; Ayala, A.R.; Jampol, L.M.; Aiello, L.P.; Antoszyk, A.N.; Arnold-Bush, B.; Baker, C.W.; Bressler, N.M.; Browning, D.J.; Elman, M.J.; Ferris, F.L.; Friedman, S.M.; Melia, M.; Pieramici, D.J.; Sun, J.K.; Beck, R.W. Aflibercept, bevacizumab, or ranibizumab for diabetic macular edema. *N Engl J Med* **2015**, *372*, 1193-1203.

165. Kurihara, T.; Westenskow, P.D.; Bravo, S.; Aguilar, E.; Friedlander, M. Targeted deletion of vegfa in adult mice induces vision loss. *J Clin Invest* **2012**, *122*, 4213-4217.

166. Matuszewski, W.; Baranowska-Jurkun, A.; Stefanowicz-Rutkowska, M.M.; Modzelewski, R.; Pieczyński, J.; Bandurska-Stankiewicz, E. Prevalence of diabetic retinopathy in type 1 and type 2 diabetes mellitus patients in north-east poland. *Medicina (Kaunas)* **2020**, *56*.

167. Sinclair, S.H.; Schwartz, S.S. Diabetic retinopathy-an underdiagnosed and undertreated inflammatory, neuro-vascular complication of diabetes. *Front Endocrinol (Lausanne)* **2019**, *10*, 843.

168. Komarova, Y.A.; Kruse, K.; Mehta, D.; Malik, A.B. Protein interactions at endothelial junctions and signaling mechanisms regulating endothelial permeability. *Circ Res* **2017**, *120*, 179-206.

169. Vinores, S. Breakdown of the blood–retinal barrier. *Encyclopedia of the Eye* **2010**, 216.
170. Yang, X.; Yu, X.W.; Zhang, D.D.; Fan, Z.G. Blood-retinal barrier as a converging pivot in understanding the initiation and development of retinal diseases. *Chin Med J (Engl)* **2020**, *133*, 2586-2594.
171. Yuan, T.; Yang, T.; Chen, H.; Fu, D.; Hu, Y.; Wang, J.; Yuan, Q.; Yu, H.; Xu, W.; Xie, X. New insights into oxidative stress and inflammation during diabetes mellitus-accelerated atherosclerosis. *Redox Biol* **2019**, *20*, 247-260.
172. Ly, A.; Yee, P.; Vessey, K.A.; Phipps, J.A.; Jobling, A.I.; Fletcher, E.L. Early inner retinal astrocyte dysfunction during diabetes and development of hypoxia, retinal stress, and neuronal functional loss. *Invest Ophthalmol Vis Sci* **2011**, *52*, 9316-9326.
173. Kruk, J.; Kubasik-Kladna, K.; Aboul-Enein, H.Y. The role oxidative stress in the pathogenesis of eye diseases: Current status and a dual role of physical activity. *Mini Rev Med Chem* **2015**, *16*, 241-257.
174. Ganesh Yerra, V.; Negi, G.; Sharma, S.S.; Kumar, A. Potential therapeutic effects of the simultaneous targeting of the nrf2 and nf-κb pathways in diabetic neuropathy. *Redox Biol* **2013**, *1*, 394-397.
175. Wang, D.; Wang, H.; Gao, H.; Zhang, H.; Zhang, H.; Wang, Q.; Sun, Z. P2x7 receptor mediates nlrp3 inflammasome activation in depression and diabetes. *Cell Biosci* **2020**, *10*, 28.
176. Le Daré, B.; Ferron, P.J.; Gicquel, T. The purinergic p2x7 receptor-nlrp3 inflammasome pathway: A new target in alcoholic liver disease? *Int J Mol Sci* **2021**, *22*.
177. Pushpakumar, S.; Ren, L.; Kundu, S.; Gamon, A.; Tyagi, S.C.; Sen, U. Toll-like receptor 4 deficiency reduces oxidative stress and macrophage mediated inflammation in hypertensive kidney. *Sci Rep* **2017**, *7*, 6349.
178. Yuan, R.; Huang, L.; Du, L.J.; Feng, J.F.; Li, J.; Luo, Y.Y.; Xu, Q.M.; Yang, S.L.; Gao, H.; Feng, Y.L. Dihydrotanshinone exhibits an anti-

inflammatory effect in vitro and in vivo through blocking tlr4 dimerization. *Pharmacol Res* **2019**, *142*, 102-114.

179. Yu, L.; Qian, J. Dihydrotanshinone i alleviates spinal cord injury via suppressing inflammatory response, oxidative stress and apoptosis in rats. *Med Sci Monit* **2020**, *26*, e920738.
180. Zhao, W.; Li, C.; Zhang, H.; Zhou, Q.; Chen, X.; Han, Y.; Chen, X. Dihydrotanshinone i attenuates plaque vulnerability in apolipoprotein e-deficient mice: Role of receptor-interacting protein 3. *Antioxid Redox Signal* **2021**, *34*, 351-363.
181. Zhao, W.; Li, C.; Gao, H.; Wu, Q.; Shi, J.; Chen, X. Dihydrotanshinone i attenuates atherosclerosis in apoe-deficient mice: Role of nox4/nf-κb mediated lectin-like oxidized ldl receptor-1 (lox-1) of the endothelium. *Front Pharmacol* **2016**, *7*, 418.
182. Gupta, N.; Mansoor, S.; Sharma, A.; Sapkal, A.; Sheth, J.; Falatoonzadeh, P.; Kuppermann, B.; Kenney, M. Diabetic retinopathy and vegf. *Open Ophthalmol J* **2013**, *7*, 4-10.
183. Noda, K.; Nakao, S.; Ishida, S.; Ishibashi, T. Leukocyte adhesion molecules in diabetic retinopathy. *Journal of ophthalmology* **2012**, *2012*.
184. Tien, T.; Muto, T.; Zhang, J.; Sohn, E.H.; Mullins, R.F.; Roy, S. Association of reduced connexin 43 expression with retinal vascular lesions in human diabetic retinopathy. *Exp Eye Res* **2016**, *146*, 103-106.
185. Platania, C.B.M.; Lazzara, F.; Fidilio, A.; Fresta, C.G.; Conti, F.; Giurdanella, G.; Leggio, G.M.; Salomone, S.; Drago, F.; Bucolo, C. Blood-retinal barrier protection against high glucose damage: The role of p2x7 receptor. *Biochem Pharmacol* **2019**, *168*, 249-258.

LIST OF PUBLICATIONS AND SCIENTIFIC CONTRIBUTIONS

- Caruso G, Benatti C, Musso N, Fresta CG, Fidilio A, Spampinato G, Brunello N, Bucolo C, Drago F, Lunte SM, Peterson BR, Tascedda F, Caraci F.**Carnosine Protects Macrophages against the Toxicity of Aβ1-42 Oligomers by Decreasing Oxidative Stress** (2021) Biomedicines 9, 477. doi: 10.3390/biomedicines9050477.

- Caruso G*, Fresta CG*, Costantino A, Lazzarino G, Amorini AM, Lazzarino G, Tavazzi B, Lunte SM, Dhar P, Gulisano M, Caraci F.**Lung Surfactant Decreases Biochemical Alterations and Oxidative Stress Induced by a Sub-Toxic Concentration of Carbon Nanoparticles in Alveolar Epithelial and Microglial Cells** (2021) Int. J. Mol. Sci. 22, 2694. doi: 10.3390/ijms22052694. [*stesso contributo]

- Fresta CG, Caruso G, Fidilio A, Platania CBM, Musso N, Caraci F, Drago F, Bucolo C. **Dihydrotanshinone, a natural diterpenoid, preserves blood-retinal barrier integrity via P2X7 receptor** (2020) Int. J. Mol. Sci. 21, 9305. doi: 10.3390/ijms21239305.

- Fresta CG, Fidilio A, Caruso G, Caraci F, Giblin FJ, Leggio GM, Salomone S, Drago F, Bucolo C. **A New Human Blood-Retinal Barrier Model Based on Endothelial Cells, Pericytes, and Astrocytes** (2020) Int. J. Mol. Sci. 21:1636. doi: 10.3390/ijms21051636.

- Fresta CG, Fidilio A, Lazzarino G, Musso N, Grasso M, Merlo S, Amorini AM, Bucolo C, Tavazzi B, Lazzarino G, Lunte SM, Caraci F, Caruso G. **Modulation of Pro-Oxidant and Pro-Inflammatory Activities of M1 Macrophages by the Natural Dipeptide Carnosine** (2020) Int. J. Mol. Sci. 21:776. doi: 10.3390/ijms21030776.

- Bucolo C, Fidilio A, Fresta CG, Lazzara F, Platania CBM, Cantarella G, Di Benedetto G, Burgaletto C, Bernardini R, Piazza C, Barabino S, Drago F. **Ocular Pharmacological Profile of Hydrocortisone in Dry Eye Disease** (2019) Front. Pharmacol. 10:1240. doi: 10.3389/fphar.2019.01240.

- Platania CBM, Lazzara F, Fidilio A, Fresta CG, Conti F, Giurdanella G, Leggio GM, Salomone S, Drago F, Bucolo C. **Blood-retinal barrier protection against**

high glucose damage: The role of P2X7 receptor (2019) Biochem. Pharmacol. 168:249-258. doi: 10.1016/j.bcp.2019.07.010.

- Caruso G*, Fresta CG*, Fidilio A*, O'Donnell F, Musso N, Lazzarino G, Grasso M, Amorini AM, Tascedda F, Bucolo C, Drago F, Lazzarino G*, Lunte SM, Caraci F. **Carnosine decreases PMA-induced oxidative stress and inflammation in murine macrophages** (2019) Antioxidants (Basel). 8: pii: E281. doi: 10.3390/antiox8080281. [*stesso contributo]

- Caruso G, Fresta CG, Grasso M, Santangelo R, Lazzarino G, Lunte SM, Caraci F. **Inflammation as the common biological link between depression and cardiovascular diseases: can carnosine exerts a protective role?**(2019) Curr. Med. Chem. doi: 10.2174/0929867326666190712091515.

- Caruso G, Fresta CG, Musso N, Giambirtone M, Grasso M, Spampinato SF, Merlo S, Drago F, Lazzarino G, Sortino MA, Lunte SM, Caraci F. **Carnosine prevents Aβ-induced oxidative stress and inflammation in microglial cells: a key role of TGF-β1** (2019) Cells 8:64; doi: 10.3390/cells8010064.

- Siegel JM, Schilly KM, Wijesinghe MB, Caruso G, Fresta CG, Lunte SM. **Optimization of a microchip electrophoresis method with electrochemical detection for the determination of nitrite in macrophage cells as an indicator of nitric oxide production** (2018) Anal. Methods 11:148-156.

- Caruso G, Fresta CG, Lazzarino G, Distefano DA, Parlascino P, Lunte SM, Lazzarino G, Caraci F. **Sub-toxic human amylin fragment concentrations promote the survival and proliferation of SH-SY5Y cells via the release of VEGF and HspB5 from endothelial RBE4 cells** (2018) Int. J. Mol. Sci. 19:3659; doi:10.3390/ijms19113659

CONFERENCES

- A New Human Blood–Retinal Barrier Model Based on Endothelial Cells, Pericytes, and Astrocytes. 40° Congresso Nazionale della Società Italiana di Farmacologia – Digital Edition, Marzo 9-13, 2019.

- Blood-retinal barrier protection against high glucose damage: the role of P2X7 receptor. 39° Congresso Nazionale della Società Italiana di Farmacologia, Firenze, Novembre 19-23, 2019.
- Monitoring carnosine uptake by RAW 264.7 macrophage cells using microchip electrophoresis with fluorescence detection. Biomedical Sciences Symposium, Lawrence (KS), Aprile 18, 2019.

La borsa di dottorato è stata cofinanziata con risorse del
Programma Operativo Nazionale Ricerca e Innovazione 2014-2020 (CCI 2014IT16M2OP005),
Fondo Sociale Europeo, Azione I.1 "Dottorati Innovativi con caratterizzazione Industriale"

UNIONE EUROPEA
Fondo Sociale Europeo